MOLECULAR DOCKING ASSESSMENT OF THE ANTIMIGRAINE POTENTIAL OF THE PHYTOCONSTITUENTS OF SOME MEDICINAL PLANTS

BY

NWEKE ISAAC CHINECHEREM

PHA1908546

DEPARTMENT OF PHARMACEUTICAL CHEMISTRY

FACULTY OF PHARMACY

UNIVERISTY OF BENIN

BENIN CITY

NOVEMBER 2025

MOLECULAR DOCKING ASSESSMENT OF THE ANTIMIGRAINE POTENTIAL OF THE PHYTOCONSTITUENTS OF SOME MEDICINAL PLANTS

BY

NWEKE ISAAC CHINECHEREM

PHA1908546

A DISSERTATION SUBMITTED TO THE DEPARTMENT OF PHARMACEUTICAL CHEMISTRY, FACULTY OF PHARMACY, UNIVERSITY OF BENIN, BENIN CITY IN PARTIAL FULFILMENT OF THE REQUIREMENT FOR THE AWARD OF DOCTOR OF PHARMACY DEGREE HONOURS IN PHARMACY

NOVEMBER 2025

CERTIFICATION

This is to certify that this work was done by **Nweke Isaac Chinecherem** in the Department of Pharmaceutical Chemistry, Faculty of Pharmacy, University of Benin, Benin City, Nigeria in partial fulfilment of the requirement of the award of the Doctor of Pharmacy Degree (PharmD)

_____ _____

Dr. UYI M. OGBEIDE **Date**

Supervisor

_____ _____

Dr. VINCENT O. IMIEJE **Date**

Head of Department

DEDICATION

To God Almighty, the source of all grace, strength, and guidance, without whom this achievement would not be possible.

With the deepest love and appreciation, I dedicate this work to Mum, whose sacrifice and unwavering support have been my constant foundation.

ACKNOWLEDGEMENT

My sincere gratitude goes to God almighty for His grace, mercies, love, provision and strength throughout the period of my project work and stay in the university.

I am very grateful to my supervisor, Dr. Uyi M. Ogbeide, whose understanding, experience, willingness to listen and patience made the entire work a huge success. I cannot fully express my sincere gratitude to you, thank you so much Sir. To Kluvet, Rock, Priscilla and Regina, thank you for your time and assistance.

My special appreciation goes to my parents; Mr. Japhet and Mrs. Lebechi Nweke, my lovely siblings; Nnenna, Blessing, Ezinne, Victor, and Samuel, and my beloved grandmother for their constant support, prayers and inspiration. Big thanks to my guys; Emma, Bard, Sammy, Ochuko and to my colleagues who have been part of this journey in any aspect. Diana, my therapist, thank you so much for your care.

Finally, I want to appreciate myself for pushing through and growing through it all.

TABLE OF CONTENT

Title page - - - - - - - - - - - i

Certification - - - - - - - - - - - ii

Dedication - - - - - - - - - - - iii

Acknowledgement - - - - - - - - - - iv

Table of content - - - - - - - - - - v

List of tables - - - - - - - - - - ix

List of figures - - - - - - - - - - x

List of abbreviations - - - - - - - - - xii

Abstract - - - - - - - - - - xiv

CHAPTER ONE

INTRODUCTION AND LITERATURE REVIEW

1 MIGRAINE 1

1.1 Migraine Therapy 3

1.1.1 Mechanisms of Action 3

1.1.2 Simple Analgesics and NSAIDs 4

1.1.3 Ergot Alkaloids 5

1.1.4 Triptans 5

1.1.5 Ditans 6

1.1.6 Gepants 7

1.1.7 Antidepressants 8

1.1.8 Antiepileptics 9

1.1.9 Beta-Blockers 10

1.1.10 Monoclonal antibodies 11

1.1.11 OnabotulinumtoxinA 12

1.1.12 Non-Pharmacological and Complementary Interventions 12
1.2 MEDICINAL PLANTS IN MIGRAINE MANAGEMENT 12
1.2.1 Crassocephalum crepidioides (Benth) Asteraceae 13
1.2.1.1 Trado-Medical Uses of Crassocephalum crepidioides 15
1.2.1.2 Phytochemical Constituents of *Crassocephalum crepidioides* 15
1.2.2 *Nigella sativa* (Linn) Ranunculaceae 16
1.2.2.1 Trado-Medical Uses of Nigella sativa 17
1.2.2.2 Phytochemical Constituents of Nigella sativa 17
1.2.3 Petasites hybridus (Linn) Asteraceae 18
1.2.3.1 Trado-Medical Uses of Petasites hybridus 19
1.2.3.2 Phytochemical Constituents of Petasites hybridus 19
1.2.4 Tanacetum parthenium (Linn.) Asteraceae 20
1.2.4.1 Trado-Medical Uses of *Tanacetum Parthenium* 20
1.2.4.2 Phytochemical Constituents of *Tanacetum parthenium* 21
1.3 Molecular Docking Studies 21
1.3.1 Molecular Docking Models 22
1.3.2 Docking Methods According to Flexibility Modelling 23
1.3.3 Docking Process 23
1.3.4 Docking Software 24
1.4 Aim and Objectives 25
1.4.1 Specific Objectives 25

CHAPTER TWO

MATERIALS AND METHODS

2 MATERIALS AND METHODS 26
2.1 Materials 26
2.1.1 RCSB PDB 26
2.1.1.1 Serotonin 5-HT$_1$B Receptor 26
2.1.1.2 Serotonin 5-HT$_1$D Receptor 27

2.1.1.3 Serotonin 5-HT$_1$F Receptor 28
2.1.1.4 CGRP (CLR + RAMP1) Receptor 29
2.1.2 PyRx 30
2.1.3 PyMOL 30
2.1.4 ADMETlab 3.0 31
2.2 METHODS 32
2.2.1 Identification and Preparation of Protein Target 32
2.2.2 Identification and Preparation of Ligands 32
2.2.3 Identification of Binding Site 33
2.2.4 Molecular Docking and Post-docking Analysis 33
2.2.5 ADMET Profiling 34

CHAPTER THREE

RESULT

3 Binding Site Amino Acids 35
3.1 Molecular Docking Analysis 36
3.1.1 Crassocephalum crepidioides 36
3.1.2 Nigella sativa 36
3.1.3 Petasites hybridus 36
3.1.4 Tanacetum parthenium 37
3.2 ADME Profiling of ligands 113
3.3 Toxicity Prediction 123

CHAPTER FOUR

DISCUSSION

4 DISCUSSION 138
4.1 Binding Affinity 138
4.1.1 Crassocephalum crepidioides 140
4.1.2 Nigella sativa 142

4.1.3 Petasites hybridus 144
4.1.4 Tanacetum parthenium 146
4.2 ADMET Profiling 149
CHAPTER FIVE
CONCLUSION
REFERENCES 153

LIST OF TABLES

Table 3.0: Binding site amino acids identified in 6G79, 7E32, 7EXD and 6E3Y - - 35

Table 3.1.1 Binding affinities of *Crassocephalum crepidioides* compounds with 6G79, 7E32, 7EXD, and 6E3Y - - - - - - - - - - 38

Table 3.1.2 Binding affinities of *Nigella sativa* compounds with 6G79, 7E32, 7EXD, and 6E3Y- - - - - - - - - - - - - 40

Table 3.1.3 Binding affinities of *Petasites hybridus* compounds with 6G79, 7E32, 7EXD, and 6E3Y - - - - - - - - - - - - 43

Table 3.1.4 Binding affinities of *Tanacetum parthenium* compounds with 6G79, 7E32, 7EXD, and 6E3Y - - - - - - - - - - - 48

Table 3.2.1 ADME Profiling of ligands from *Crassocephalum crepidioides* - - 113

Table 3.2.2 ADME Profiling of ligands from *Nigella sativa* - - - - - 114

Table 3.2.3. ADME Profiling of ligands from *Petasites hybridus* - - - - 117

Table 3.2.4 ADME Profiling of ligands from *Tanacetum parthenium* - - - 120

Table 3.3.1 Toxicity prediction of selected ligands from *Crassocephalum crepidioides* - 123

Table 3.3.2 Toxicity prediction of selected ligands from *Nigella sativa* - - - 125

Table 3.3.3 Toxicity prediction of selected ligands from *Petasites hybridus*- - - 128

Table 3.3.4 Toxicity prediction of selected ligands from *Tanacetum parthenium* - - 133

LIST OF FIGURES

Figure 1.1.2 Chemical structure of Aspirin - - - - - - - 4

Figure 1.1.3 Chemical structure of Ergotamine - - - - - - 5

Figure 1.1.4 Chemical structure of Sumatriptan - - - - - - 6

Figure 1.1.5 Chemical structure of Lasmiditan - - - - - - 7

Figure 1.1.6 Chemical structure of Rimegepant - - - - - - 8

Figure 1.1.7 Chemical structure of Amitriptyline - - - - - - 9

Figure 1.1.8 Chemical structure of Valproate - - - - - - 10

Figure 1.1.9 Chemical structure of Propranolol - - - - - - 11

Figure 1.2.1 fresh leaves of *Crassocephalum crepidioides* - - - - - 14

Figure 1.2.2 Dry seeds of *Nigella sativa* - - - - - - - 16

Figure 1.2.3 Leaves of *Petasites hybridus* - - - - - - - 18

Figure 1.2.4 Leaves of *Tanacetum parthenium* - - - - - - 20

Figure 2.1.1.1 Coupling specificity of heterotrimeric Go to the serotonin 5-HT1B receptor (6G79) - - - - - - - - - - - - 27

Figure 2.1.1.2 Serotonin 1D (5-HT1D) receptor-Gi protein complex - - - 28

Figure 2.1.1.3 Lasmiditan-bound serotonin 1F (5-HT1F) receptor-Gi protein complex - 28

Figure 2.1.1.4 Cryo-EM structure of the active, Gs-protein complexed, human CGRP receptor - - - - - - - - - - - - - 29

Figure 3.1.1.1 2D and 3D views of the molecular interactions of amino-acid residues of 5-HT$_1$B Receptor with ligands in *Crassocephalum crepidioides* - -- - - 55

Figure 3.1.1.2 2D and 3D views of the molecular interactions of amino-acid residues of 5-HT$_1$D Receptor with ligands in *Crassocephalum crepidioides* - - - - - 59

Figure 3.1.1.3 2D and 3D views of the molecular interactions of amino-acid residues of 5-HT$_1$F Receptor with ligands in *Crassocephalum crepidioides* - -- - - 60

Figure 3.1.2.1 2D and 3D views of the molecular interactions of amino-acid residues of 5-HT$_1$B Receptor with ligands in *Nigella sativa* - - - - - - - 65

Figure 3.1.2.2 2D and 3D views of the molecular interactions of amino-acid residues of 5-HT$_1$D Receptor with ligands in *Nigella sativa* - - - - - - - 71

Figure 3.1.2.3 2D and 3D views of the molecular interactions of amino-acid residues of 5-HT$_1$F Receptor with ligands in *Nigella sativa* - - - - - - 76

Figure 3.1.3.1 2D and 3D views of the molecular interactions of amino-acid residues of 5-HT$_1$B Receptor with ligands in *Petasites hybridus* - - -- - - - 79

Figure 3.1.3.2 2D and 3D views of the molecular interactions of amino-acid residues of 5-HT$_1$D Receptor with ligands in *Petasites hybridus* - - - - - - - 91

Figure 3.1.3.3 2D and 3D views of the molecular interactions of amino-acid residues of 5-HT$_1$F Receptor with ligands in *Petasites hybridus* - - - - - - - 95

Figure 3.1.4.1 2D and 3D views of the molecular interactions of amino-acid residues of 5-HT$_1$B Receptor with ligands in *Tanacetum parthenium* -- - - - - 98

Figure 3.1.4.2 2D and 3D views of the molecular interactions of amino-acid residues of 5-HT$_1$D Receptor with ligands in *Tanacetum parthenium* - - - - - - 108

Figure 3.1.4.3 2D and 3D views of the molecular interactions of amino-acid residues of 5-HT$_1$F Receptor with ligands in *Tanacetum parthenium* - - - - - - 111

Figure 3.1.4.4 2D and 3D views of the molecular interactions of amino-acid residues of CGRP Receptor with ligands in *Tanacetum parthenium* - - - - - - 112

LIST OF ABBREVIATIONS

2D: Two-Dimensional

3D: Three-Dimensional

5-**HT5:** Hydroxytryptamine (Serotonin)

5-HT$_1$B: Serotonin 1B receptor subtype

5-HT$_1$D: Serotonin 1D receptor subtype

5-HT$_1$F: Serotonin 1F receptor subtype

ADME: Absorption, Distribution, Metabolism, and Excretion

ADMET: Absorption, Distribution, Metabolism, Excretion, and Toxicity

AHS: American Headache Society

ALA: Alanine

ASN: Asparagine

ASP: Aspartic Acid

BMC: BioMed Central

CADD: Computer-Aided Drug Design

CGRP: Calcitonin Gene-Related Peptide

CLR: Calcitonin Receptor-Like Receptor

CNS: Central Nervous System

CYS: Cysteine

Cryo-EM: Cryo-electron microscopy

CSD: Cambridge Structural Database

CYP3A4: Cytochrome P450 3A4 enzyme

DALY: Disability-Adjusted Life Year

DHE: Dihydroergotamine

DNA: Deoxyribonucleic Acid

EM: Electron Microscopy

FTDOCK: Fast Fourier Transform Docking

GABA: Gamma-Aminobutyric Acid

GC–MS: Gas Chromatography–Mass Spectrometry

GLU: Glutamic Acid

GPCR: G-Protein-Coupled Receptor

Gs: G-stimulatory protein

HIS: Histidine

ICHD-3: International Classification of Headache Disorders, 3rd Edition

ID: Identification

ILE: Isoleucine

LEU: Leucine

kcal/mol: Kilocalories per mole (unit of binding energy)

mAbs: Monoclonal Antibodies

MET: Methionine

mg: Milligram

NF-κB: Nuclear Factor kappa-light-chain-enhancer of activated B cells

NICE: National Institute for Health and Care Excellence

NSAIDs: Non-Steroidal Anti-Inflammatory Drugs

PA: Pyrrolizidine Alkaloid

PDB: Protein Data Bank

PDBQT: Protein Data Bank, Partial Charge (Q) and Atom Type (T) format

PREEMPT: Phase III Research Evaluating Migraine Prophylaxis Therapy

QSAR: Quantitative Structure–Activity Relationship

Q Site: Quantum Site Docking Program

RAMP1: Receptor Activity-Modifying Protein 1

RCSB: Research Collaboratory for Structural Bioinformatics

SER: Serine

SDI: Socio-Demographic Index

SDF: Structure Data File

SMILES: Simplified Molecular Input Line Entry System

SNRI: Serotonin–Norepinephrine Reuptake Inhibitor

SSRIs: Selective Serotonin Reuptake Inhibitors

THR: Threonine

TRPA1: Transient Receptor Potential Ankyrin 1 Channel

TRPV1: Transient Receptor Potential Vanilloid 1 Channel

TRP: Tryptophan

TYR: Tyrosine

UCSF: University of California, San Francisco

UFF: Universal Force Field

VAL: Valine

WHO: World Health Organization

YLD: Years Lived with Disability

ABSTRACT

Migraine is defined as a primary headache disorder characterized by recurrent attacks of moderate to severe headache, typically unilateral and pulsating in nature, lasting between 4 and 72 hours, and commonly accompanied by nausea, vomiting, photophobia and phonophobia. Current migraine treatments are effective but often limited by side effects, high costs, and the risk of medication-overuse headaches. Adverse effects such as vasoconstriction in cardiovascular patients, sedation from ditan, and the metabolic or teratogenic risks of some preventive agents restrict their broader use. These challenges highlight the need for safer, multi-targeted therapies and new compounds that act on established migraine targets like CGRP and 5-HT receptors. This study aims to use *in-silico* methods to assess the potential anti-migraine activity of phytoconstituents derived from *Crassocephalum crepidioides, Nigella sativa, Petasites hybridus* and *Tanacetum parthenium.* Phytoconstituents (493) present in these plants were obtained from literature sources, their 3D SDF structures were downloaded from PubChem. The protein targets: Serotonin 5-HT_1B (6G79), 5-HT_1D (7E32), 5-HT_1F (7EXD) and CGRP (63EY) receptor were obtained from Protein data bank and prepared using BIOVIA Discovery Studio 2020 and PYMOL. Molecular docking, post-docking analysis and ADMET profiling were done using PyRx, BIOVIA discovery studio 2020 and ADMETlab 3.0 web server respectively. Fourteen (14) phytoconstituents present in *Crassocephalum crepidioides,* twenty four (24) phytoconstituents present in *Nigella sativa,* forty three (43) phytoconstituents present in *Petasites hybridus,* and thirty nine (39) phytoconstituents present in *Tanacetum parthenium* had binding affinity comparable to their reference drugs in the range of -6.9 to -11 kcal/mol. ADMET profiling of the phytoconstituents showed good oral bioavailability, and an overall balanced toxicity profile suggesting acceptable safety. These findings suggest that certain phytoconstituents from the selected plants may possess potential anti-migraine activity against key migraine-associated targets.

CHAPTER ONE

INTRODUCTION AND LITERATURE REVIEW

1 MIGRAINE

Migraine is a highly prevalent neurological disorder, affecting about 1.16 billion people globally, and ranking among the top causes of years lived with disability (YLD) (GBD 2019; WHO, 2021; Dong *et al*., 2024). Migraine is a leading cause of chronic disability rather than mortality (ICHD-3, 2018). Between 1990 and 2021, global migraine prevalence increased by approximately 58%, majorly due to population growth and aging, while age-standardized rates remained relatively stable (GBD 2021; Dong *et al*., 2024). High Socio-Demographic Index (SDI) regions show higher reported rates, likely reflecting better diagnosis and access to neurological care, whereas low-SDI regions hide large numbers of undiagnosed and untreated cases (WHO, 2021).

As migraine is a non-fatal condition, its overall burden is primarily reflected in Years Lived with Disability (YLDs) rather than Disability-Adjusted Life Years (DALYs) confirming its major contribution to non-fatal health loss (GBD 2021). Migraine ranked as the second leading global cause of YLD and the first among young women (Dong *et al*., 2024). It ranked 4th–5th overall, contributing 4–5% of total YLDs worldwide, while its DALY rank (19th overall, 3rd among neurological disorders) demonstrates that its enormous morbidity is masked by mortality-weighted metrics (GBD 2021; Dong *et al.*, 2024). Though the female burden remains higher, male migraine incidence and prevalence have increased more rapidly in recent decades (Dong *et al*., 2024). Migraine typically begins in adolescence (10–14 years) and peaks in functional disability and prevalence between 30–49 years, corresponding to the global working-age period

(GBD 2021; Dong *et al*., 2024). Migraine sufferers are up to three times more likely to experience anxiety and insomnia than non-sufferers (Amiri *et al*., 2022). These relationships worsen frequency of headache and overall quality of life, highlighting the need for holistic neurological and mental health care (Dong *et al*., 2024).

In Nigeria, migraine represents a significant yet under-recognized public health burden. Awareness as a neurological disorder remains low in Nigeria, diagnostic resources are limited, and many patients practice self-medication instead of appropriate medical care ((Aderinto *et al*., 2024; Osonuga *et al*., 2025). More recent reviews estimate prevalence between 15% and 20%, with urban populations reaching as high as 26% (Osonuga *et al*., 2025). Young adults and women are unequally affected, and common triggers include stress, lack of sleep, fatigue, and intense exercise (Aderinto *et al*., 2024). The disorder has been strongly associated with reduced productivity, poor academic performance, absenteeism, and reduced quality of life.

Migraine is defined as a primary headache disorder characterized by recurrent attacks of moderate to severe headache, typically unilateral and pulsating in nature, lasting between 4 and 72 hours, and commonly accompanied by nausea, vomiting, photophobia (abnormal sensitivity to light), and phonophobia (abnormal sensitivity to sound) (Olesen, 2018). The classification distinguishes between migraine with aura, characterized by transient neurological disturbances such as visual or sensory symptoms that precede or accompany the headache, and migraine without aura, in which such focal neurological signs are absent (Olesen, 2018).

The understanding of migraine pathophysiology has shifted from vascular theory to neurovascular models. The vascular theory proposed that aura symptoms were caused by cerebral vasoconstriction followed by vasodilation, which resulted in headache pain. However, current models view migraine as a neurovascular disorder involving complex interactions

between neuronal and vascular mechanisms (Hoffmann *et al*., 2017). Activation of the trigeminovascular system leads to the release of vasoactive neuropeptides such as calcitonin gene-related peptide (CGRP), substance P, and neurokinin A. These mediators promote vasodilation, neurogenic inflammation, and increased nociceptive transmission, which together drive the pain and associated symptoms of migraine (Villalón *et al*., 2009). Serotonin (5-HT) pathways are also central, particularly through the 5-HT_1B, 5-HT_1D, and 5-HT_1F receptor subtypes, which modulate vascular tone and pain signaling (Iyengar *et al*., 2019). Recognition of these mechanisms has guided the development of therapeutic agents such as triptans and CGRP receptor antagonists that specifically target these pathways (Edvinsson, 2022).

1.1 Migraine Therapy

The dual approach to migraine therapy combines fast-acting medications for acute attacks, which is administered at the onset of a migraine attack with the primary goal of reversing the attack, relieving pain, and minimizing disability and with long-term preventive medicines, which can greatly reduce the daily impact of the condition and improve overall quality of life (Cady and Cady, 2012). A balanced migraine management plan is thus a synergy of both acute and preventive treatments, tailored to the patient's specific clinical profile.

1.1.1 Mechanisms of Action

The various therapies for migraine target different aspects of the underlying pathophysiology. Non-specific agents, such as simple analgesics and non-steroidal anti-inflammatory drugs (NSAIDs), work by reducing inflammation and pain signals throughout the body. Migraine-specific agents like triptans and ergot alkaloids act as vasoconstrictors, narrowing the blood

vessels in the brain and modulate neurotransmitters, such as serotonin, which are implicated in the pain pathways of migraine (American Academy of Family Physicians, 2018).

In contrast, newer, more targeted treatments such as Gepants act as CGRP receptor antagonists. Ditans selectively activates serotonin receptor (5-HT1F) on nerves, interrupting pain signals without causing the blood vessel constriction associated with older agents (Goadsby *et al*., 2023).

1.1.2 Simple Analgesics and NSAIDs

For mild-to-moderate migraine attacks, non-specific drugs are recommended first-line medications, especially when taken early during an attack (American Academy of Neurology,p 2012). Simple analgesics like acetaminophen and non-steroidal anti-inflammatory drugs (NSAIDs) such as aspirin, ibuprofen, and diclofenac are widely used for this purpose (American Academy of Neurology, 2012). Acetaminophen at a dose of 1000 mg is an effective treatment for mild attacks (Cady and Cady, 2012), and there is good quality evidence supporting the use of NSAIDs for acute migraine treatment (American Academy of Neurology, 2012).

The efficacy of simple analgesics can be enhanced with pro-kinetic, anti-emetic agents like metoclopramide or domperidone as adjunctive therapies, stop nausea and ensure that oral medications are absorbed more effectively (Cady and Cady, 2012).

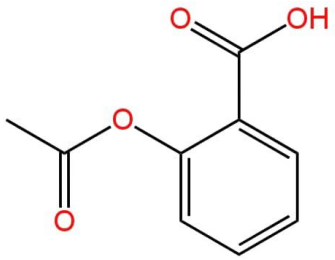

FIGURE 1.1.2: Chemical structure of Aspirin.

1.1.3 Ergot Alkaloids

Ergot alkaloids, primarily ergotamine and dihydroergotamine (DHE), are established but less commonly used medications for acute migraine. They act as 5-HT_1B/5-HT_1D serotonin receptor agonists. These drugs cause cranial blood vessel constriction and inhibit neuropeptide release. DHE is administered parenterally or intranasally and is useful for status migrainosus. Ergotamine can be taken orally with caffeine to boost absorption (Silberstein, 2019).

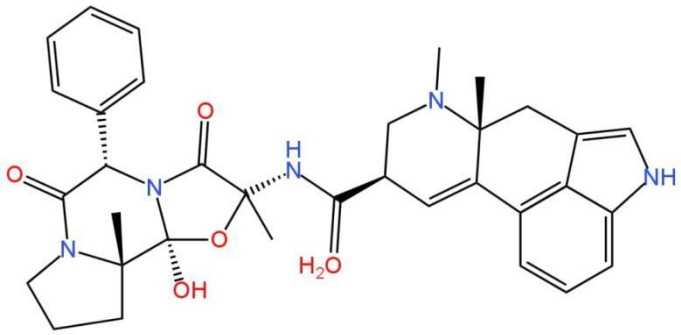

FIGURE 1.1.3: Chemical structure of Ergotamine

Adverse effects include nausea and vomiting, serious risk of ischemic events from potent vasoconstriction. Contraindications include pregnancy and uncontrolled hypertension. Ergot alkaloids are now reserved for patients who do not respond to or cannot take other treatments, requiring careful screening and limited use (Shafqat *et al*., 2020). Triptans are generally preferred over ergotamine for better tolerability (Colman *et al*., 2005).

1.1.4 Triptans

Triptans are considered the gold standard for treating moderate to severe migraines. They act as selective 5-$HT_1B/_1D$ receptor agonists, causing cranial vasoconstriction and inhibiting the release of CGRP and other neuropeptides (Goadsby *et al*., 2002). These drugs, including sumatriptan

and rizatriptan, are available in various oral, subcutaneous, and intranasal forms. Randomized trials show that triptans provide faster and more complete pain relief than NSAIDs or ergot derivatives, with better outcomes when used early in an attack (Derry *et al*., 2014). Shorter-acting triptans like sumatriptan offer rapid relief, while longer-acting options such as frovatriptan help reduce headache recurrence (Dodick *et al*., 2019).

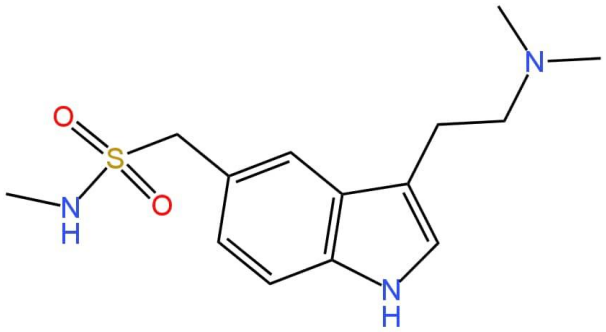

FIGURE 1.1.4: Chemical structure of Sumatriptan

Common side effects are typically mild and include dizziness, tingling sensations, and chest or throat discomfort. Due to their vasoconstrictive effect, triptans are contraindicated in patients with coronary artery disease, stroke, or uncontrolled hypertension. While rare, serious ischemic events can occur. To prevent medication overuse headache, patients should not take triptans more than ten days per month (Tfelt-Hansen *et al*., 2000).

1.1.5 Ditans

Ditans are a new class of acute migraine drugs and as an alternative to triptans. Lasmiditan, the first approved agent, is a selective 5-HT_1F receptor agonist that inhibits trigeminal nociceptive activity and CGRP release without causing vasoconstriction (Goadsby *et al*., 2019). Clinical

studies have shown that Lasmiditan reduces pain and relieve associated symptoms within two hours of dosing, including patients with cardiovascular disease who cannot use triptans.

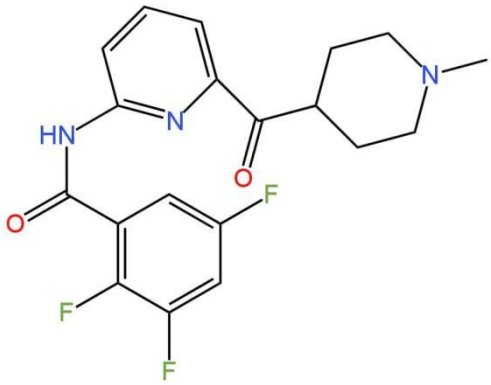

FIGURE 1.1.5: Chemical structure of Lasmiditan

The most common side effects are dizziness, drowsiness, and fatigue. Patients are adviced to avoid driving or operating machinery for at least eight hours after taking a dose (Goadsby *et al*., 2019).

1.1.6 Gepants

Gepants are CGRP receptor antagonists that block the vasodilatory and pro-inflammatory effects of CGRP, interrupting migraine pain pathways (Wang *et al*., 2024; Goadsby *et al*., 2023). They are effective for both acute and preventive treatment. For acute therapy, ubrogepant and rimegepant are oral agents, while zavegepant nasal spray provides rapid relief within 15 minutes (Lipton *et al*., 2023). For prevention, atogepant is approved for episodic and chronic migraine, and rimegepant is unique for dual acute and preventive use (Goadsby *et al*., 2023). Gepants lack vasoconstrictive effects, making them safer for patients with cardiovascular risk (Sacco *et al*., 2023). They are generally well tolerated, with nausea, constipation, fatigue, and, for zavegepant,

distorted taste and nasal discomfort as common side effects. Long-term safety of chronic CGRP blockade remains under investigation (Goadsby *et al*., 2023).

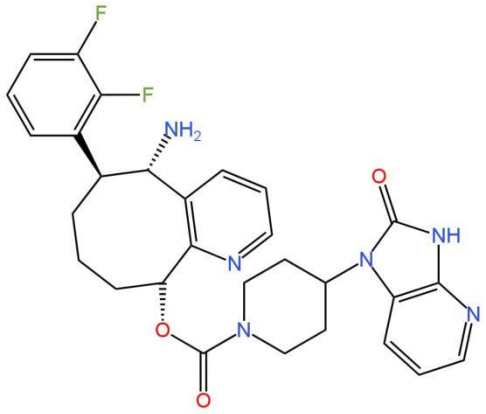

FIGURE 1.1.6: Chemical structure of Rimegepant

1.1.7 Antidepressants

Antidepressants are important in migraine prevention because they modulate serotonergic and noradrenergic pathways involved in pain. They act to modulate pain signaling through enhanced descending inhibition and reduced central sensitization, offering advantage in addition to mood effects (Loder *et al*., 2012). They are clinically recommended as second-line preventive agents, typically after beta-blockers or antiepileptics, but they remain valuable in patients with comorbid depression, anxiety, or insomnia due to their dual therapeutic benefits and low cost (AHS, 2021).

Amitriptyline is primary choice, prescribed at 10–75 mg at night, with effects usually evident after 2–3 months. Its sedative action can improve sleep, but anticholinergic effects, weight gain, and daytime drowsiness often limit use (Silberstein, 2015). Other examples include Venlafaxine, an SNRI, which may reduce migraine frequency and is useful when comorbid psychiatric

symptoms exist. However, nausea, insomnia, and hypertension restrict its use. SSRIs are not recommended (Banzi *et al*., 2015).

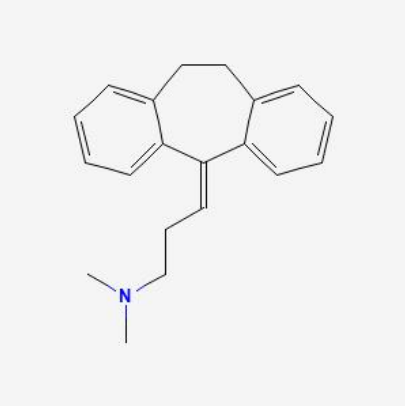

FIGURE 1.1.7: Chemical structure of Amitriptyline

1.1.8 Antiepileptics

Antiepileptics, specifically topiramate and valproate, are first-line options for migraine prevention. These drugs reduce cortical excitability and modulate neurotransmission by enhancing GABA activity, inhibiting voltage-gated sodium and calcium channels, and dampening glutamatergic signaling, thereby limiting cortical spreading depression and trigeminovascular activation (Silberstein, 2015). Topiramate (50–100 mg/day) is clinically used in patients with comorbid obesity due to associated weight loss (Silberstein, 2015). Valproate (500–1500 mg/day) with similar effective is useful in those with comorbid epilepsy or bipolar disorder, though its teratogenicity and metabolic adverse effects restrict its use especially in women of childbearing age (Mathew, 2011).

Common side effects of topiramate include paresthesia, slow thinking, and kidney stones, while valproate presents risks of weight gain, tremor, and hepatotoxicity (Linde *et al*., 2013). Other

antiepileptics, such as gabapentin and lamotrigine, are not recommended for routine migraine prophylaxis due to minimal benefit and inconsistency (Silberstein, 2015)

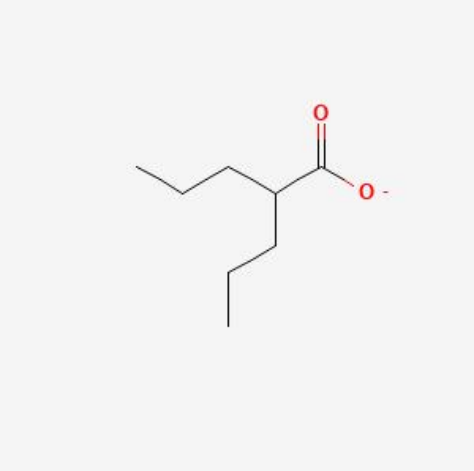

FIGURE 1.1.8: Chemical structure of Valproate

1.1.9 Beta-Blockers

Beta-adrenergic blockers are widely used as first-line therapy for prevention of frequent migraines, particularly in patients with hypertension or anxiety. They have shown good efficacy for migraine prevention and are affordability (Goadsby *et al*., 2017). The exact mechanism of action is not fully understood, but it's believed they work by modulating adrenergic and serotonergic neurotransmission, reducing cortical hyperexcitability, and stabilizing vascular tone. Propranolol and metoprolol commonly used clinically. Treatment typically starts at a low dose and gradually increased, with effects seen within four to six weeks of continuous use (Linde *et al*., 2013).

Common side effects include fatigue, dizziness, sleep disturbance, and reduced exercise tolerance due to decreased sympathetic activity. More serious risks like bradycardia, hypotension, and bronchospasm limit their use. They are contraindicated in patients with asthma, chronic

obstructive pulmonary disease, severe bradyarrhythmia, or decompensated heart failure (Linde *et al*., 2013).

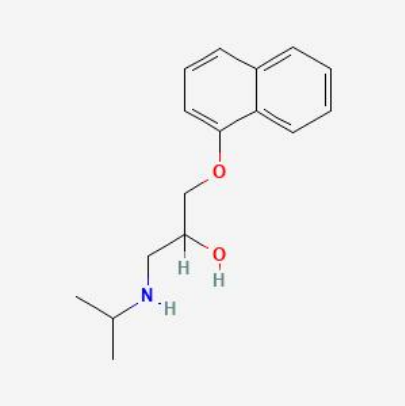

FIGURE 1.1.9: Chemical structure of Propranolol

1.1.10 Monoclonal antibodies

Monoclonal antibodies are newest class of preventive migraine therapies and are used as second-line drugs, typically for patients who fail or cannot take beta-blockers, antiepileptics, or antidepressants (AHS, 2021). They act by targeting the calcitonin gene-related peptide (CGRP) pathway. Agents include erenumab (CGRP receptor blocker), and fremanezumab, galcanezumab, and eptinezumab (CGRP ligand blockers). By inhibiting CGRP signaling, these drugs reduce vasodilation and neurogenic inflammation (Goadsby *et al*., 2020). These therapies are administered via monthly or quarterly subcutaneous or intravenous injections, offering a convenient alternative to daily oral medications. Reductions in monthly migraine days, improved quality of life, and favorable have been seen in conducted clinical studies (Skljarevski *et al*., 2018).

Common side effects include injection-site reactions and constipation, with rare reports of hypersensitivity, minimal drug–drug interactions and no risk of weight gain and sedation. However, high cost and limited long-term safety remain challenges (Ashina *et al*., 2021).

1.1.11 OnabotulinumtoxinA

OnabotulinumtoxinA is approved for prevention of chronic migraine. It is administered every 12 weeks following the Phase III Research Evaluating Migraine Prophylaxis Therapy (PREEMPT) injection protocol and greatly reduces monthly headache days. Common side effects include injection-site pain, neck weakness, and drooping eyelid (Dodick *et al*., 2010).

1.1.12 Non-Pharmacological and Complementary Interventions

Lifestyle modification, which includes regular sleep, hydration, exercise, and trigger avoidance, is the basis of migraine care. Behavioral approaches such as biofeedback and cognitive-behavioral therapy have shown effectiveness in reducing frequency of attack (Nestoriuc *et al*., 2008). Neuromodulation devices such as external trigeminal nerve stimulators, non-invasive vagus nerve stimulators, and transcranial magnetic stimulators are alternative therapies for patients not responding to medication (Puledda *et al*., 2020). Nutritional supplements such as magnesium, riboflavin, coenzyme Q10, feverfew, and butterbur also show preventive benefit, although concerns about standardization and safety remain (Holland *et al*., 2012).

1.2 MEDICINAL PLANTS IN MIGRAINE MANAGEMENT

Traditional medicine systems in Africa, Asia, and Europe have described various plants with claimed activity against headache and migraine-like syndromes. Modern research has attempted

to validate these ethnomedicinal claims, elucidate their pharmacological basis, and isolate bioactive constituents implicated in migraine pathophysiology (Rajapakse and Davenport, 2019).

Examples of medicinal plants traditionally used for migraine treatment and management include *Petasites hybridus* (Butterbur) and *Tanacetum parthenium* (Feverfew), which have been scientifically validated for migraine prophylaxis, as well as *Crassocephalum crepidioides* (Ebolo, Thickhead), and *Nigella sativa* (Black seed) which are traditionally used for managing headache and migraine symptoms but remain largely unexplored at the molecular level (Moscano *et al*., 2019). *Petasites hybridus* has been shown to inhibit CGRP release from trigeminal afferents through modulation of TRPA1 and TRPV1 receptor channels (Kleeberg-Hartmann *et al*., 2021) while *Tanacetum parthenium* exhibits anti-inflammatory and neuromodulatory effects and its principal compound parthenolide has been shown to modulate TRPA1 channels (Materazzi *et al*., 2013). However, their molecular interactions with the CGRP receptor, and serotonin receptors, remain unexplored. There is currently no molecular or computational evidence confirming their anti-migraine activity or elucidating their mechanisms of action of phytochemicals from *Crassocephalum crepidioides* and *Nigella sativa*. This gap limits the integration of these plants into evidence-based migraine therapeutics.

Through *in-silico* analysis of phytochemicals derived from these four selected medicinal plants against migraine-associated molecular targets, traditional medicinal knowledge with computational pharmacology can reveal novel bioactive compounds.

1.2.1 Crassocephalum crepidioides (Benth) Asteraceae

Crassocephalum crepidioides (Benth.) S. Moore, also known as thickhead, belongs to the Asteraceae family, which comprises about 1,600 genera and over 23,000 species worldwide

(Baldwin, 2009). The genus Crassocephalum consists of approximately 24 species, many of which are edible leafy vegetables or medicinal herbs (Adebayo *et al*., 2013)

It is native to tropical Africa but widely distributed and naturalized in Asia, particularly in tropical and subtropical regions such as India, China, Malaysia, and Indonesia (Ogunlesi *et al*., 2010; Liu *et al*., 2010). In Nigeria and West Africa, it is cultivated as a traditional leafy vegetable and is abundant in-home gardens. The plant is commonly referred to as Ebolo or Gbolo (Yoruba), Worowo (Igbo), Ebodu (Edo state), and Thickhead (English) (Ogunlesi *et al*., 2010; Adebayo *et al*., 2013).

Crassocephalum crepidioides is an erect, annual herbaceous plant that can grow up to 1–1.8 metres tall, depending on location and soil conditions (Liu *et al*., 2010). The stems are soft, fleshy, and slightly succulent with mucilaginous sap. The leaves are alternate, simple, and vary in shape from ovate to lyrate-pinnatifid, with irregularly serrated margins; they are green in colour and slightly succulent to touch (Adebayo *et al*., 2013). The inflorescence is a nodding capitulum with orange to red tubular florets surrounded by involucral bracts, bearing a conspicuous white pappus that aids in wind dispersal of seeds (Frontiers, 2019). The plant produces flowers and fruits almost all year round in suitable environment, particularly in the most soil and distributed lands. The seeds are small and lightweight, easily dispersed by wind, allowing the species to colonize rapidly (Frontiers, 2019).

FIGURE 1.2.1 fresh leaves of *Crassocephalum crepidioides*

1.2.1.1 Trado-Medical Uses of Crassocephalum crepidioides

Crassocephalum crepidioides (Ebolo, Thickhead) has been traditionally used across tropical Africa, particularly in Nigeria, for the treatment of wounds, burns, indigestion, stomachache, headache and ulcers (Ajao *et al*., 2018). The leaves and stems are also widely consumed as vegetables, incorporated into soups and stews in West and Central Africa, and are regarded as a common leafy food plant in both rural and urban communities (Ugwu *et al*., 2016). The leaf extract has also been shown to promote wound healing in excision wound models, supported by its antioxidant and anti-inflammatory activity (Osuala *et al*., 2019).

Crassocephalum crepidioides has been found to accumulate pyrrolizidine alkaloids such as jacobine, which are hepatotoxic and tumorigenic, thus raising safety concerns regarding its uncontrolled use (Ngokere *et al*, 2019).

1.2.1.2 Phytochemical Constituents of *Crassocephalum crepidioides*

Crassocephalum crepidioides contains a variety of phytochemicals, including saponins, tannins, reducing sugars, flavonoids, alkaloids, steroids, hydrogen cyanides, glycosides, terpenoids, fats

and oils, balsams, free anthraquinones, and soluble carbohydrates (Achi *et al*. 2017; Esievo, Onuche, and Fatokun 2018; Nawaz 2020).

Gas chromatography-mass spectrometry (GC-MS) analysis of the ethanol extract from *Crassocephalum crepidioides* has identified several isolated compounds, including heptanoic acid, 2,2-dimethyl butane, 5-cyclomethylidadiene, hepta-3,5-dien-1-ol, hepta-1,3-dien-1-ol, hepta-1,5-diene-1-ol, hepta-2,4,6-trienoic acid, oct-1,5-dien-1-ol, n-hexadecanoic acid, glycerine, tetradecanoic acid, 4-(2,6,6-trimethylcyclohexa-1,3-dienyl)but-3-en-2-one, 3-acetoxy-4-cyano-2,5-dimethylpyridine, pentadecanoic acid, 11-octadecanoic acid, nanodecanoic acid, octadecanoic acid, 13-docosenamide, methyl ester, and Z,11-hexadecanoic acid (Akachukwu and Uchegbu, 2016).

1.2.2 *Nigella sativa* (Linn) Ranunculaceae

Nigella sativa L., commonly known as black seed or black cumin, belongs to the family Ranunculaceae which comprises about 60 genera and over 2,000 species (Woo *et al*., 2024). The plant is indigenous to Southwest Asia, the Middle East, and North Africa, and can also be cultivated in West Africa and Nigeria (Elhariri *et al*., 2024). In Nigeria and other West African countries, the seeds are popularly used as spice, condiment, and medicine, and are locally called “Habbatul barakah” or “Habbatus-sauda” (Arabic/Hausa), “Black seed” (English), and sometimes “Girin-girin” (Hausa) (Abdulelah and Zainal-Abidin, 2007).

Nigella sativa is an annual herb that grows about 20–30 cm tall with finely divided leaves and pale blue to white flowers; the fruits are capsule-like follicles containing angular black seeds with a characteristic aroma (Woo *et al*., 2024).

FIGURE 1.2.2 Dry seeds of *Nigella sativa*

1.2.2.1 Trado-Medical Uses of Nigella sativa

N. sativa seeds play an important role in the traditional treatment of various diseases, especially fever, chronic headache, migraine, hypertension, and paralysis. Additionally, the extracts of *N. sativa* are traditionally used as a laxative, intestinal antiprotozoal agent, and carminative (Mashayekhi-Sardoo H, *et al*.) The seeds are used in folk medicine in Nigeria for the management of cough, asthma, hypertension, and diabetes, and as an immune booster (Elhariri *et al*., 2024).

1.2.2.2 Phytochemical Constituents of Nigella sativa

Nigella sativa possesses a wide spectrum of phytochemicals, including alkaloids, phenolic compounds, flavonoids, tannins, saponins, terpenoids, anthraquinones, glycosides, essential fatty acids, proteins, amino acids, reducing sugars, mucilage, resins, crude fiber, vitamins, and minerals (Saleh *et al*. 2018; Ravi *et al*. 2024; Rahman *et al*. 2024).

Gas chromatography–mass spectrometry (GC-MS) of the ethanol and methanol extracts of *Nigella sativa* revealed the presence of several compounds, including thymoquinone,

thymohydroquinone, dithymoquinone, thymol, carvacrol, p-cymene, trans-anethole, terpineol, α-pinene, longifolene (Saleh *et al*., 2018; Rahman *et al*., 2024).

1.2.3 Petasites hybridus (Linn) Asteraceae

Petasites hybridus (Linn.) G. Gaertn., B. Mey. and Scherb., known as butterbur, belongs to the Asteraceae family which has over 1,600 genera and more than 23,000 species (Andres *et al*., 2005). The genus Petasites consists of about 18 perennial species found mainly in temperate Europe and Asia. The name is derived from the Greek petasos, meaning broad hat, in reference to its large leaves (Andres *et al*., 2005).

Petasites hybridus is indigenous to Europe and parts of Asia and can also be cultivated in West Africa and Nigeria. It is a perennial rhizomatous herb that can grow up to 1 m tall, with very large reniform basal leaves (40–90 cm wide) and stout flowering stems bearing dense clusters of purple-pink florets which appear in spring before the leaves (Andres *et al*., 2005).

FIGURE 1.2.3: Leaves of *Petasites hybridus*

1.2.3.1 Trado-Medical Uses of Petasites hybridus

Petasites hybridus (butterbur) has been traditionally used in Europe for the management of wounds, coughs, asthma, fever, and urinary disorders (Frei *et al*., 2015; Lipton *et al*., 2004). Extracts from the rhizomes and leaves have also been used as herbal teas or decoctions (Roeder and Wiedenfeld, 2013). Rhizomes and leaves are used in herbal medicine for migraine prophylaxis, asthma, and allergic rhinitis. The active sesquiterpene esters petasin and isopetasin are reported to inhibit leukotriene synthesis and smooth muscle spasm (Grossmann, 2011). However, the plant also contains hepatotoxic pyrrolizidine alkaloids, and only standardized PA-free extracts are considered safe for medicinal use (Andres *et al*., 2005; Grossmann, 2011).

1.2.3.2 Phytochemical Constituents of Petasites hybridus

Petasites hybridus contains sesquiterpene esters, flavonoids, essential oils, bitter substances, mucilage, and pyrrolizidine alkaloids (Grossmann, 2011; Halbsguth *et al*. (2025).

Gas chromatography–mass spectrometry (GC–MS) and phytochemical studies of *Petasites hybridus* rhizomes and leaves revealed the presence of petasin, isopetasin, neopetasin, S-petasin, iso-S-petasin, furanopetasins, oxopetasins, petasol, nepetasol, neopetasol, furanoeremophilanes, eremophilanolides, bakkenolides, senecionine, integerrimine, senkirkine, as well as flavonoids and phenolic acids. These constituents have been identified as the major bioactive compounds of the plant (Halbsguth *et al*., 2025).

1.2.4 Tanacetum parthenium (Linn.) Asteraceae

Tanacetum parthenium (Linn.) Sch. Bip., commonly called feverfew, is a member of the Asteraceae family. The genus Tanacetum includes about 160 species distributed across Europe and Asia (Pareek *et al*., 2011).

The plant is indigenous to the Balkans and the Caucasus region and can also be cultivated in West Africa and Nigeria. *Tanacetum parthenium* is a bushy perennial herb about 30–70 cm tall, with strongly aromatic pinnatifid leaves and small daisy-like flower heads, each about 2 cm in diameter, with yellow disc florets surrounded by white ray florets (Pareek *et al*., 2011).

FIGURE 1.2.4: Leaves of *Tanacetum parthenium*

1.2.4.1 Trado-Medical Uses of *Tanacetum Parthenium*

Tanacetum parthenium (feverfew) has been traditionally used in Europe and the Mediterranean for the treatment of fever, stomachache, menstrual disorders, toothache, insect bites, and headaches (Pareek *et al*., 2011). The fresh or dried leaves are sometimes consumed directly, brewed as tea, or added to food as an herbal remedy (Pareek *et al*., 2011).

1.2.4.2 Phytochemical Constituents of *Tanacetum parthenium*

Tanacetum parthenium contains sesquiterpene lactones, flavonoids, volatile oils, and other constituents including camphor and pinenes. These phytochemicals have been associated with the anti-inflammatory, anticancer, cardiotonic, and antispasmodic properties of the plant (Majdi *et al*. 2015; Al-Snafi 2021).

Gas chromatography–mass spectrometry (GC–MS) and phytochemical investigations of *Tanacetum parthenium* have revealed more than 30 sesquiterpene lactones such as parthenolide, artecanin, artemorin, balchanin, canin, reynosin, santamarine, costunolide, 1β-hydroxyarbusculin, magnoliolide, chrysartemin A, chrysartemin B, 3β-hydroxyparthenolide, secotanaparthenolide A, 8α-hydroxy-10α-(H)1,4,5,6,7,11b-hexahydro-12H-benzocyclodecen-9(8aH)-one, 9α-hydroxyparthenolide, 9β-hydroxyparthenolide, and parthenolide-3β,9α-epoxide. Other sesquiterpene lactones include eudesmanolides, germacranolides, and guaianolides, with parthenolide recognized as the main bioactive germacranolide (Pareek *et al*., 2011; Majdi *et al*., 2015).

1.3 Molecular Docking Studies

Molecular docking is a computational technique that involves fitting a ligand into the binding site of a target molecule. This process optimizes and combines various factors such as steric, hydrophobic, and electrostatic complementarity. The primary goal of molecular docking is to predict the framework of interactions between a protein and a ligand, as well as to estimate the free energy associated with their binding (Sethi et al., 2019). The technique involves placing a molecule (ligand) into the preferred binding site of a specific region of DNA or protein

(receptor), primarily through non-covalent interactions, to form a stable complex that possesses potential efficacy and greater specificity (Dar and Mir, 2017).

Docking is typically the initial step in the identification of active compounds from an existing pool of chemicals within drug discovery projects. It categorizes biomolecules into ligands, proteins, and nucleic acids, leading to three main types of docking systems: protein-ligand, protein-protein, and nucleic acid-protein interactions (Wang and Zhu, 2016). Molecular docking serves as a valuable approach for understanding drug-biomolecular interactions. It is used to facilitate rational drug design and discovery, as well as mechanistic studies

Knowledge of the binding site prior to docking significantly increases the efficiency of the docking process. Such information is often obtained from proteins that have been co-crystallized with similar ligands (Meng et al., 2012). Results from docking studies provide insights into the binding energy and stability of the complexes formed. These predictions help determine the binding affinity between a ligand and a protein, the structure of the protein-ligand complex, and the activity of the ligand (Prakash, 2010; Wang and Zhu, 2016; Dar and Mir, 2017)

Structures of various compounds used in molecular docking are available from several databases, including Drug Bank, ZINC, Chem ID, ChemBank, PDB Bind, PubChem, Asinax, and the Cambridge Structural Database (CSD) (Hwa, Chaudhary and Mishra, 2016; Dar and Mir, 2017).

1.3.1 Molecular Docking Models

Various molecular docking models have been introduced and they include:

Lock and Key Model- This was introduced in 1890 by Emil Fischer; the substrate here is expected to fit into the reactive site of the macromolecule (receptor/protein) just like a key fit in a lock. It is also known as the rigid model (Tripathi and Misra, 2020).

- Induced Fit Model- This model was introduced by Daniel Koshland in 1958, also known as flexible docking. Here, both ligand and protein target are to mutually adapt to each other using small conformational changes till an optimal fit is achieved; both ligand and receptor are flexible thus the ligand binds flexibly to the active site of the receptor (Tripathi and Misra, 2020).
- Conformation Ensemble Model- This model recognizes that proteins may undergo larger conformational changes due to their nature of plasticity which allows it to change from one state to another.

1.3.2 Docking Methods According to Flexibility Modelling

- Rigid ligand and rigid receptor docking- Here, the receptor and ligand are treated as inflexible bodies; examples of docking programs used include FTDOCK and FLOG (Meng *et al.*, 2012).
- Flexible ligand and rigid receptor docking- The ligand used here is flexible while the receptor is kept rigid during docking; docking programs used here include AutoDock, FlexX and Autodock Vina (Meng *et al.*, 2012).
- Flexible ligand and flexible receptor docking- Glide can be used as a docking program here (Meng *et al.*, 2012).

1.3.3 Docking Process

Docking involves 3 processes namely:

- Ligand preparation; where duplicate structures are removed (Roy, Kar and Das, 2015).
- Protein preparation; where hydrogen atoms are added, protein minimized, charges and atoms are set properly and other modifications done (Roy, Kar and Das, 2015).
- Ligand-protein docking- A grid box can be generated at the centroid of the ligand bound to the receptor's active site or the active pockets of the protein can be found to dock the prepared ligand. The interaction energy is then compared with that of the bound ligand of the crystallized protein structure so as to assess the degree of fit into the receptor (Roy, Kar and Das, 2015).

1.3.4 Docking Software

Examples of docking software include (Roy, Kar and Das, 2015):

- Autodock- A suite which predicts the way small molecules (that is, drug candidates or substrates) bind to a receptor of a known 3-dimensional structure.
- Discovery Studio
- Dock- A program which examines possible binding orientations of protein-protein and protein-DNA complexes.
- Glide- A fast and accurate docking program.
- Q Site- Docking program with very accurate calculations of the energy of protein-ligand interactions in the active site.

Molecular docking can be applied in lead optimization, hit identification, prediction of Drug-DNA interaction, protein engineering and binding site prediction (Hwa, Chaudhary and Mishra, 2016; Dar and Mir, 2017). Currently marketed drugs using the structure based drug design-docking study include Captopril and Indinavir (Roy, Kar and Das, 2015).

For this research, molecular docking approaches will be used in evaluating and determining the mode of action of the phytochemical constituents present in these medicinal plants which have been reported to possess anti-migraine effect by screening these phytochemicals against known targets.

1.4 Aim and Objectives

This study aims to use *in-silico* methods to assess the potential anti-migraine activity of phytoconstituents derived from *Crassocephalum crepidioides, Nigella sativa, Petasites hybridus* and *Tanacetum parthenium.*

1.4.1 Specific Objectives

The specific objectives were to:

1. Obtain phytoconstituents reported from *Crassocephalum crepidioides, Nigella sativa, Petasites hybridus* and *Tanacetum parthenium.*
2. Obtain the protein targets associated with migraine from protein data bank.
3. Carry out molecular docking studies of the phytoconstituents against migraine-relevant protein targets (5-HT1B/1D, 5-HT1F, and CGRP receptor complex).
4. Carry out post-docking analysis of the protein-ligands complex.
5. Determine the Absorption, Distribution, Metabolism, Excretion, Toxicity (ADMET) properties of selected ligands.

CHAPTER 2

MATERIALS AND METHODS

2 MATERIALS AND METHODS

2.1 Materials

2.1.1 RCSB PDB

The Research Collaboratory for Structural Bioinformatics (RCSB) Protein Data Bank (PDB) is an open-access resource for experimentally determined three-dimensional structures of biological macromolecules, including proteins, nucleic acids, and large complexes. Advances in cryo-electron microscopy, integrative and computational modeling have significantly improved the quantity and quality of ligand-bound, active-state GPCR and receptor–effector complex structures in the PDB, making structural data essential for research and drug discovery (Burley, 2022; Parajulee, 2023). These developments enable researchers to combine high-resolution structures with functional pharmacology to explain how ligands engage receptors, how subtle sequence and loop differences drive subtype selectivity, and how receptor conformations bias downstream signaling understandings that are directly relevant to rational design of antimigraine drugs (Burley, 2022; Tan *et al*., 2022).

2.1.1.1 Serotonin 5-HT$_1$B Receptor

The activated 5-HT$_1$B receptor bound to donitriptan and coupled to a G protein has been used as a central structural template for understanding activation mechanics in the 5-HT$_1$ subfamily (PDB ID: 6G79). Using those recent syntheses as the interpretive framework preserves the

original mechanistic points about donitriptan's binding mode while incorporating updated insight into how receptor microenvironments and conserved microswitches control activation (Parajulee, 2023; Tan *et al*., 2022).

FIGURE 2.1.1.1: Coupling specificity of heterotrimeric Go to the serotonin 5-HT1B receptor(6G79).

2.1.1.2 Serotonin 5-HT$_1$D Receptor

High-quality structural data for 5-HT$_1$D (PDB ID: 7E32) now provide a reliable template for the orthosteric pocket and intracellular G-protein interface that improves docking and mutational interpretation relative to older homology models (Parajulee, 2023). Although a structure of 5-HT$_1$D co-crystallized with sumatriptan has not yet been reported, recent structural frameworks allow modern docking and functional assays to model and test sumatriptan interactions with much greater precision than earlier computational work. (Parajulee, 2023).

FIGURE 2.1.1.2: Serotonin 1D (5-HT1D) receptor-Gi protein complex

2.1.1.3 Serotonin 5-HT$_1$F Receptor

The structural basis of Lasmiditan's selectivity for the 5-HT$_1$F subtype is now defined by cryo-EM structures showing Lasmiditan bound within the orthosteric pocket and stabilizing an active, G-protein-coupled conformation (PDB ID: 7EXD). These structures explain the unique ligand–residue contacts responsible for 1F selectivity and are the most direct mechanistic sources for why Lasmiditan avoids vasoconstrictive off-targets while retaining clinical antimigraine efficacy (Huang *et al*., 2021; Parajulee, 2023).

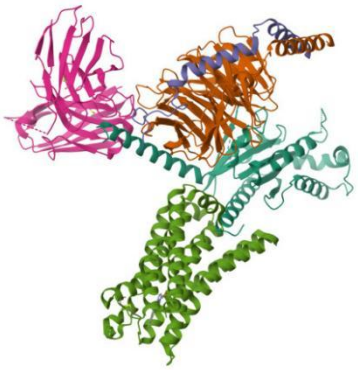

FIGURE 2.1.1.3: Lasmiditan-bound serotonin 1F (5-HT1F) receptor-Gi protein complex

2.1.1.4 CGRP (CLR + RAMP1) Receptor

Mechanistic and clinical literature over the last few years has clarified how small-molecule gepants (for example rimegepant, atogepant, ubrogepant) antagonize the CGRP receptor: by occupying or allosterically disrupting sites formed at the CLR–RAMP1 interface and thereby preventing CGRP peptide binding and receptor activation (PDB ID: 6E3Y) (Edvinsson, 2024; Aoh, 2024). Recent reviews summarize how gepants inhibit peptide-receptor interactions and stabilize inactive receptor states, and they integrate these molecular mechanisms with clinical efficacy and safety data emerging from trials and real-world use (Edvinsson, 2024; Aoh, 2024). Recent analyses also emphasize tissue-dependent expression of receptor subunits and vascular heterogeneity, clarifying why antagonist effects may vary across vascular beds and clinical contexts (Edvinsson, 2024; Younis, 2024).

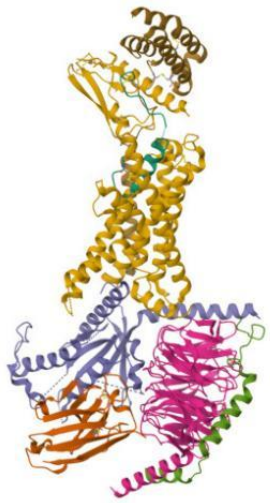

FIGURE 2.1.1.4: Cryo-EM structure of the active, Gs-protein complexed, human CGRP receptor.

2.1.2 PyRx

PyRx is an open-source virtual screening software widely used in computational drug discovery. It allows researchers to perform high-throughput screening of compound libraries against potential drug targets, making it a valuable tool in Computer-Aided Drug Design (CADD) workflows (Dallakyan and Olson, 2015; James *et al*., 2023). PyRx integrates multiple programs within a unified graphical user interface, simplifying the workflow from ligand preparation to docking analysis.

PyRx utilizes several plug-in software components, including:

- AutoDock Vina, which serves as the docking engine for screening multiple ligands against a target macromolecule with high computational efficiency (Trott and Olson, 2010; Eberhardt *et al*., 2021).
- Open Babel, which is used for importing molecular structures in formats such as Structure Data Format (SDF), performing energy minimization, and converting ligands to a dockable format — typically PDBQT, which contains information on partial charges (Q) and atom types (T) (O'Boyle *et al*., 2011; Banerjee *et al*., 2022).
- Python, which serves as the core scripting and programming language that supports the PyRx interface and automation tools (van Rossum and Drake, 2009).

Together, these components make PyRx a powerful and accessible platform for virtual screening, molecular docking, and early-stage drug discovery studies (James *et al*., 2023).

2.1.3 PyMOL

PyMOL is a molecular visualization software used for three-dimensional (3D) visualization of proteins, nucleic acids, and other macromolecules. Through the integration of various plug-ins, it

can also be employed for macromolecular analysis, pharmacophore and homology modeling, protein–ligand docking, and other molecular simulations (Schrödinger, LLC, 2023; Mahmud *et al*., 2022). PyMOL was utilized in this study to identify the binding or active site amino acid residues of the receptor proteins prior to conducting target-directed molecular docking.

2.0.4 Biovia Discovery Studio 2020

BIOVIA Discovery Studio 2020 is an integrated software suite used for molecular modeling, pharmacophore generation, quantitative structure–activity relationship (QSAR) analysis, and various in silico simulations in computational drug discovery (Dassault Systèmes, 2020; Li *et al*., 2021). The software provides an interactive visual interface for analyzing and interpreting protein–ligand interactions, predicting binding affinities, and evaluating structural conformations. In this study, Discovery Studio was employed to view and analyze the active or binding sites, inspect ligand conformations, and visualize the docking poses and binding interactions of each ligand with the target receptor (Zhao *et al*., 2023).

2.1.4 ADMETlab 3.0

ADMETlab 3.0 is a freely accessible web-based platform designed for the comprehensive prediction of ADMET (Absorption, Distribution, Metabolism, Excretion, and Toxicity) properties, physicochemical parameters, and drug-likeness of small molecules, thereby facilitating computer-aided drug discovery and development (Fu *et al*., 2024). The platform integrates advanced AI models to predict 119 pharmacokinetic and toxicity parameters with improved accuracy and reliability (Fu *et al*., 2024; Liu *et al*., 2022). ADMETlab 3.0 enables researchers to evaluate candidate molecules for crucial pharmacokinetic properties such as oral bioavailability, blood–brain barrier permeability, cytochrome P450 enzyme interactions, and

various toxicity parameters, including hepatotoxicity and cardiotoxicity, which are essential for early-stage drug design and optimization (Fu *et al*., 2024; Xu *et al*., 2024).

2.2 METHODS

2.2.1 Identification and Preparation of Protein Target

The target receptors used for this study; serotonin 5-HT$_1$B, 5-HT$_1$D, 5-HT$_1$F, and CGRP receptors were identified and retrieved from the RCSB PDB. All receptor structures were prepared using BIOVIA Discovery Studio 2020 and PyMOL, where heteroatoms, water molecules, and unwanted chains were deleted. The structures were then energy-minimized, hydrogen atoms were added, and partial charges were assigned to optimize each receptor's geometry for molecular docking analysis. The refined protein structures were subsequently saved in PDB format for further computational studies (Dassault Systèmes, 2020; Zhao *et al*., 2023).

2.2.2 Identification and Preparation of Ligands

Compounds from the selected medicinal plants were retrieved from the PubChem database (Kim *et al*., 2023) in Structure Data File (SDF) format. The downloaded compounds were then imported into PyRx 0.8 software using the Open Babel plug-in, where they were subjected to energy minimization to obtain the most stable conformations. The Universal Force Field (UFF) and Steepest Descent algorithm were applied during optimization to reduce steric strain and ensure accurate docking geometry. Following minimization, all ligand structures were converted to PDBQT format, which is compatible with AutoDock Vina-based docking protocols. The optimized ligands were subsequently saved for molecular docking simulations against the prepared receptor targets (Olawale *et al*., 2023; Dallakyan and Olson, 2015).

2.2.3 Identification of Binding Site

The active/binding amino acid residues of the receptors were identified using PyMOL molecular visualization software (Yuan, Chan, and Hu, 2017). This was possible because the 5-HT_1B receptor (6G79) is co-crystallized with the triptan agonist donitriptan, the 5-HT_1F receptor (7EXD) is co-crystallized with the anti-migraine drug lasmiditan, and the CGRP receptor (6E3Y) is co-crystallized with the native CGRP peptide. Visualization of these co-crystallized complexes in PyMOL enabled the identification of the specific amino acid residues constituting the active/binding sites used for docking studies.

For the 5-HT_1D receptor, which was not co-crystallized with a ligand, the identification of potential active or binding site residues was performed through literature-based structural analysis. The amino acid residues constituting the proposed binding pocket were identified using insights derived from recent structural studies on the serotonin receptor family (Wang *et al*., 2023).

The amino acid residues identified using PyMOL for the receptors that were co-crystallized with their respective ligands were confirmed using published structural analyses.

2.2.4 Molecular Docking and Post-docking Analysis

The protein targets that were previously prepared and saved in PDB format were loaded into PyRx and designated as macromolecules, while all ligands from each plant, including both natural products and their metabolites, were imported into the platform. The binding amino acid residues on the macromolecules were identified and labeled, and molecular docking was performed using the AutoDock Vina plugin, with the grid boxes positioned over the respective

binding residues. Docking simulations were executed at an exhaustiveness of 8 to ensure adequate conformational sampling.

For each plant, all ligands were docked against each protein target, and the binding affinities were obtained. Ligands exhibiting binding affinities equal to or more favorable than those of the respective standard ligands were selected for further receptor–ligand interaction analysis. The binding conformations of the selected ligands for each protein target were subsequently saved from PyRx in PDB format for detailed visualization and evaluation.

The interactions between the identified amino acid residues and the selected ligands were then analyzed using BIOVIA Discovery Studio Visualizer 2020. Both three-dimensional and two-dimensional analyses were performed to visualize the binding models of each ligand and to identify those with the highest potential for anti-migraine activity**.**

2.2.5 ADMET Profiling

Ligands that exhibited binding affinities equal to or more favorable than the respective standard ligands for each protein target were selected for ADMET profiling. The SMILES notation of each selected ligand was obtained and used to evaluate their pharmacokinetic properties using the ADMETlab 3.0 web server. Ligands that did not violate any of Lipinski's rule of five were selected.

CHAPTER THREE

RESULT

3 Binding Site Amino Acids

The binding site amino acids identified with the aid of PyMOL and through literature-based structural analysis are:

Table 3.0: Binding site amino acids identified in 6G79, 7E32, 7EXD and 6E3Y

6G79 (5-HT 1B)	7E32 (5-HT 1D)	7EXD (5-HT 1F)	6E3Y (CGRP)
TYR75	ASP118	ASP103	THR191
ASP129	ILE119	ILE104	LEU195
ILE130	CYS122	CYS107	HIS219
CYS133	SER201	ILE174	MET223
THR134	ALA205	HIS176	TYR227
VAL200	TRP314	THR182	TRP283
VAL201	PHE317	SER185	ILE284
THR203	PHE318	TRP306	SER286
TRP327	SER321	PHE309	ASP287
PHE330	TYR346	PHE310	HIS295
PHE331		GLU313	ILE298
SER334		ASN317	LEU302
MET337		TYR337	ASP366
PHE351			
TYR359			

3.1 Molecular Docking Analysis

Compounds from *Crassocephalum crepidioides, Nigella sativa, Petasites hybridus,* and *Tanacetum parthenium* all showed varying degrees of binding affinities for the protein targets (6G79, 7E32, 7EXD, and 6E3Y); this is shown in **Tables 3.1.1 – 3.1.4**.

3.1.1 Crassocephalum crepidioides

Four (4) standard/control ligands, marked with asterisks (*), bound with different affinities to their respective target proteins, and Sixteen (16) compounds interacted with one or more of the target proteins, exhibiting varying binding affinities, as shown in **Table 3.1.1**. The various binding models/ interaction with the binding site amino acids in 3D and 2D views can also be seen in **Figure 3.1.1.1, Figure 3.1.1.2, and Figure 3.1.1.3.**

3.1.2 Nigella sativa

Four (4) standard/control ligands, marked with asterisks (*), bound with different affinities to their respective target proteins, and twenty eight (28) compounds interacted with one or more of the target proteins, exhibiting varying binding affinities, as shown in **Table 3.1.2**. The various binding interaction of each ligand with the binding site amino acids in 3D and 2D views can be seen in **Figure 3.1.2.1, Figure 3.1.2.2, and Figure 3.1.2.3.**

3.1.3 Petasites hybridus

Four (4) standard/control ligands, marked with asterisks (*), bound with different affinities to their respective target proteins, and forty seven (47) compounds interacted with one or more of the target proteins, exhibiting varying binding affinities, as shown in **Table 3.1.3**. The various

binding interaction of each ligand with the binding site amino acids in 3D and 2D views can be seen in **Figure 3.1.3.1, Figure 3.1.3.2, and Figure 3.1.3.3.**

3.1.4 Tanacetum parthenium

Four (4) standard/control ligands, marked with asterisks (*), bound with different affinities to their respective target proteins, and forty three (43) compounds interacted with one or more of the target proteins, exhibiting varying binding affinities, as shown in **Table 3.1.4**. The various binding interaction of each ligand with the binding site amino acids in 3D and 2D views can be seen in **Figure 3.1.4.1, Figure 3.1.4.2, Figure 3.1.4.3, and Figure 3.1.4.4.**

Table 3.1.1: Binding affinities of *Crassocephalum crepidioides* compounds with 6G79, 7E32, 7EXD, and 6E3Y

Compounds	Compound Cid	6G79 ΔG (Kcal/mol)	7E32 ΔG (Kcal/mol)	7EXD ΔG (Kcal/mol)	6E3Y ΔG (Kcal/mol)
Donitriptan*	197706	-9.2			
Sumatriptan*	5358		-6.9		
Lasmiditan*	11610526			-9.8	
Rimegepant*	51049968				-9.1
[(1S,2S,3E,5R,7E,11R)-8-formyl-5-[(E)-4-hydroxy-4-methylpent-2-enyl]-1,5-dimethyl-12-oxabicyclo[9.1.0]dodeca-3,7-dien-2-yl]3-methylbut-2-enoate	162897130	-9.2			
2-[(1S,2R,3S,9S,11S)-11-methoxy-3,9-dimethyl-3-(4-methylpent-3-enyl)-8,12-dioxatricyclo[7.2.1.01,6]dodec-5-en-2-yl]ethenyl3-methlbut-2-enoate	162889473	-9.2			
Vibsanin T	11441439	-9.4			
(1S,4S,5R,8R,13S,14R,17S,18R)-4,5,9,9,13,20,20-heptamethyl-24 oxahexacyclo[15.5.2.01,18.04,17.05,14.08,13]tetracos-15-en-10-one	15385431	-9.4			

[(E)-2-[(1S,5S,7R,8S,11S)-8-methyl-5-(2-oxopropyl)-11-prop-1-en-2-yl-4-oxatricyclo[6.3.1.02,6]dodec-2(6)-en-7-yl]ethenyl] 3-methylbut-2-enoate	11188728	-9.4		
7-but-2-enyl-6,8-dihydroxy-3-pent-3-enyl-3,4-dihydroisochromen-1-one	73814489		-7.3	
2-(4-hydroxy-3-methoxyphenyl)-3-(hydroxymethyl)-5-[(E)-3-hydroxyprop-1-enyl]-1-benzofuran-7-ol	10246758		-7.0	
2-[(3aS,5R,8aR)-3-methyl-8-methylidene-3a,4,5,6,7,8a-hexahydro-1H-azulen-5-yl]propan-2-ol	10656574		-7.4	
[(2R,3R,4S,5R,6S)-3,5-dihydroxy-2-(hydroxymethyl)-6-(6-methoxy-2-oxochromen-7-yl)oxyoxan-4-yl] acetate	162902217		-7.1	
2-[(3R,3aR,5S,8aS)-3-hydroperoxy-3-methyl-8-methylidene-3a,4,5,6,7,8a-hexahydroazulen-5-yl]propan-2-ol	162915438		-7.6	
[(2R,3S,4S,5R,6S)-5-acetyloxy-3,4-dihydroxy-6-(6-methoxy-2-oxochromen-7-yl)oxyoxan-2-yl]methyl acetate	21636119		-7.0	
[(2R,3R,4S,5R,6S)-4-acetyloxy-3,5-dihydroxy-6-(6-methoxy-2-oxochromen-7-yl)oxyoxan-2-yl]methyl acetate	21636120		-7.0	
Scopolin	439514		-7.1	
7-butyl-6,8-dihydroxy-3-pent-3-enyl-3,4-dihydroisochromen-1-one	73814488		-7.0	
Neovibsanin I	10788065			-10
[(E)-2-[(4S,6S,7S,8S,11R,15S)-4-methoxy-4,8,12,12-tetramethyl-3,13-dioxatetracyclo[6.6.2.02,6.011,15]hexadec-	12068760			-10.1

1-en-7-yl]ethenyl]3-methylbut-2-enoate

Table 3.1.2: Binding affinities of *Nigella sativa* compounds with 6G79, 7E32, 7EXD, and 6E3Y

Compounds	Compound Cid	6G79 ΔG (Kcal/mol)	7E32 ΔG (Kcal/mol)	7EXD ΔG (Kcal/mol)	6E3Y ΔG (Kcal/mol)
Donitriptan*	197706	-9.2			
Sumatriptan*	5358		-7.0		
Lasmiditan*	11610526			-9.8	
Rimegepant*	51049968				-9.1
4alpha,24-Dimethyl-5alpha-cholest-8(9)-en-3beta-ol	101614264	-10			
Butyrospermol	12302182	-10.5		-11	
(3S,5S,9S,10S,13R,14R,17R)-17-[(E,2S,5S)-5-ethyl-6-methylhept-3-en-2-yl]-10,13-dimethyl-2,3,4,5,6,9,11,12,14,15,16,17-dodecahydro-1H-cyclopenta[a]phenanthren-3-ol	162958795	-10	-7.0	-10.4	
(3S,8R,9R,10R,13R,14R,17R)-17-[(2R,5R)-5,6-dimethylheptan-2-yl]-10,13-dimethyl-2,3,4,7,8,9,11,12,14,15,16,17-dodecahydro-1H-	163015454	-9.3		-10.7	

cyclopenta[a]phenanthren-3-ol				
(3S)-3-hydroxy-3-methyl-11-(4-oxocyclohexa-2,5-dien-1-ylidene)-2,4,6,7,8,9-hexahydropyridazino[1,2-a]indazol-1-one	163185263	-9.2	-8.3	-9.8
Campesterol	173183	-9.3		-10.3
5-Dehydroavenasterol	44263331	-9.4		
Alpha-Spinasterol	5281331	-9.3		
24-Ethyllophenol	541368	-9.7		
(3R,3aR,5aS,6S,7S,9aR,9bS)-3a,9b-dimethyl-7-prop-1-en-2-yl-3-[(2R,4R)-4,6,6-trimethyl-5-methylideneoctan-2-yl]spiro[1,2,3,4,5,5a,7,8,9,9a-decahydrocyclopenta[a]naphthalene-6,5'-oxolane]-2'-one	643558	-9.3		
(+)-Obtusifoliol	65252	-9.6		
(3S,6R)-6-[(8R,9S,10S,13R,14S,17R)-10,13-dimethyl-2,3,4,5,6,7,8,9,11,12,14,15,16,17-tetradecahydro-1H-cyclopenta[a]phenanthren-17-yl]-3-propan-2-ylheptan-1-ol	56924079	-9.2	-7.2	
4-(1-methoxy-3-methyl-6,7,8,9-tetrahydropyridazino[1,2-a]indazol-11-ylidene)cyclohexa-2,5-dien-1-one	102103090		-8.4	
[3-methyl-11-(4-oxocyclohexa-2,5-dien-1-ylidene)-6,7,8,9-tetrahydropyridazino[1,2-a]indazol-1-yl] hydrogen sulfate	102575929		-8.6	-10.3

11-(4-hydroxyphenyl)-3-methyl-6,7,8,9-tetrahydropyridazino[1,2-a]indazol-10-ium-1-ol	118717506	-7,4	
6,7,8,9-Tetrahydro-11-(4-hydroxyphenyl)-3-methyl-1H-pyridazino(1,2-a)indazol-1-one	136828302	-7,8	
[11-(4-hydroxycyclohexa-2,5-dien-1-ylidene)-3-methyl-6,7,8,9-tetrahydropyridazino[1,2-a]indazol-1-yl]hydrogen sulfate	163104975	-8.4	-9.8
(6aR)-1,2-dimethoxy-6,6-dimethyl-5,6,6a,7-tetrahydro-4H-dibenzo[de,g]quinolin-6-ium-10,11-diol	163190058	-8.1	
4-(1-methoxy-3-methyl-6,7,8,9-tetrahydropyridazino[1,2-a]indazol-10-ium-11-yl)phenol	72201751	-7.7	
Nigelladine B	86302611	-7.2	
Nigelladine A	86302612	-8.1	
(8aR)-2,2,4-trimethyl-6,8a-di(propan-2-yl)-8,9-dihydrocyclopenta[g]quinolin-7-one	90670767	-8.1	-10.2
(3S)-3-hydroxy-11-(4-hydroxyphenyl)-3-methyl-2,4,6,7,8,9-hexahydropyridazino[1,2-a]indazol-10-ium-1-one	118717505	-7.6	
Salfredin B11	636462	-7.8	
(+)-Tirucallol	101257		-10.4
(3S,8R,9R,10R,13R,14R,17R)-17-[(2R,5R)-5-ethyl-6-methylheptan-2-yl]-10,13-dimethyl-2,3,4,7,8,9,11,12,14,15,16,17-dodecahydro-1H-	11870456		-10.3

cyclopenta[a]phenanthren-3-ol					
(3S,8R,9R,10R,13R,14R,17R)-17-[(E,2S,5S)-5-ethyl-6-methylhept-3-en-2-yl]-10,13-dimethyl-2,3,4,7,8,9,11,12,14,15,16,17-dodecahydro-1H-cyclopenta[a]phenanthren-3-ol	124762119			-11	
(3S,8R,9R,10R,13R,14R,17R)-10,13-dimethyl-17-[(2R)-6-methylheptan-2-yl]-2,3,4,7,8,9,11,12,14,15,16,17-dodecahydro-1H-cyclopenta[a]phenanthren-3-ol	7055705			-10.6	

Table 3.1.3: Binding affinities of *Petasites hybridus* compounds with 6G79, 7E32, 7EXD, and 6E3Y

Compounds	**Compound Cid**	**6G79 ΔG (Kcal/mol)**	**7E32 ΔG (Kcal/mol)**	**7EXD ΔG (Kcal/mol)**	**6E3Y ΔG (Kcal/mol)**
Donitriptan	197706	-9.2			
Sumatriptan	5358		-6.9		
Lasmiditan	11610526			-9.8	
Rimegepant	51049968				-9.0
[(4aR,5S,7S,8aR)-3,4a,5-trimethyl-9-oxo-4,5,6,7,8,8a-hexahydrobenzo[f][1]benzofuran-7-yl](Z)-2-methylbut-2-enoate	101596893	-9.2			

[(4aR,5S,7S,8aR)-3,4a,5-trimethyl-9-oxo-4,5,6,7,8,8a-hexahydrobenzo[f][1]benzofuran-7-yl] 2-methylbut-2-enoate	162963127	-9.2		
[(4aR,5S,7R,8aR,9aS)-3,4a,5-trimethyl-2-oxo-4,5,6,7,8,8a,9,9a-octahydrobenzo[f][1]benzofuran-7-yl]3-methylbut-2-enoate	163010411	-9.2	-7.0	
4-[(2E,4S,6S)-6-hydroperoxy-4-hydroxy-3,7-dimethylocta-2,7-dienoxy]-5-methylchromen-2-one	163029109	-9.2		
5-methyl-4-[(2Z)-2-[(5R)-5-(2-methylprop-1-enyl)oxolan-3-ylidene]ethoxy]chromen-2-one	163193385	-9.4		
Rhamnazin	5320945	-9.2	-6.9	
(9-acetyloxy-1-methyl-6-oxo-[1]benzofuro[3,2-c]chromen-8-yl) acetate	85557854	-9.2		-10
[(2E)-2-[(8S,8aR)-8,8a-dimethyl-3-oxo-5,6,7,8-tetrahydro-1H-naphthalen-2-ylidene]propyl] (Z)-2-methylbut-2-enoate	101928816		-6.9	
[(1R,2R,8aR)-1,8a-dimethyl-6-oxo-7-propan-2-ylidene-2,3,4,8-tetrahydro-1H-naphthalen-2-yl] 3-methylbut-2-enoate	101928817		-7.0	
[(4aR,5S,7R,8aR,9aS)-3,4a,5-trimethyl-2-oxo-4,5,6,7,8,8a,9,9a-octahydrobenzo[f][1]benzofuran-7-yl] (Z)-2-methylbut-2-enoate	101996396		-7.0	
Pethybrene	11052748		-7.2	
Albene	11084199		-7.0	

Euparin	119039	-7.4
(4aR,5S,8aS)-3,4a,5-trimethyl-5,6,7,8,8a,9-hexahydro-4H-benzo[f][1]benzofuran	12309960	-8.1
4-Geranyloxy-5-methyl coumarin	129866803	-8.4
(4aR,5S,8aR)-3,4a,5-trimethyl-4,5,6,7,8,8a-hexahydrobenzo[f][1]benzofuran-9-one	13819512	-8.4
4-[(2Z,5R)-5-hydroxy-3-(hydroxymethyl)-7-methylocta-2,6-dienoxy]-5-methylchromen-2-one	162912731	-7.3
[(2E,4R)-3,7-dimethyl-1-(5-methyl-2-oxochromen-4-yl)oxyocta-2,6-dien-4-yl] acetate	162946861	-7.1
[(4aR,5S,7R,8aR,9aS)-3,4a,5-trimethyl-2-oxo-4,5,6,7,8,8a,9,9a-octahydrobenzo[f][1]benzofuran-7-yl] (E)-2-methylbut-2-enoate	162966470	-7.1
(4aR,5S,8aR,9aR)-3,4a,5-trimethyl-4,5,6,7,8,8a,9,9a-octahydro-1H-benzo[f]indol-2-one	162974730	-6.9
(4aR,5R,8aR,9aR)-3,4a,5-trimethyl-4,5,6,7,8,8a,9,9a-octahydrobenzo[f][1]benzofuran-2-one	162983895	-7.3
(3S)-3-ethenyl-9-methyl-3-(4-methylpent-3-enyl)-2H-furo[3,2-c]chromen-4-one	163034952	-8.4
4-[(2E,4R)-4-hydroxy-3-(hydroxymethyl)-7-methylocta-2,6-dienoxy]-5-methylchromen-2-one	163041276	-8.6
4-[(2E,4R)-4-hydroxy-3,7-dimethylocta-2,6-dienoxy]-5-methylchromen-2-one	163057208	-9.0

4-[10-Oxo-neryloxy]-5-methylcoumarin	163184474	-7.8
4-[10-Oxo-geranyloxyl]-5-methylcoumarin	163184475	-8.1
4-(10-Hydroxyneryloxy)-5-methylcoumarin	163184477	-7.5
4-(10-Hydroxygeranyloxy)-5-methylcoumarin	163184481	-8.2
4-[5-Formyl-3-methyl-pent-2E,4E-dien-1-yl]-5-methylcoumarin	163184483	-7.8
5-[6,10-Dioxo-neryloxy]-5-methyl coumarin	163184484	-7.0
4-[(2Z,6S)-6-hydroperoxy-3-(hydroxymethyl)-7-methylocta-2,7-dienoxy]-5-methylchromen-2-one	163186576	-7.2
4-[(2Z,6R)-6-hydroxy-3-(hydroxymethyl)-7-methylocta-2,7-dienoxy]-5-methylchromen-2-one	163189873	-7.1
Dehydrofukinone	177072	-7.2
[(2Z)-6-methyl-2-[2-(5-methyl-2-oxochromen-4-yl)oxyethylidene]hept-5-enyl] acetate	23786283	-7.5
Quercetin	5280343	-7.2
Neopetasane	5320106	-7.0

4-Hydroxy-5-methylcoumarin	54688203	-6.9	
4a,5-dimethyl-3-propan-2-ylidene-5,6,7,8-tetrahydro-4H-naphthalen-2-one	612721	-7.7	
Petasitene	636697	-7.4	
Diisobutyl phthalate	6782	-7.1	
(R)-beta-bisabolene	68128	-7.3	
Beta-Elemene	6918391	-7.2	
[(4aR,5S,7R,8aR,9aR)-3,4a,5-trimethyl-2-oxo-4,5,6,7,8,8a,9,9a-octahydrobenzo[f][1]benzofuran-7-yl] (Z)-2-methylbut-2-enoate	101996395		-10.3
[(4aR,5S,7R,8aR,9aR)-3,4a,5-trimethyl-2-oxo-4,5,6,7,8,8a,9,9a-octahydrobenzo[f][1]benzofuran-7-yl] 2-methylprop-2-enoate	102469295		-10
[(4aR,5S,7R,8aR,9aR)-3,4a,5-trimethyl-2-oxo-4,5,6,7,8,8a,9,9a-octahydrobenzo[f][1]benzofuran-7-yl] 2-methylpropanoate	102469296		-9.9
[(4aS,5R,6R,8aR,9aR)-3,4a,5-trimethyl-2-oxo-4,5,6,7,8,8a,9,9a-octahydrobenzo[f][1]benzofuran-6-yl] (Z)-2-methylbut-2-enoate	162933325		-9.8
[(4aR,5S,7R,8aR,9aR)-3,4a,5-trimethyl-2-oxo-4,5,6,7,8,8a,9,9a-octahydrobenzo[f][1]benzofuran-7-yl] (E)-2-methylbut-2-enoate	162966469		-9.8

Table 3.1.4: Binding affinities of *Tanacetum parthenium* compounds with 6G79, 7E32, 7EXD, and 6E3Y

Compounds	Compound Cid	6G79 ΔG (Kcal/mol)	7E32 ΔG (Kcal/mol)	7EXD ΔG (Kcal/mol)	6E3Y ΔG (Kcal/mol)
Donitriptan	197706	-9.7			
Sumatriptan	5358		-6.9		
Lasmiditan	11610526			-9.8	
Rimegepant	51049968				-9.1
(3S,8R,9S,10R,12S,13S,14S,17R)-10,13-dimethyl-17-[(1S)-1-[(3S)-3-methyl-2,3,4,5-tetrahydropyridin-6-yl]ethyl]-2,3,4,7,8,9,11,12,14,15,16,17-dodecahydro-1H-cyclopenta[a]phenanthrene-3,12-diol	101861833	-9.9		-10.8	
7-[[(1S,4aR,6S,8aS)-6-hydroxy-5,5,8a-trimethyl-2-methylidene-3,4,4a,6,7,8-hexahydro-1H-naphthalen-1-yl]methoxy]-6,8-dimethoxychromen-2-one	102328535	-11		-10.3	
Phelligridin C	10248188	-10			
Phelligridin D	10339712	-10.1			

Rubijervine	253295	-10.2		
Fucosterol	5281328	-9.7		-10.6
Ergosterol Peroxide	5351516	-10.2		
Hypholomine B	54730031	-10.8		
(3S,3'R,3'aS,6'S,6aS,6bS,7'aR,9S,11aS,11bR)-3',6',10,11b-tetramethylspiro[2,3,4,6,6a,6b,7,8,11,11a-decahydro-1H-benzo[a]fluorene-9,2'-3a,4,5,6,7,7a-hexahydro-3H-furo[3,2-b]pyridine]-3-o	86287406	-10.2		
(4R,5S)-5-[(1S,2R)-2-hydroxy-5-oxocyclopent-3-en-1-yl]-3-methylidene-4-(2-oxopropyl)oxolan-2-one	101254614		-7.4	
(4R,5S)-5-[(1S,2S)-2-hydroxy-5-oxocyclopent-3-en-1-yl]-3-methylidene-4-(2-oxopropyl)oxolan-2-one	101254615		-7.4	
Secotanapartholide B	10265551		-7.5	
Secotanapartholide A	10356188		-7.1	
(1S,2R,5S,9S,10S,11R)-2-hydroxy-2,11-dimethyl-6-methylidene-8,12,13-trioxatetracyclo[9.2.2.01,10.05,9]pentadec-14-en-7-one	14219462		-8.7	
Methyl-gamma-costate	14707110		-8.2	

(3aS,6R,9aS,9bS)-6-hydroxy-6,9-dimethyl-3-methylidene-4,5,9a,9b-tetrahydro-3aH-azuleno[4,5-b]furan-2-one	15406669	-7.5
Santamarin	188297	-7.4
1,3-dimethyl-8-propan-2-yltricyclo[4.4.0.02,7]dec-3-ene	19725	-7.1
(+-)-Cannabichromene	30219	-7.5
Reynosin	482788	-7.2
Apigenin	5280443	-8.3
Luteolin	5280445	-8.2
Chrysoeriol	5280666	-8.4
Artemorin	5281428	-8.0
Hispidulin	5281628	-7.2
6-Hydroxykaempferol	5281638	-7.1
Ellagic Acid	5281855	-7.6
Chrysanthenyl isovalerate	529750	-7.0

4-[(E)-2-(3,5-dihydroxyphenyl)ethenyl]-2-methoxybenzene-1,3-diol	5315205	-7.9		
Nepetin	5317284	-7.4		
Isofraxidin	5318565	-6.9		
Jaceosidin	5379096	7.2		
Jaceidin	5464461	-6.9		
1-beta-Hydroxyarbusculin A	60199554	-7.0		
3-O-methyl-isosecotanapartholide	70697791	-6.9		
(+)-Alantolactone	72724	-7.5		
Chrysanthenyl angelate	91748888	-6.9		
(1R,2S,7S,8S)-1,3-dimethyl-8-propan-2-yltricyclo[4.4.0.02,7]dec-3-ene	92042749	-6.9		
7-(alpha-D-Glucopyranosyloxy)-5-hydroxy-2-(4-hydroxyphenyl)-4H-1-benzopyran-4-one	12304095		-9.8	
Isofucosterol	5281326		-10.7	
(1R,3S,3'R,3'aS,4aR,6'S,6aS,6bS,7'aR,9R,11aS,11bS)-1,3-dihydroxy-3',6',10,11b-	16723933		-10.2	-9.2

tetramethylspiro[1,2,3,4,4a,5,6,6a,6b,7,8,11a-dodecahydrobenzo[a]fluorene-9,2'-3a,4,5,6,7,7a-hexahydro-3H-furo[3,2-b]pyridine]-11-one		
22,23-Dihydrobrassicasterol	5283637	-10.6
Solanidine	65727	-10

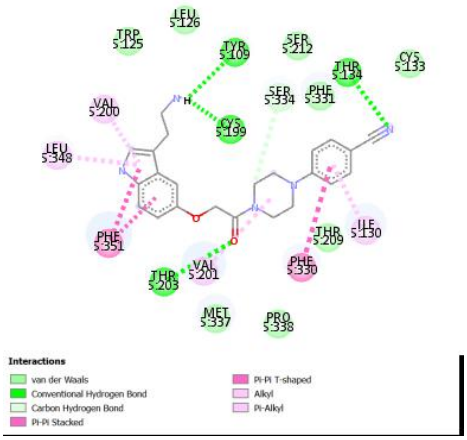
LEU S:126
TRP S:125
TYR S:109
SER S:212
THR S:134
CYS S:133
VAL S:200
SER S:334
PHE S:331
CYS S:139
LEU S:548
PHE S:351
THR S:209
ILE S:130
VAL S:201
PHE S:330
THR S:203
MET S:337
PRO S:338
Interactions
van der Waals
Conventional Hydrogen Bond
Carbon Hydrogen Bond
Pi-Pi Stacked
Pi-Pi T-shaped
Alkyl
Pi-Alkyl

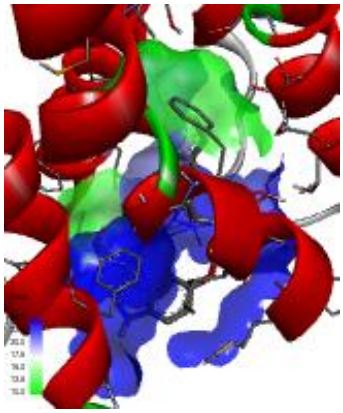

I

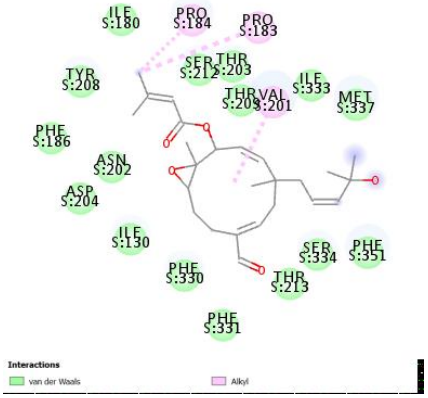
ILE S:180
PRO S:184
PRO S:183
SER S:212
THR S:203
TYR S:208
ILE S:333
THR S:209
VAL S:201
MET S:337
PHE S:186
ASN S:202
ASP S:204
ILE S:130
SER S:334
PHE S:351
PHE S:330
THR S:213
PHE S:331
Interactions
van der Waals
Alkyl

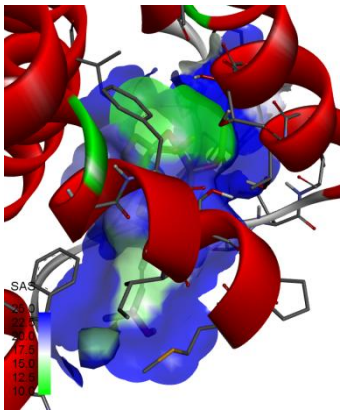
SAS

II

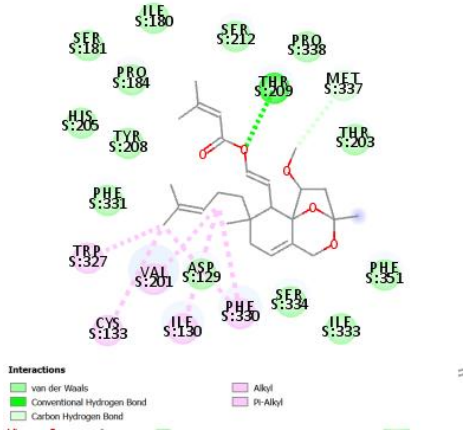
ILE S:180
SER S:181
SER S:212
PRO S:338
PRO S:184
THR S:209
MET S:337
HIS S:205
TYR S:208
THR S:203
PHE S:331
TRP S:327
VAL S:201
ASP S:129
PHE S:351
SER S:334
PHE S:330
CYS S:133
ILE S:130
ILE S:333
Interactions
van der Waals
Conventional Hydrogen Bond
Carbon Hydrogen Bond
Alkyl
Pi-Alkyl

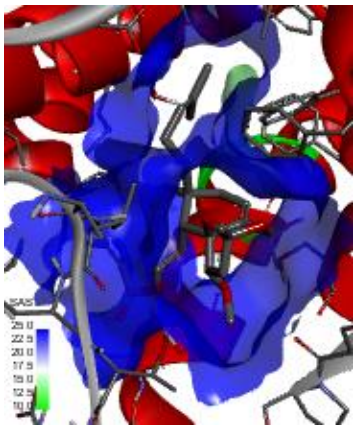

III

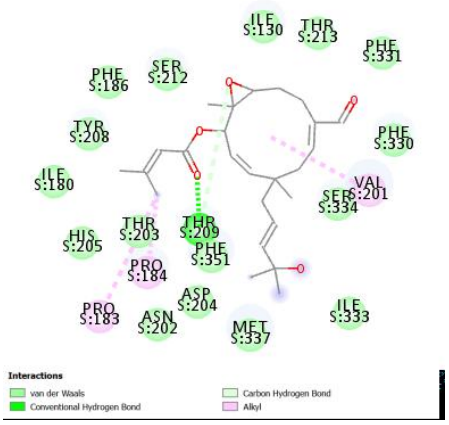
ILE S:130
THR S:213
PHE S:331
SER S:212
PHE S:186
TYR S:208
PHE S:330
ILE S:180
VAL S:201
SER S:334
THR S:203
THR S:209
HIS S:205
PHE S:351
PRO S:184
ASP S:204
PRO S:183
ASN S:202
MET S:337
ILE S:333
Interactions
van der Waals
Carbon Hydrogen Bond
Conventional Hydrogen Bond
Alkyl

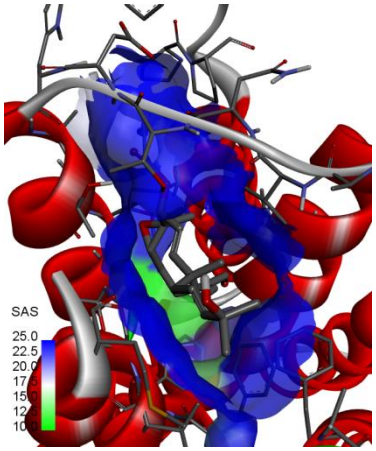
SAS
25.0
22.5
20.0
17.5
15.0
12.5
10.0

IV

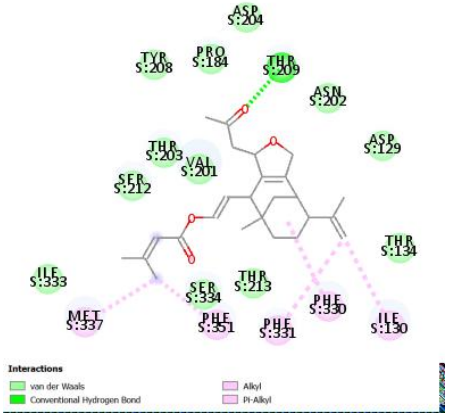
ASP S:204
TYR S:208
PRO S:184
THR S:209
ASN S:202
ASP S:129
THR S:203
VAL S:201
SER S:212
THR S:134
ILE S:333
THR S:213
SER S:334
PHE S:330
MET S:337
PHE S:351
PHE S:331
ILE S:130
Interactions
van der Waals
Alkyl
Conventional Hydrogen Bond
Pi-Alkyl

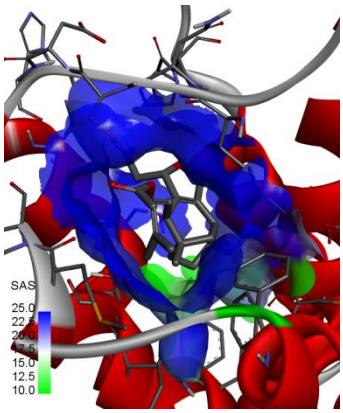
SAS
25.0
22.5
20.0
17.5
15.0
12.5
10.0

V

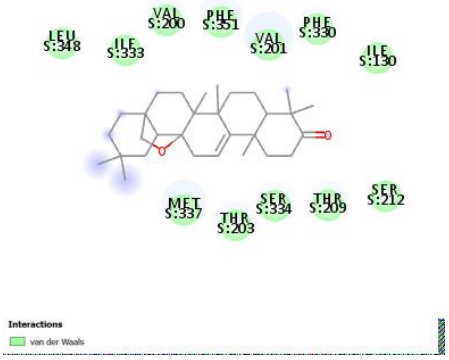
VAL S:200
PHE S:351
PHE S:330
LEU S:348
ILE S:333
VAL S:201
ILE S:130
MET S:337
SER S:334
THR S:209
SER S:212
THR S:203
Interactions
van der Waals

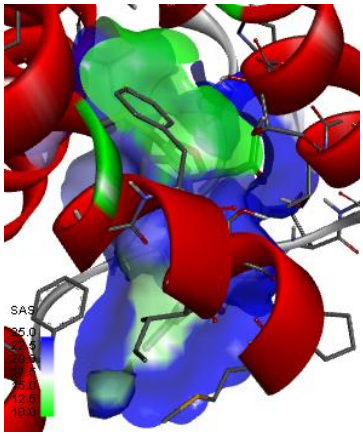
SAS
25.0
22.5
20.0
17.5
15.0
12.5
10.0

VI

Figure 3.1.1.1: 2D (left) and 3D (right) views of the molecular interactions of amino-acid residues of 5-HT$_1$B receptor with (I) Donitriptan (II) [(1S,2S,3E,5R,7E,11R)-8-formyl-5-[(E)-4-hydroxy-4-methylpent-2-enyl]-1,5-dimethyl-12-oxabicyclo[9.1.0]dodeca-3,7-dien-2-yl] 3-methylbut-2-enoate (III) 2-[(1S,2R,3S,9S,11S)-11-methoxy-3,9-dimethyl-3-(4-methylpent-3-enyl)-8,12-dioxatricyclo[7.2.1.01,6]dodec-5-en-2-yl]ethenyl 3-methylbut-2-enoate (IV) Vibsanin T (V) [(E)-2-[(1S,5S,7R,8S,11S)-8-methyl-5-(2-oxopropyl)-11-prop-1-en-2-yl-4-oxatricyclo[6.3.1.02,6]dodec-2(6)-en-7-yl]ethenyl] 3-methylbut-2-enoate (VI) (1S,4S,5R,8R,13S,14R,17S,18R)-4,5,9,9,13,20,20-heptamethyl-24oxahexacyclo[15.5.2.01,18.04,17.05,14.08,13] -15-en-10-one in *Crassocephalum crepidioides.*

I

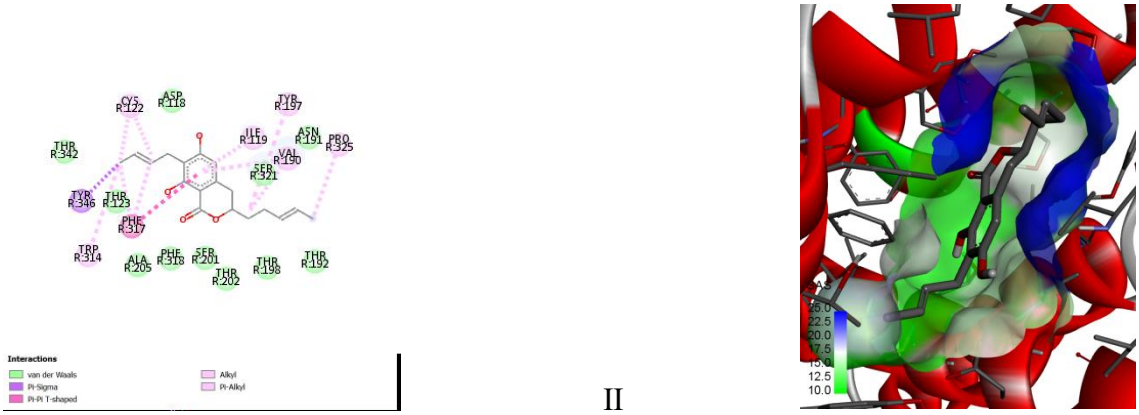

II

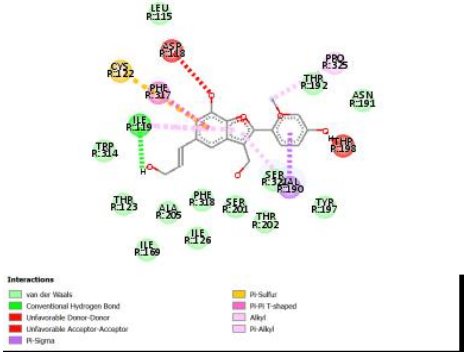
LEU R:115
ASP R:118
CYS R:122
PHE R:317
PRO R:325
THR R:192
ASN R:191
ILE R:119
TRP R:314
THR R:198
SER R:321
VAL R:190
THR R:123
ALA R:205
PHE R:318
SER R:201
THR R:202
TYR R:197
ILE R:126
ILE R:169
Interactions
van der Waals
Conventional Hydrogen Bond
Unfavorable Donor-Donor
Unfavorable Acceptor-Acceptor
Pi-Sigma
Pi-Sulfur
Pi-Pi T-shaped
Alkyl
Pi-Alkyl

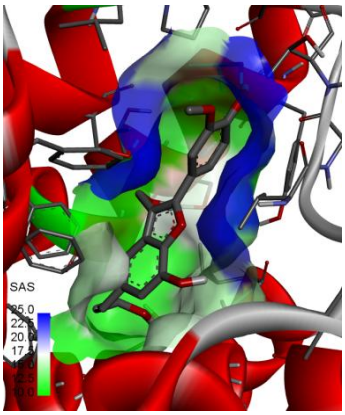
SAS

III

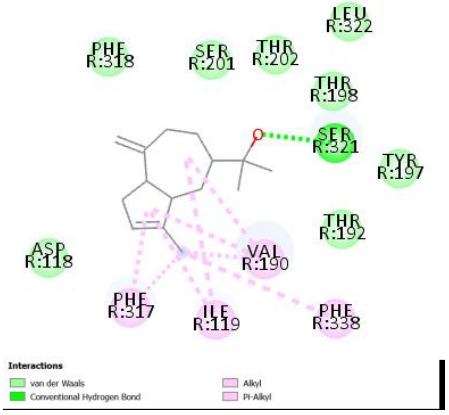
LEU R:322
PHE R:318
SER R:201
THR R:202
THR R:198
SER R:321
TYR R:197
THR R:192
ASP R:118
VAL R:190
PHE R:317
ILE R:119
PHE R:338
Interactions
van der Waals
Conventional Hydrogen Bond
Alkyl
Pi-Alkyl

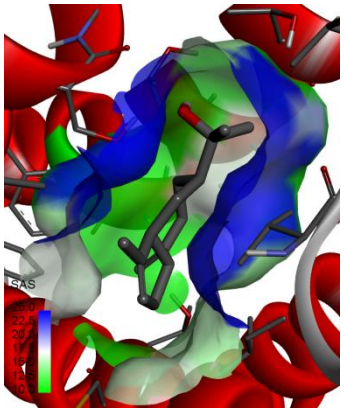
SAS

IV

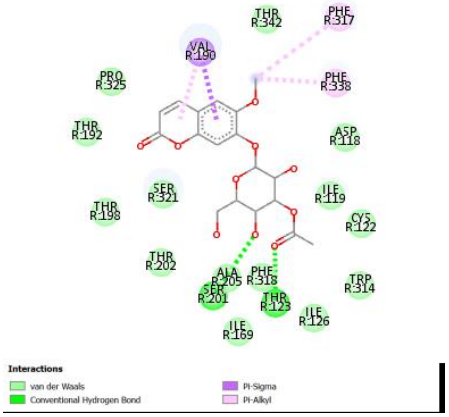
THR R:342
PHE R:317
VAL R:190
PRO R:325
PHE R:338
THR R:192
ASP R:118
SER R:321
ILE R:119
THR R:198
CYS R:122
THR R:202
ALA R:205
PHE R:318
TRP R:314
SER R:201
THR R:123
ILE R:126
ILE R:169
Interactions
van der Waals
Conventional Hydrogen Bond
Pi-Sigma
Pi-Alkyl

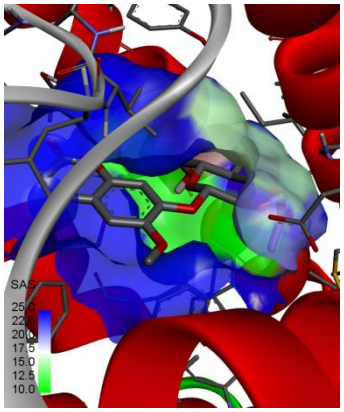
SAS
25.0
22.5
20.0
17.5
15.0
12.5
10.0

V

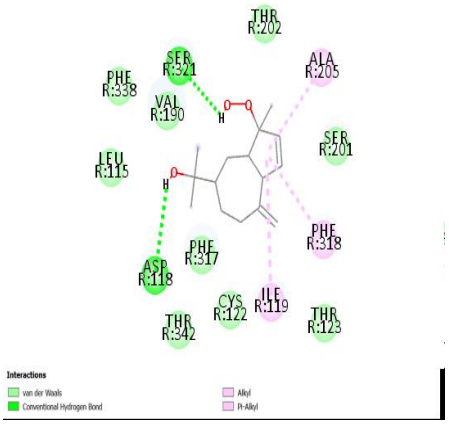
THR R:202
SER R:321
ALA R:205
PHE R:338
VAL R:190
SER R:201
LEU R:115
PHE R:318
PHE R:317
ASP R:118
CYS R:122
ILE R:119
THR R:342
THR R:123
Interactions
van der Waals
Conventional Hydrogen Bond
Alkyl
Pi-Alkyl

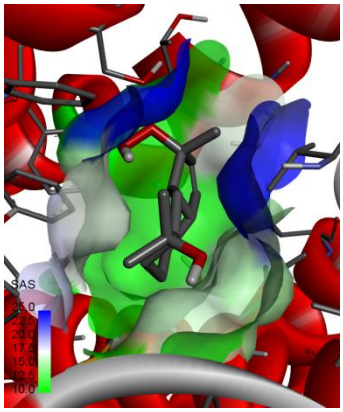
SAS

VI

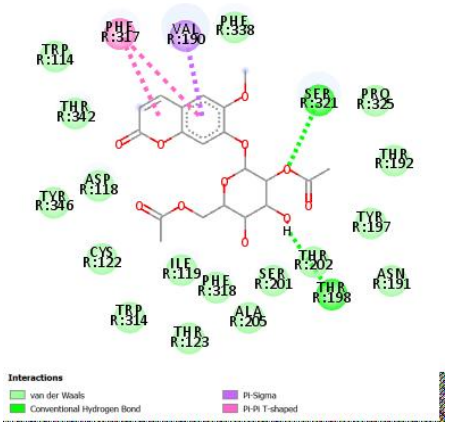
PHE R:317
VAL R:190
PHE R:338
TRP R:114
THR R:342
SER R:321
PRO R:325
THR R:192
ASP R:118
TYR R:346
TYR R:197
CYS R:122
ILE R:119
PHE R:318
SER R:201
THR R:202
ASN R:191
THR R:198
TRP R:314
ALA R:205
THR R:123
Interactions
van der Waals
Conventional Hydrogen Bond
Pi-Sigma
Pi-Pi T-shaped

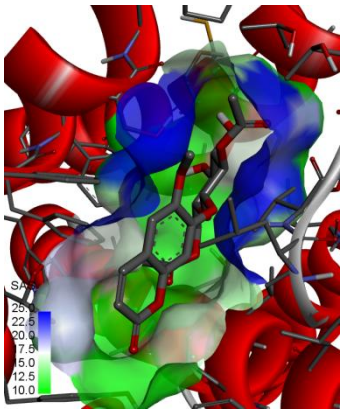
SAS

VII

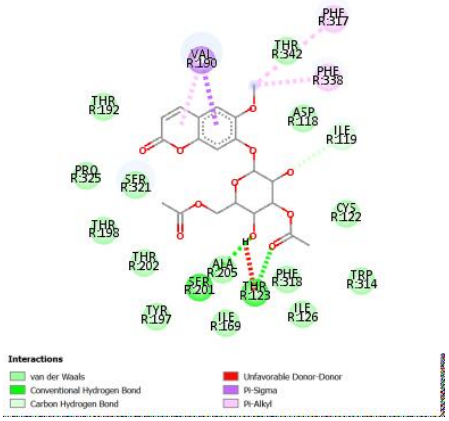
PHE R:317
VAL R:190
THR R:342
PHE R:338
THR R:192
ASP R:118
ILE R:119
PRO R:325
SER R:321
CYS R:122
THR R:198
THR R:202
ALA R:205
SER R:201
PHE R:318
THR R:123
TRP R:314
TYR R:197
ILE R:169
ILE R:126
Interactions
van der Waals
Conventional Hydrogen Bond
Carbon Hydrogen Bond
Unfavorable Donor-Donor
Pi-Sigma
Pi-Alkyl

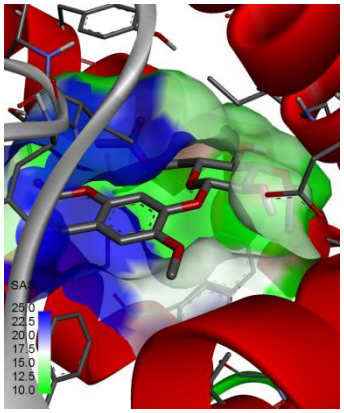
SAS

VIII

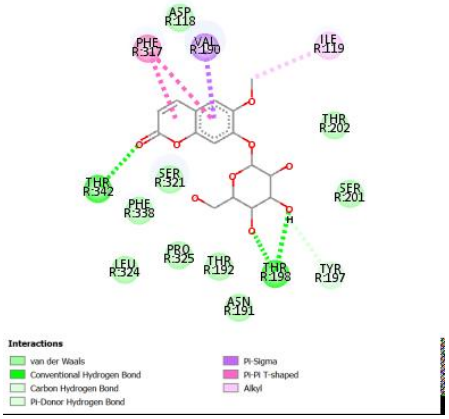

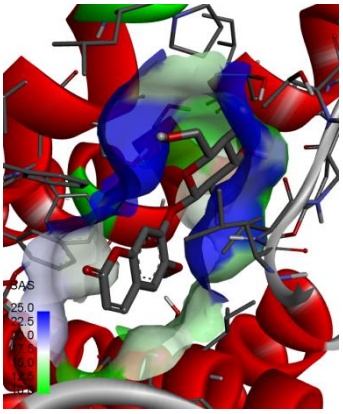

IX

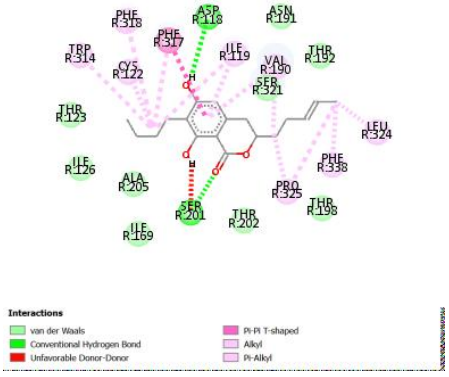

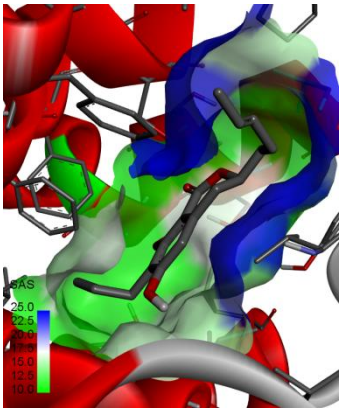

X

Figure 3.1.1.2: 2D (left) and 3D (right) views of the molecular interactions of amino-acid residues of 5-HT1D receptor with (I) Sumatriptan (II) 7-but-2-enyl-6,8-dihydroxy-3-pent-3-enyl-3,4-dihydroisochromen-1-one (III) 2-(4-hydroxy-3-methoxyphenyl)-3-(hydroxymethyl)-5-[(E)-3-hydroxyprop-1-enyl]-1-benzofuran-7-ol (IV) 2-[(3aS,5R,8aR)-3-methyl-8-methylidene-3a,4,5,6,7,8a-hexahydro-1H-azulen-5-yl]propan-2-ol (V) [(2R,3R,4S,5R,6S)-3,5-dihydroxy-2-(hydroxymethyl)-6-(6-methoxy-2-oxochromen-7-yl)oxyoxan-4-yl] acetate (VI) 2-[(3R,3aR,5S,8aS)-3-hydroperoxy-3-methyl-8-methylidene-3a,4,5,6,7,8a-hexahydroazulen-5-yl]propan-2-ol (VII) [(2R,3S,4S,5R,6S)-5-acetyloxy-3,4-dihydroxy-6-(6-methoxy-2-

oxochromen-7-yl)oxyoxan-2-yl]methyl acetate (VIII) [(2R,3R,4S,5R,6S)-4-acetyloxy-3,5-dihydroxy-6-(6-methoxy-2-oxochromen-7-yl)oxyoxan-2-yl]methyl acetate (IX) Scopolin (X) 7-butyl-6,8-dihydroxy-3-pent-3-enyl-3,4-dihydroisochromen-1-one in *Crassocephalum crepidioides*.

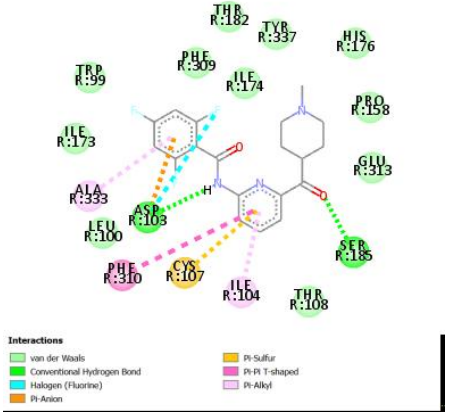

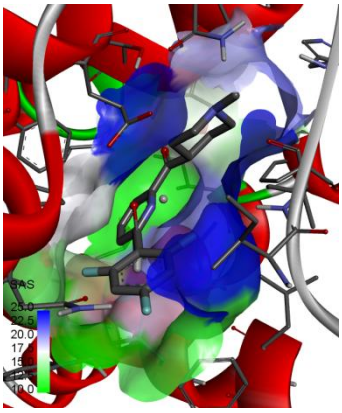

I

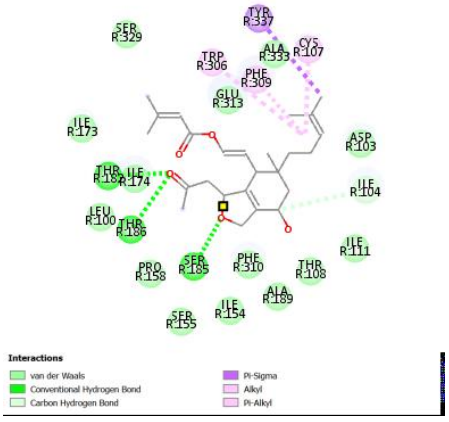

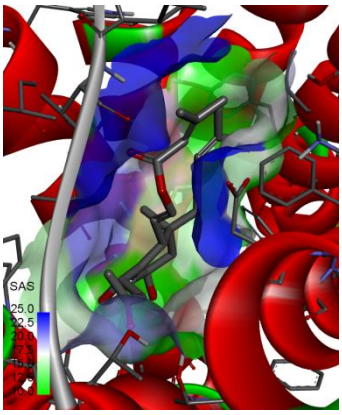

II

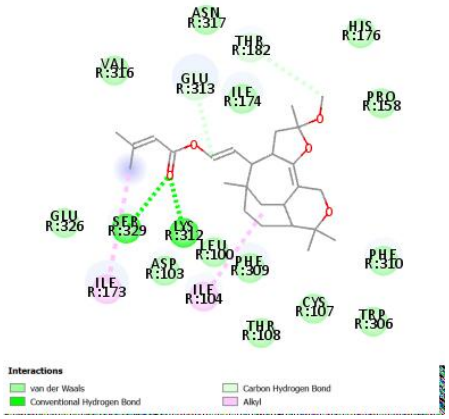

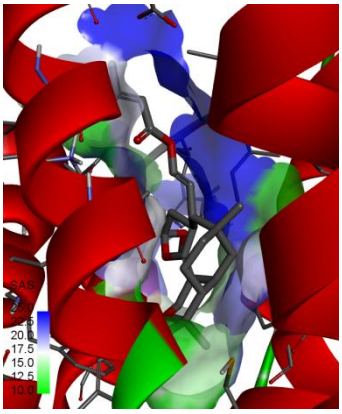

III

Figure 3.1.1.3: 2D (left) and 3D (right) views of the molecular interactions of amino-acid residues of 5-HT1F receptor with (I) Lasmiditan (II) Neovibsanin I (III) [(E)-2-[(4S,6S,7S,8S,11R,15S)-4-methoxy-4,8,12,12-tetramethyl-3,13-dioxatetracyclo[6.6.2.02,6.011,15]hexadec-1-en-7-yl]ethenyl] 3-methylbut-2-enoate in *Crassocephalum crepidioides.*

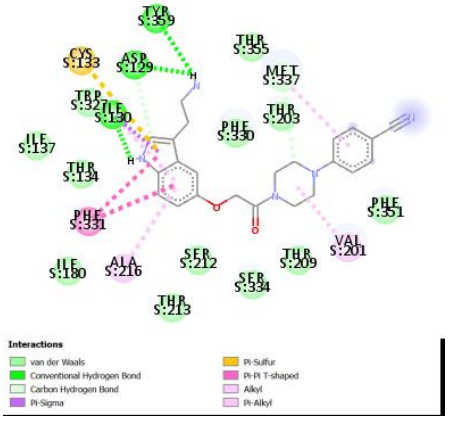

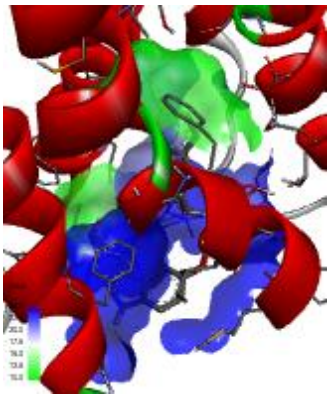

I

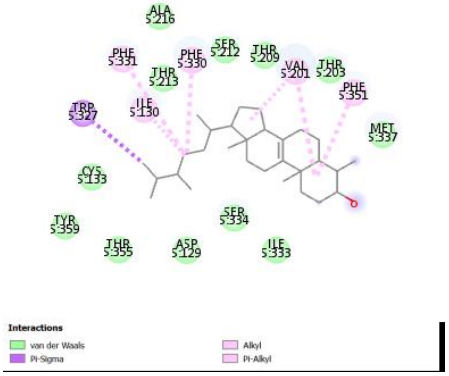
ALA S:216
PHE S:331
PHE S:330
SER S:212
THR S:209
VAL S:201
THR S:203
THR S:213
PHE S:351
TRP S:327
ILE S:130
MET S:337
CYS S:133
SER S:334
TYR S:359
THR S:355
ASP S:129
ILE S:333
Interactions
van der Waals
Alkyl
Pi-Sigma
Pi-Alkyl

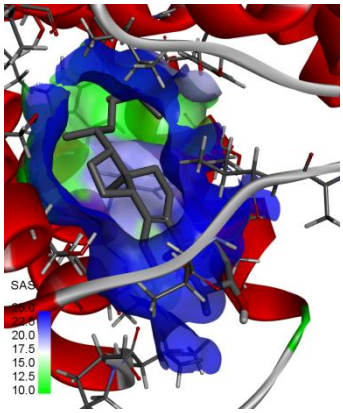
SAS
20.0
17.5
15.0
12.5
10.0

II

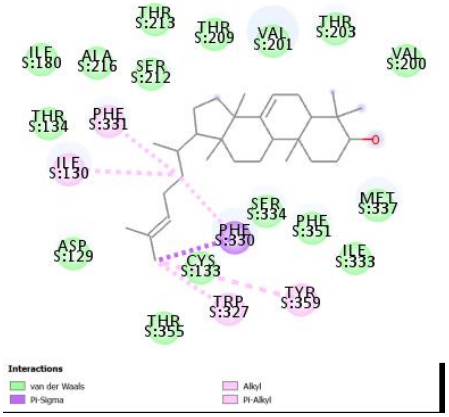
THR S:213
THR S:209
VAL S:201
THR S:203
ILE S:180
ALA S:216
SER S:212
VAL S:200
THR S:134
PHE S:331
ILE S:130
SER S:334
MET S:337
PHE S:330
PHE S:351
ASP S:129
CYS S:133
ILE S:333
TRP S:327
TYR S:359
THR S:355
Interactions
van der Waals
Alkyl
Pi-Sigma
Pi-Alkyl

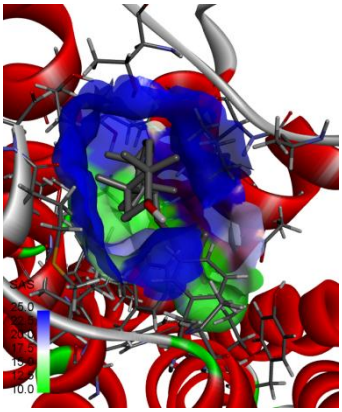
10.0

III

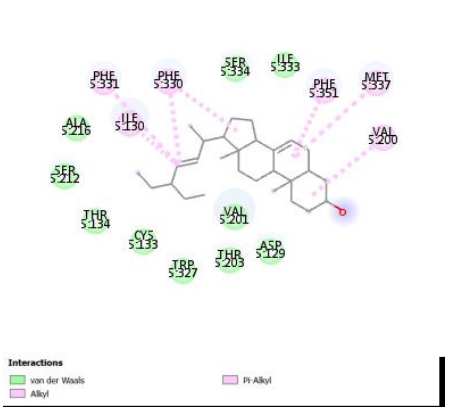
PHE S:331
PHE S:330
SER S:334
ILE S:333
PHE S:351
MET S:337
ILE S:130
ALA S:216
VAL S:200
SER S:212
VAL S:201
THR S:134
CYS S:133
ASP S:129
TRP S:327
THR S:203
Interactions
van der Waals
Alkyl
Pi-Alkyl

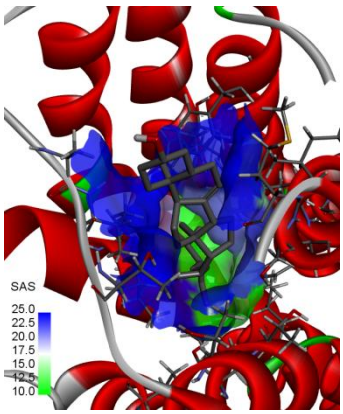
SAS
25.0
22.5
20.0
17.5
15.0
12.5
10.0

IV

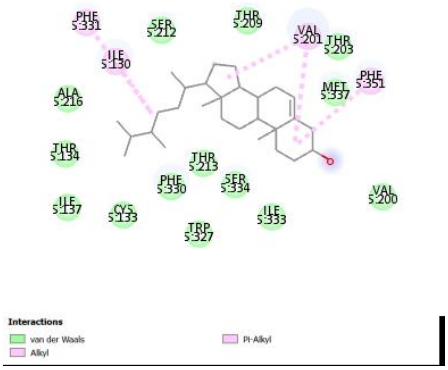
PHE S:331
SER S:212
THR S:209
VAL S:201
THR S:203
ILE S:130
PHE S:351
MET S:337
ALA S:216
THR S:134
THR S:213
PHE S:330
SER S:334
VAL S:200
ILE S:137
CYS S:133
ILE S:333
TRP S:327
Interactions
van der Waals
Alkyl
Pi-Alkyl

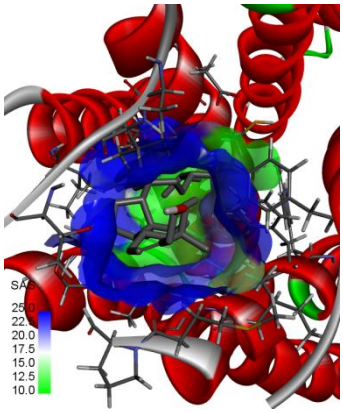
SAS
25.0
22.5
20.0
17.5
15.0
12.5
10.0

V

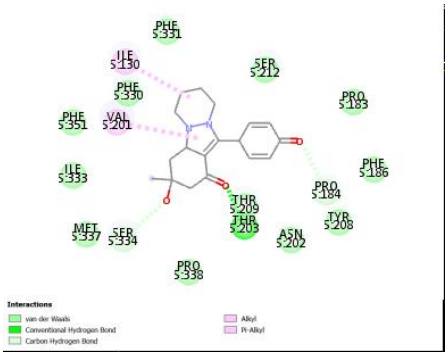
PHE S:331
ILE S:130
SER S:212
PHE S:330
PRO S:185
PHE S:351
VAL S:201
PHE S:186
ILE S:333
PRO S:184
THR S:209
THR S:203
TYR S:208
MET S:337
SER S:334
ASN S:202
PRO S:338
Interactions
van der Waals
Conventional Hydrogen Bond
Carbon Hydrogen Bond
Alkyl
Pi-Alkyl

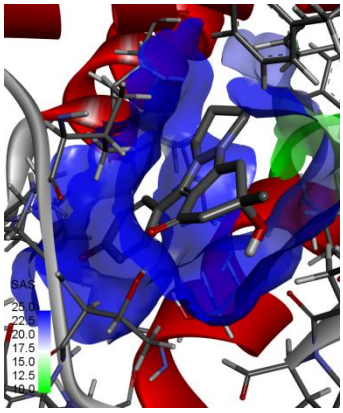
SAS
25.0
22.5
20.0
17.5
15.0
12.5
10.0

VI

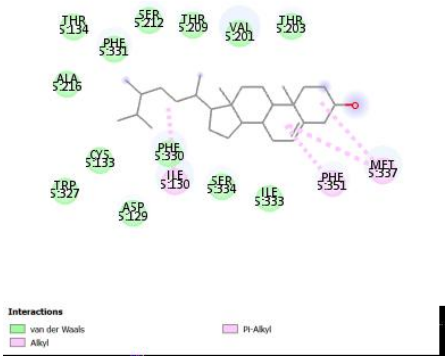
THR S:134
SER S:212
THR S:209
VAL S:201
THR S:203
PHE S:331
ALA S:216
CYS S:133
PHE S:330
MET S:337
ILE S:130
SER S:334
PHE S:351
TRP S:327
ILE S:333
ASP S:129
Interactions
van der Waals
Alkyl
Pi-Alkyl

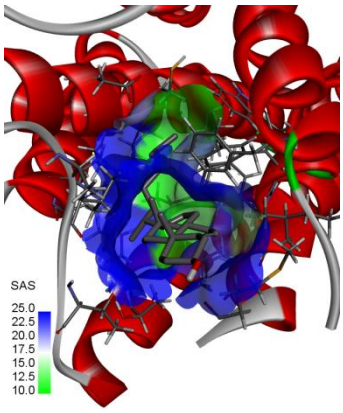
SAS
25.0
22.5
20.0
17.5
15.0
12.5
10.0

VII

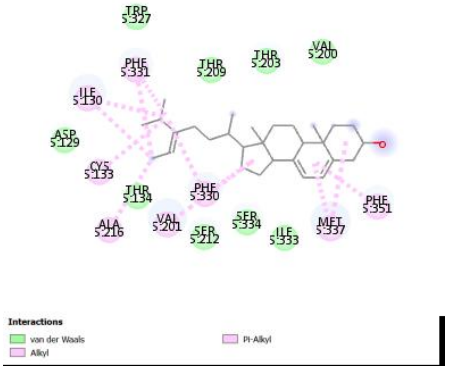
TRP S:327
PHE S:331
THR S:209
THR S:203
VAL S:200
ILE S:130
ASP S:129
CYS S:133
THR S:134
PHE S:330
PHE S:351
ALA S:216
VAL S:201
SER S:334
SER S:212
ILE S:333
MET S:337
Interactions
van der Waals
Alkyl
Pi-Alkyl

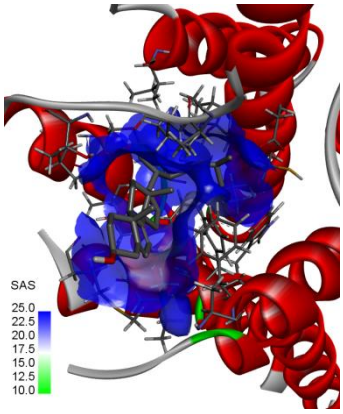
SAS
25.0
22.5
20.0
17.5
15.0
12.5
10.0

VIII

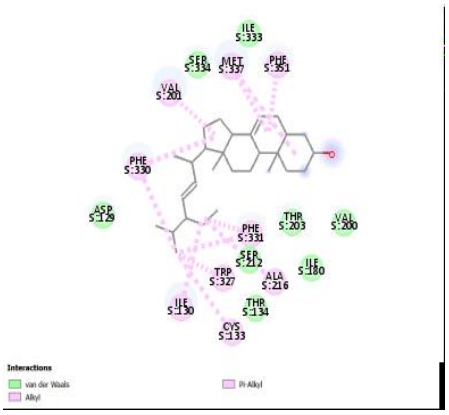
ILE S:333
SER S:334
MET S:337
PHE S:351
VAL S:201
PHE S:330
ASP S:129
THR S:203
VAL S:200
PHE S:331
SER S:212
ILE S:180
TRP S:327
ALA S:216
ILE S:130
THR S:134
CYS S:133
Interactions
van der Waals
Alkyl
Pi-Alkyl

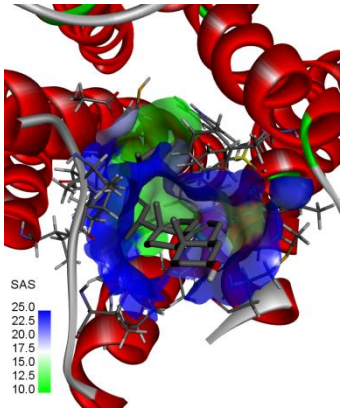
SAS
25.0
22.5
20.0
17.5
15.0
12.5
10.0

IX

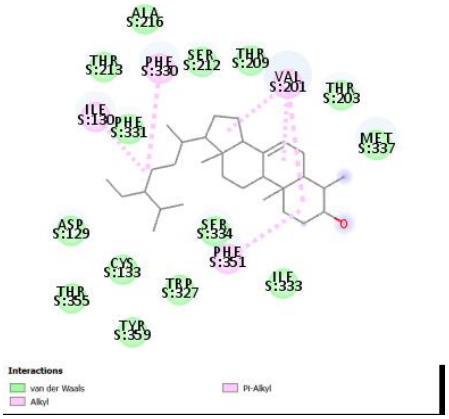
ALA S:216
THR S:213
PHE S:330
SER S:212
THR S:209
VAL S:201
THR S:203
ILE S:130
PHE S:331
MET S:337
ASP S:129
SER S:334
PHE S:351
CYS S:133
TRP S:327
ILE S:333
THR S:355
TYR S:359
Interactions
van der Waals
Alkyl
Pi-Alkyl

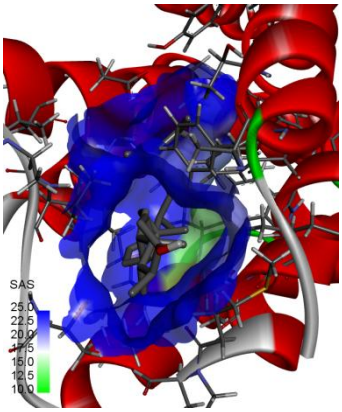
SAS
25.0
22.5
20.0
17.5
15.0
12.5
10.0

X

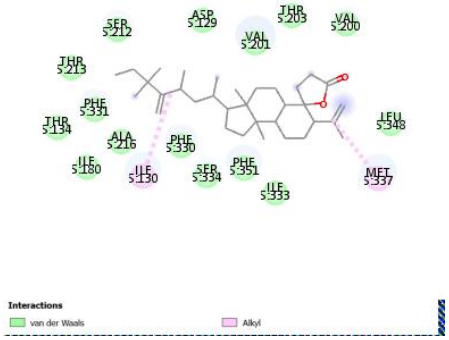
SER S:212
ASP S:129
THR S:203
VAL S:200
VAL S:201
THR S:213
PHE S:331
THR S:134
ALA S:216
PHE S:330
LEU S:348
ILE S:180
ILE S:130
SER S:334
PHE S:351
ILE S:333
MET S:337
Interactions
van der Waals
Alkyl

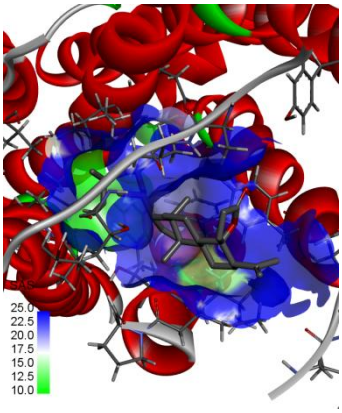
25.0
22.5
20.0
17.5
15.0
12.5
10.0

XI

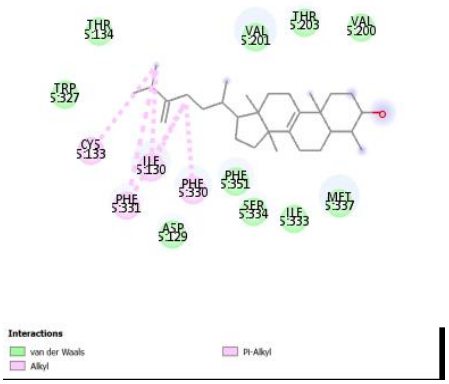
THR S:134
VAL S:201
THR S:203
VAL S:200
TRP S:327
CYS S:133
ILE S:130
PHE S:351
PHE S:330
PHE S:331
SER S:334
ILE S:333
MET S:337
ASP S:129
Interactions
van der Waals
Pi-Alkyl
Alkyl

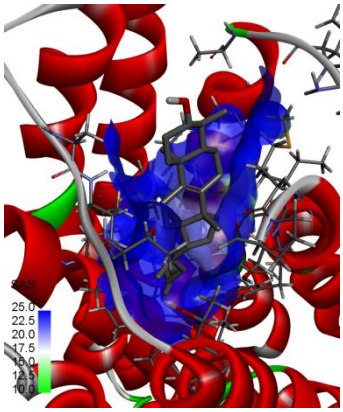
25.0
22.5
20.0
17.5

XII

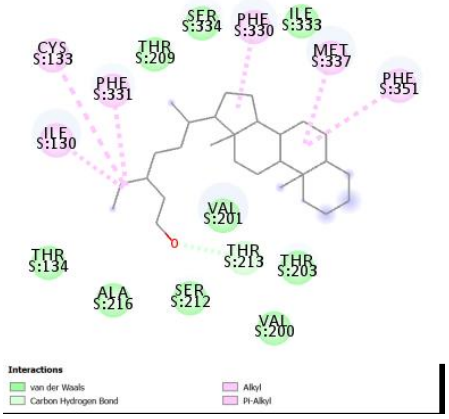
SER S:334
PHE S:330
ILE S:333
CYS S:133
THR S:209
MET S:337
PHE S:331
PHE S:351
ILE S:130
VAL S:201
THR S:134
THR S:213
THR S:203
ALA S:216
SER S:212
VAL S:200
Interactions
van der Waals
Carbon Hydrogen Bond
Alkyl
Pi-Alkyl

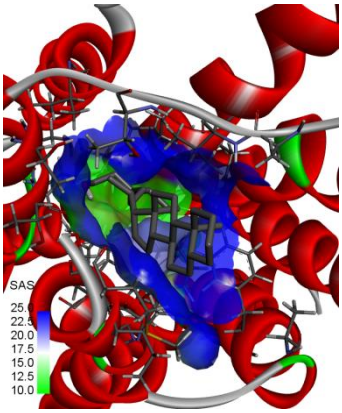
SAS
25.0
22.5
20.0
17.5
15.0
12.5
10.0

XIII

Figure 3.1.2.1: 2D (left) and 3D (right) views of the molecular interactions of amino-acid residues of 5-HT1B receptor with (I) Donitriptan (II) 4alpha,24-Dimethyl-5alpha-cholest-8(9)-en-3beta-ol (III) Butyrospermol (IV) (3S,5S,9S,10S,13R,14R,17R)-17-[(E,2S,5S)-5-ethyl-6-methylhept-3-en-2-yl]-10,13-dimethyl-2,3,4,5,6,9,11,12,14,15,16,17-dodecahydro-1H-cyclopenta[a]phenanthren-3-ol (V) (3S,8R,9R,10R,13R,14R,17R)-17-[(2R,5R)-5,6-dimethylheptan-2-yl]-10,13-dimethyl-2,3,4,7,8,9,11,12,14,15,16,17-dodecahydro-1H-cyclopenta[a]phenanthren-3-ol (VI) (3S)-3-hydroxy-3-methyl-11-(4-oxocyclohexa-2,5-dien-1-ylidene)-2,4,6,7,8,9-hexahydropyridazino[1,2-a]indazol-1-one (VII) Campesterol (VIII) 5-Dehydroavenasterol (IX) Alpha-Spinasterol (X) 24-Ethyllophenol (XI) (3R,3aR,5aS,6S,7S,9aR,9bS)-3a,9b-dimethyl-7-prop-1-en-2-yl-3-[(2R,4R)-4,6,6-trimethyl-5-methylideneoctan-2-yl]spiro[1,2,3,4,5,5a,7,8,9,9a-decahydrocyclopenta[a]naphthalene-6,5'-oxolane]-2'-one (XII) (+)-Obtusifoliol (XIII) (3S,6R)-6-[(8R,9S,10S,13R,14S,17R)-10,13-dimethyl-2,3,4,5,6,7,8,9,11,12,14,15,16,17-tetradecahydro-1H-cyclopenta[a]phenanthren-17-yl]-3-propan-2-ylheptan-1-ol in *Nigella sativa.*

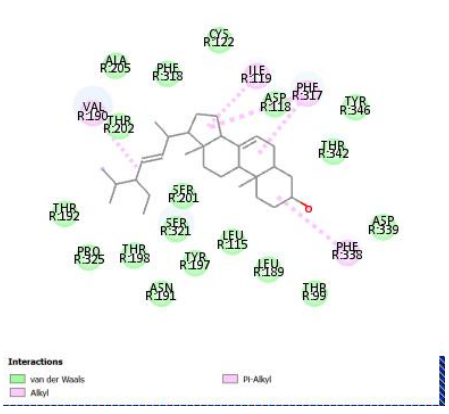

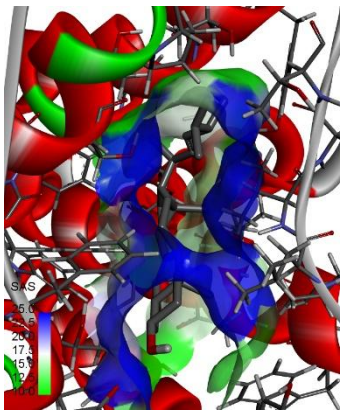

I

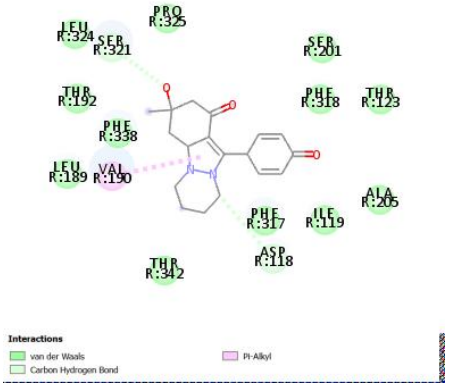
PRO R:325
LEU R:324
SER R:321
SER R:201
THR R:192
PHE R:318
THR R:123
PHE R:338
LEU R:189
VAL R:190
ALA R:205
PHE R:317
ILE R:119
ASP R:118
THR R:342
Interactions
van der Waals
Carbon Hydrogen Bond
Pi-Alkyl

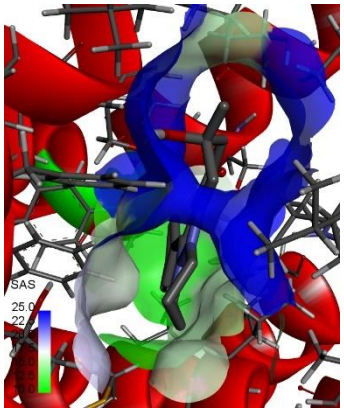
SAS

II

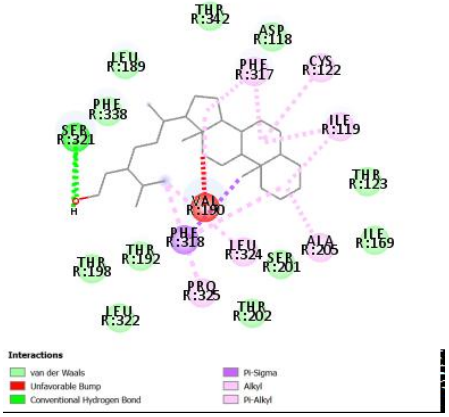
THR R:342
ASP R:118
LEU R:189
PHE R:317
CYS R:122
PHE R:338
ILE R:119
SER R:321
THR R:123
VAL R:190
PHE R:318
LEU R:324
ALA R:205
ILE R:169
THR R:192
SER R:201
THR R:198
PRO R:325
THR R:202
LEU R:322
Interactions
van der Waals
Unfavorable Bump
Conventional Hydrogen Bond
Pi-Sigma
Alkyl
Pi-Alkyl

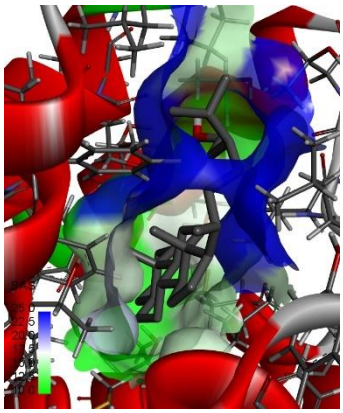

III

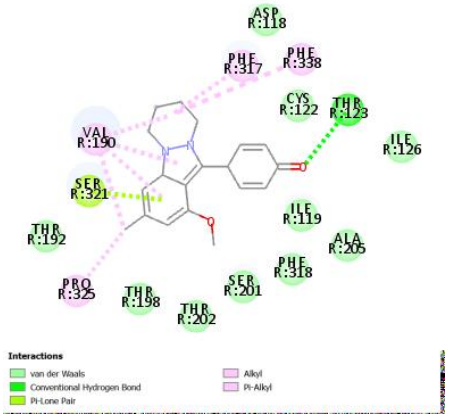
ASP R:118
PHE R:317
PHE R:338
CYS R:122
THR R:123
VAL R:190
ILE R:126
SER R:321
ILE R:119
THR R:192
ALA R:205
PHE R:318
PRO R:325
SER R:201
THR R:198
THR R:202
Interactions
van der Waals
Conventional Hydrogen Bond
Pi-Lone Pair
Alkyl
Pi-Alkyl

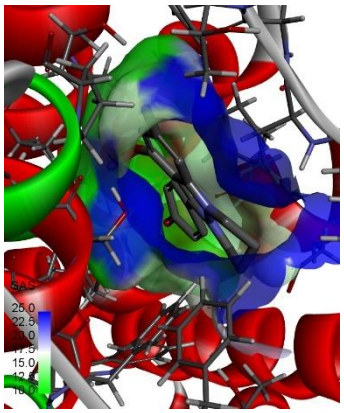

IV

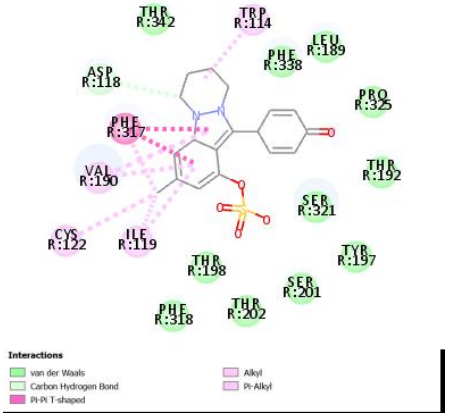
THR R:342
TRP R:114
LEU R:189
PHE R:338
ASP R:118
PRO R:325
PHE R:317
THR R:192
VAL R:190
SER R:321
CYS R:122
ILE R:119
TYR R:197
THR R:198
SER R:201
PHE R:318
THR R:202
Interactions
van der Waals
Carbon Hydrogen Bond
Pi-Pi T-shaped
Alkyl
Pi-Alkyl

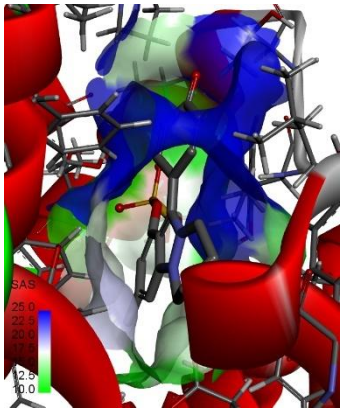
SAS
25.0
22.5
20.0
17.5
12.5
10.0

V

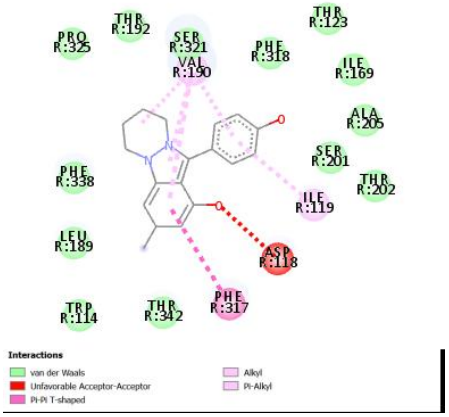
THR R:123
THR R:192
PRO R:325
SER R:321
PHE R:318
VAL R:190
ILE R:169
ALA R:205
SER R:201
PHE R:338
THR R:202
ILE R:119
LEU R:189
ASP R:118
TRP R:114
THR R:342
PHE R:317
Interactions
van der Waals
Unfavorable Acceptor-Acceptor
Pi-Pi T-shaped
Alkyl
Pi-Alkyl

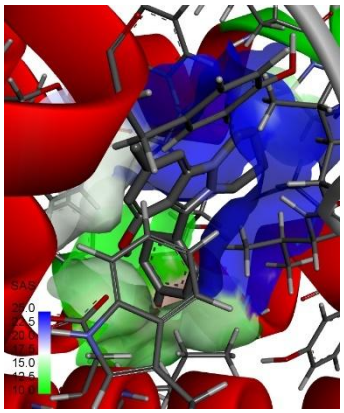
SAS
15.0
12.5
10.0

VI

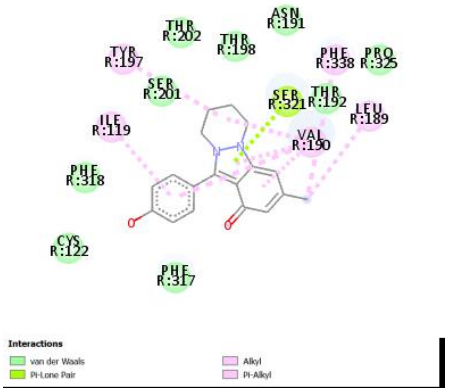
ASN R:191
THR R:202
THR R:198
TYR R:197
PHE R:338
PRO R:325
SER R:201
SER R:321
THR R:192
LEU R:189
ILE R:119
VAL R:190
PHE R:318
CYS R:122
PHE R:317
Interactions
van der Waals
Pi-Lone Pair
Alkyl
Pi-Alkyl

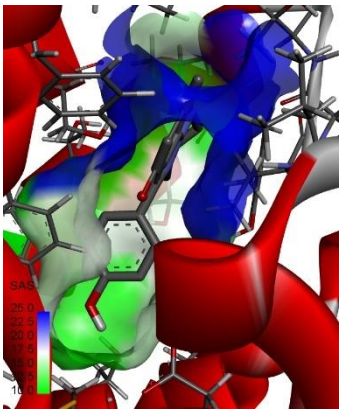
SAS
25.0
22.5
20.0
17.5
15.0

VII

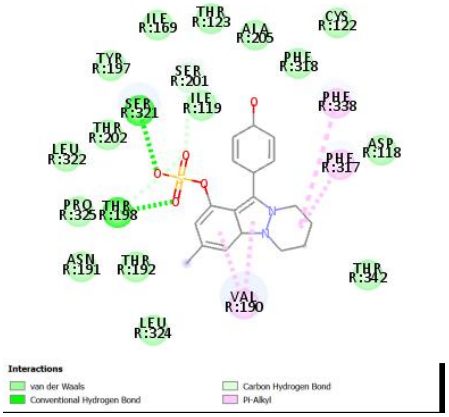
ILE R:169
THR R:123
ALA R:205
CYS R:122
TYR R:197
SER R:201
PHE R:318
SER R:321
ILE R:119
PHE R:338
THR R:202
LEU R:322
ASP R:118
PHE R:317
PRO R:325
THR R:198
ASN R:191
THR R:192
THR R:342
VAL R:190
LEU R:324
Interactions
van der Waals
Conventional Hydrogen Bond
Carbon Hydrogen Bond
Pi-Alkyl

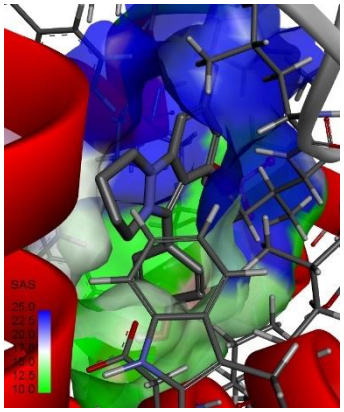
SAS

VIII

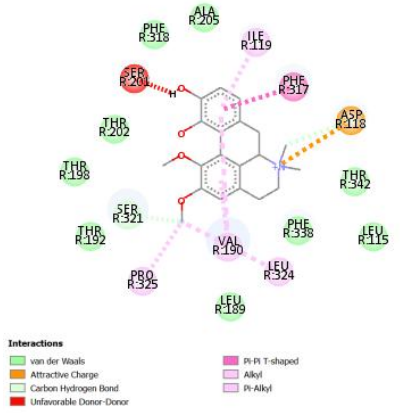
ALA R:205
PHE R:318
ILE R:119
SER R:201
PHE R:317
ASP R:118
THR R:202
THR R:198
THR R:342
SER R:321
THR R:192
VAL R:190
PHE R:338
LEU R:115
PRO R:325
LEU R:324
LEU R:189
Interactions
van der Waals
Attractive Charge
Carbon Hydrogen Bond
Unfavorable Donor-Donor
Pi-Pi T-shaped
Alkyl
Pi-Alkyl

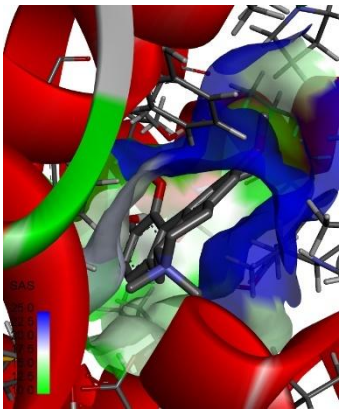
SAS

IX

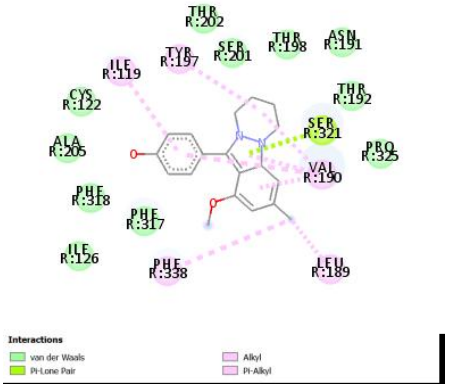
THR R:202
THR R:198
ASN R:191
SER R:201
TYR R:197
ILE R:119
THR R:192
CYS R:122
SER R:321
ALA R:205
PRO R:325
VAL R:190
PHE R:318
PHE R:317
ILE R:126
PHE R:338
LEU R:189
Interactions
van der Waals
Pi-Lone Pair
Alkyl
Pi-Alkyl

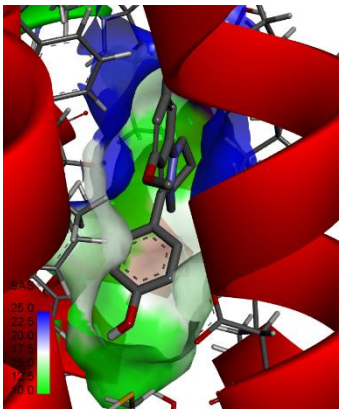
SAS

X

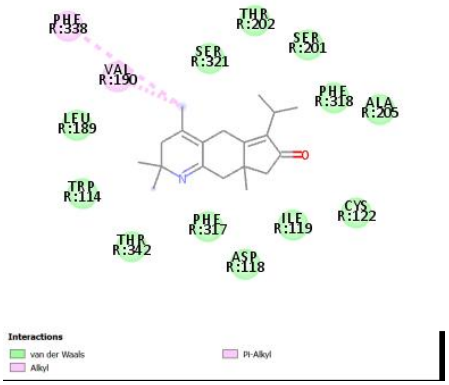
PHE R:338
THR R:202
SER R:201
SER R:321
VAL R:190
PHE R:318
ALA R:205
LEU R:189
TRP R:114
CYS R:122
PHE R:317
ILE R:119
THR R:342
ASP R:118
Interactions
van der Waals
Pi-Alkyl
Alkyl

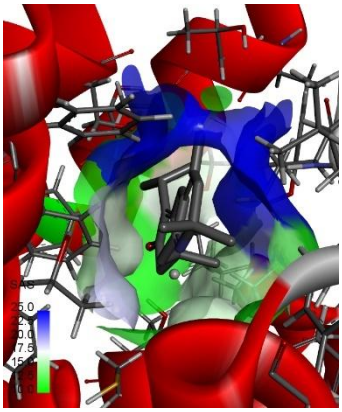

XI

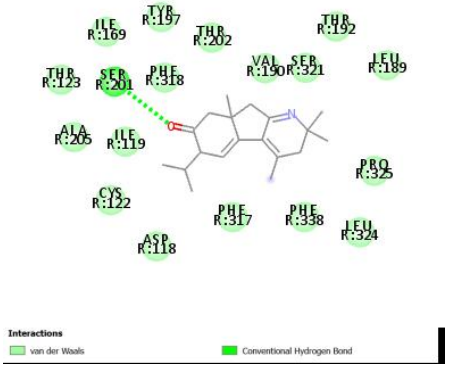
TYR R:197
ILE R:169
THR R:202
THR R:192
VAL R:190
SER R:321
LEU R:189
THR R:123
SER R:201
PHE R:318
ALA R:205
ILE R:119
PRO R:325
CYS R:122
PHE R:317
PHE R:338
LEU R:324
ASP R:118
Interactions
van der Waals
Conventional Hydrogen Bond

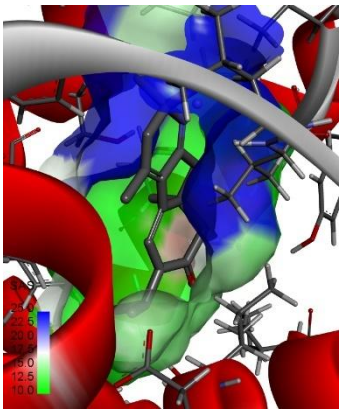

XII

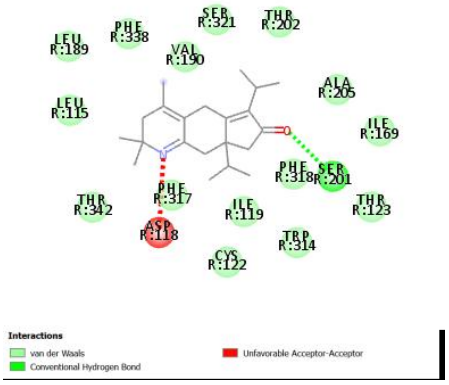
SER R:321
THR R:202
PHE R:338
LEU R:189
VAL R:190
ALA R:205
LEU R:115
ILE R:169
PHE R:318
SER R:201
PHE R:317
THR R:342
ILE R:119
THR R:123
ASP R:118
TRP R:314
CYS R:122
Interactions
van der Waals
Conventional Hydrogen Bond
Unfavorable Acceptor-Acceptor

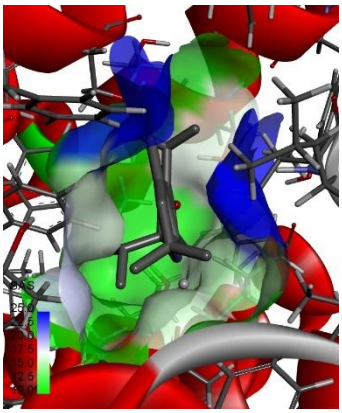

XIII

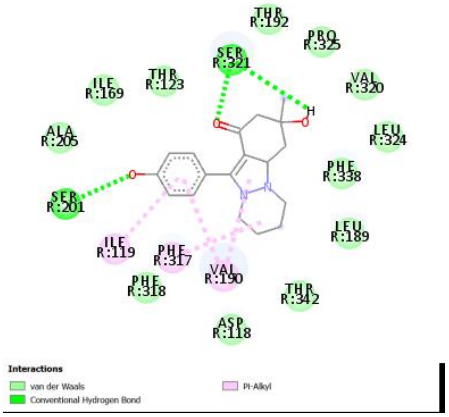

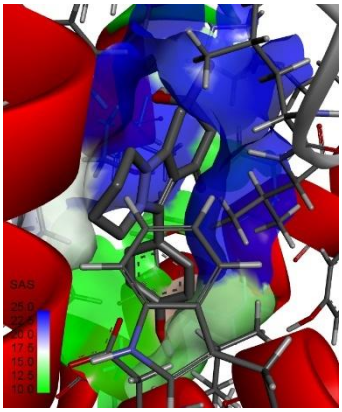

XIV

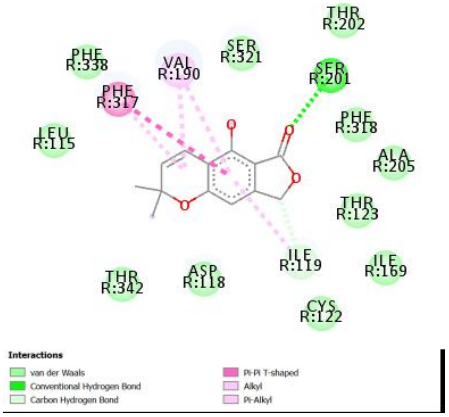

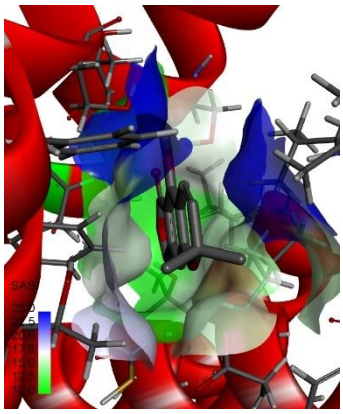

XV

Figure 3.1.2.2: 2D (left) and 3D (right) views of the molecular interactions of amino-acid residues of 5-HT1D receptor with (I) (3S,5S,9S,10S,13R,14R,17R)-17-[(E,2S,5S)-5-ethyl-6-methylhept-3-en-2-yl]-10,13-dimethyl-2,3,4,5,6,9,11,12,14,15,16,17-dodecahydro-1H-cyclopenta[a]phenanthren-3-ol (II) (3S)-3-hydroxy-3-methyl-11-(4-oxocyclohexa-2,5-dien-1-ylidene)-2,4,6,7,8,9-hexahydropyridazino[1,2-a]indazol-1-one (III) (3S,6R)-6-[(8R,9S,10S,13R,14S,17R)-10,13-dimethyl-2,3,4,5,6,7,8,9,11,12,14,15,16,17-tetradecahydro-1H-cyclopenta[a]phenanthren-17-yl]-3-propan-2-ylheptan-1-ol (IV) 4-(1-methoxy-3-methyl-6,7,8,9-tetrahydropyridazino[1,2-a]indazol-11-ylidene)cyclohexa-2,5-dien-1-one (V) [3-methyl-

11-(4-oxocyclohexa-2,5-dien-1-ylidene)-6,7,8,9-tetrahydropyridazino[1,2-a]indazol-1-yl] hydrogen sulfate (VI) 11-(4-hydroxyphenyl)-3-methyl-6,7,8,9-tetrahydropyridazino[1,2-a]indazol-10-ium-1-ol (VII) 6,7,8,9-Tetrahydro-11-(4-hydroxyphenyl)-3-methyl-1H-pyridazino(1,2-a)indazol-1-one (VIII) [11-(4-hydroxycyclohexa-2,5-dien-1-ylidene)-3-methyl-6,7,8,9-tetrahydropyridazino[1,2-a]indazol-1-yl]hydrogen sulfate (IX) (6aR)-1,2-dimethoxy-6,6-dimethyl-5,6,6a,7-tetrahydro-4H-dibenzo[de,g]quinolin-6-ium-10,11-diol (X) 4-(1-methoxy-3-methyl-6,7,8,9-tetrahydropyridazino[1,2-a]indazol-10-ium-11-yl)phenol (XI) Nigelladine B (XII) Nigelladine A (XIII) (8aR)-2,2,4-trimethyl-6,8a-di(propan-2-yl)-8,9-dihydrocyclopenta[g]quinolin-7-one (XIV) (3S)-3-hydroxy-11-(4-hydroxyphenyl)-3-methyl-2,4,6,7,8,9-hexahydropyridazino[1,2-a]indazol-10-ium-1-one (XV) Salfredin B11 in *Nigella sativa.*

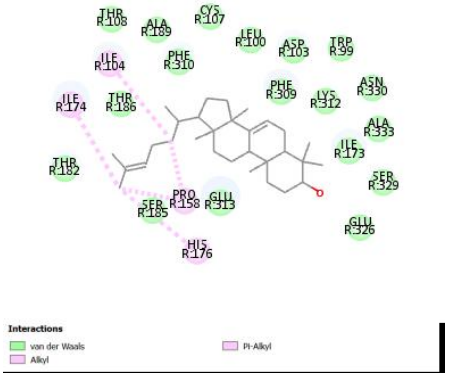

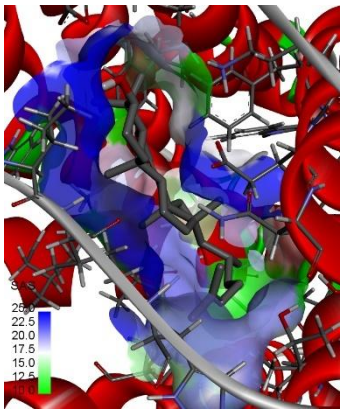

I

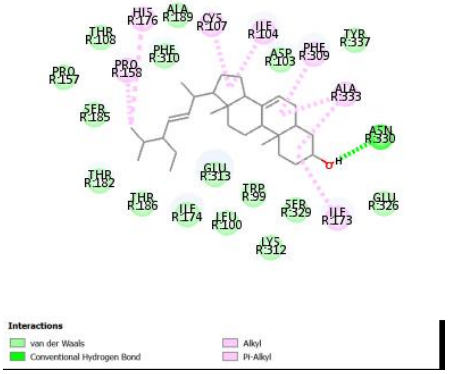
HIS R:176
ALA R:189
CYS R:107
ILE R:104
TYR R:337
THR R:108
PHE R:310
ASP R:103
PHE R:309
PRO R:157
PRO R:158
ALA R:333
SER R:185
ASN R:330
GLU R:313
THR R:182
TRP R:99
THR R:186
ILE R:174
LEU R:100
SER R:329
ILE R:173
GLU R:326
LYS R:312
Interactions
van der Waals
Conventional Hydrogen Bond
Alkyl
Pi-Alkyl

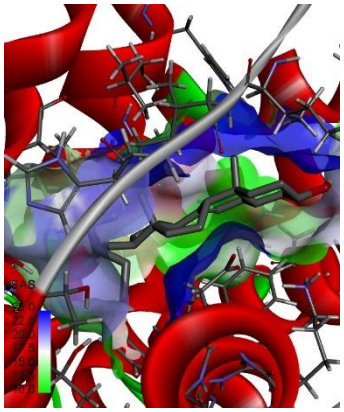

II

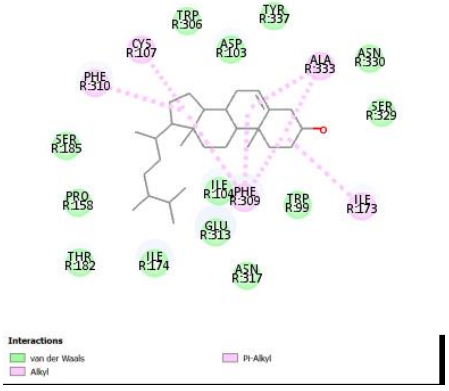
TRP R:306
TYR R:337
CYS R:107
ASP R:103
ALA R:333
ASN R:330
PHE R:310
SER R:329
SER R:185
ILE R:104
PHE R:309
TRP R:99
ILE R:173
PRO R:158
GLU R:313
THR R:182
ILE R:174
ASN R:317
Interactions
van der Waals
Alkyl
Pi-Alkyl

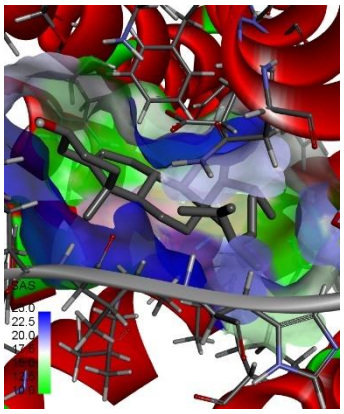

III

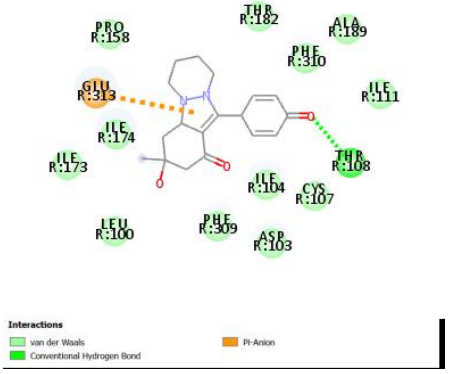
THR R:182
PRO R:158
ALA R:189
PHE R:310
GLU R:313
ILE R:111
ILE R:174
ILE R:173
THR R:108
ILE R:104
CYS R:107
LEU R:100
PHE R:309
ASP R:103
Interactions
van der Waals
Conventional Hydrogen Bond
Pi-Anion

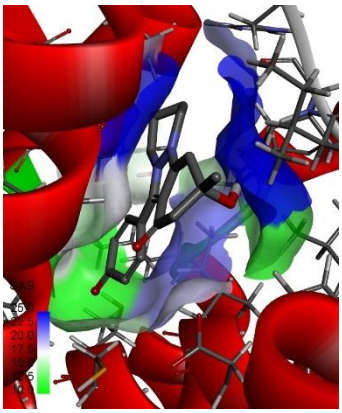

IV

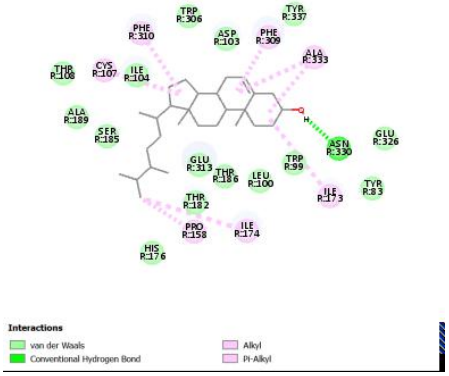
TRP R:306
TYR R:337
PHE R:310
ASP R:103
PHE R:309
ALA R:333
THR R:108
CYS R:107
ILE R:104
ALA R:189
SER R:185
GLU R:326
ASN R:330
GLU R:313
THR R:186
LEU R:100
TRP R:99
TYR R:83
ILE R:173
THR R:182
PRO R:158
ILE R:174
HIS R:176
Interactions
van der Waals
Conventional Hydrogen Bond
Alkyl
Pi-Alkyl

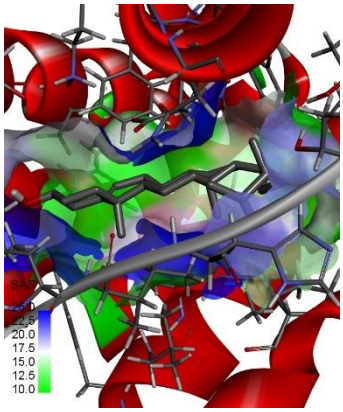
SAS
25.0
22.5
20.0
17.5
15.0
12.5
10.0

V

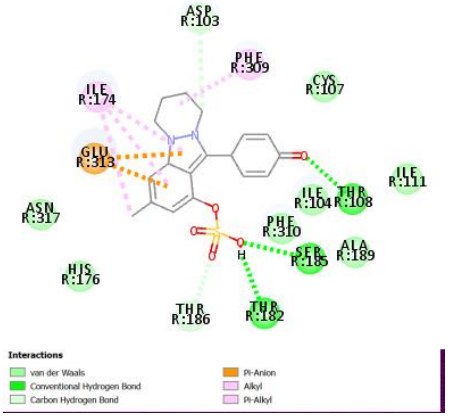
ASP R:103
PHE R:309
CYS R:107
ILE R:174
GLU R:313
ILE R:111
ILE R:104
THR R:108
ASN R:317
PHE R:310
SER R:185
ALA R:189
HIS R:176
THR R:186
THR R:182
Interactions
van der Waals
Conventional Hydrogen Bond
Carbon Hydrogen Bond
Pi-Anion
Alkyl
Pi-Alkyl

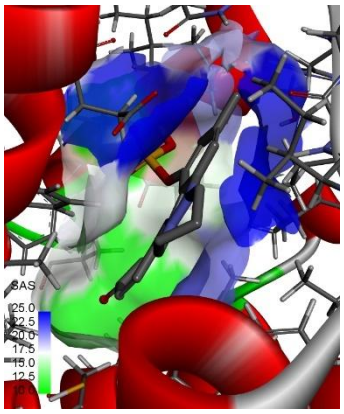
SAS
25.0
22.5
20.0
17.5
15.0
12.5

VI

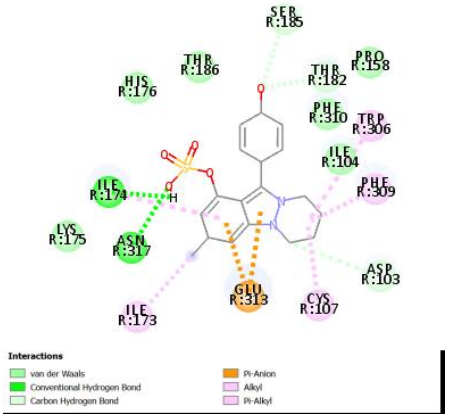
SER R:185
THR R:186
PRO R:158
HIS R:176
THR R:182
PHE R:310
TRP R:306
ILE R:104
ILE R:174
PHE R:309
LYS R:175
ASN R:317
ASP R:103
GLU R:313
CYS R:107
ILE R:173
Interactions
van der Waals
Conventional Hydrogen Bond
Carbon Hydrogen Bond
Pi-Anion
Alkyl
Pi-Alkyl

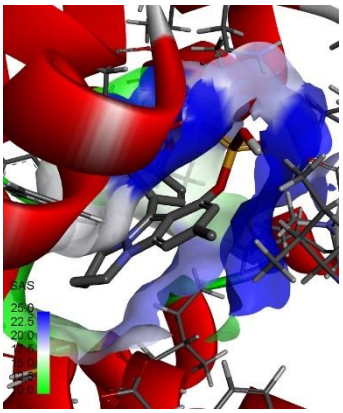
SAS
25.0
22.5
20.0

VII

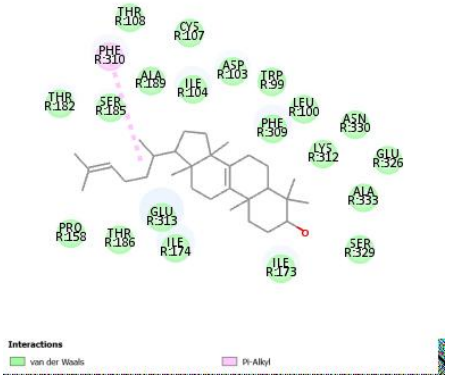
THR R:108
CYS R:107
PHE R:310
ASP R:103
ALA R:189
TRP R:99
ILE R:104
THR R:182
SER R:185
LEU R:100
PHE R:309
ASN R:330
LYS R:312
GLU R:326
ALA R:333
GLU R:313
PRO R:158
THR R:186
ILE R:174
SER R:329
ILE R:173
Interactions
van der Waals
Pi-Alkyl

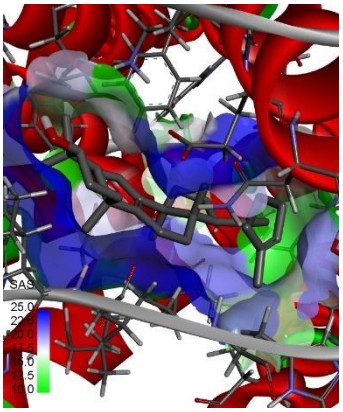
SAS

VIII

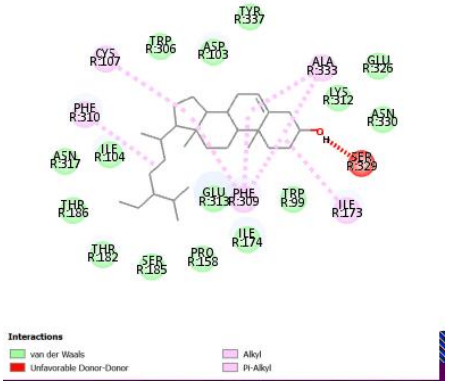
TYR R:337
TRP R:306
ASP R:103
CYS R:107
ALA R:333
GLU R:326
LYS R:312
PHE R:310
ASN R:330
ASN R:317
ILE R:104
SER R:329
GLU R:313
PHE R:309
TRP R:99
THR R:186
ILE R:173
ILE R:174
THR R:182
SER R:185
PRO R:158
Interactions
van der Waals
Unfavorable Donor-Donor
Alkyl
Pi-Alkyl

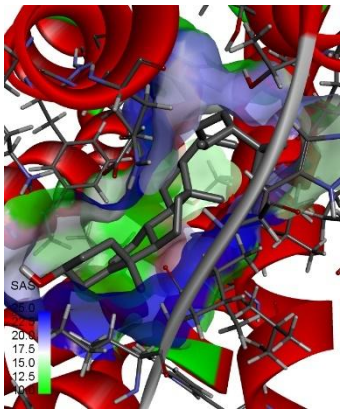
SAS
20.0
17.5
15.0
12.5

IX

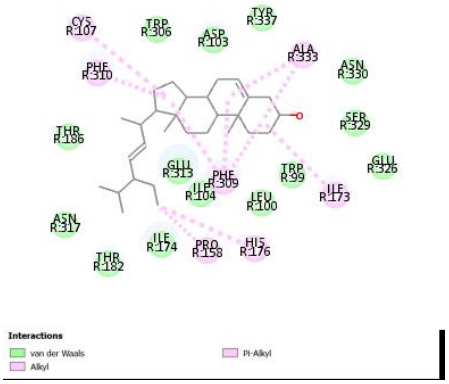
TYR R:337
CYS R:107
TRP R:306
ASP R:103
ALA R:333
PHE R:310
ASN R:330
SER R:329
THR R:186
GLU R:313
PHE R:309
TRP R:99
GLU R:326
ILE R:104
LEU R:100
ILE R:173
ASN R:317
ILE R:174
PRO R:158
HIS R:176
THR R:182
Interactions
van der Waals
Alkyl
Pi-Alkyl

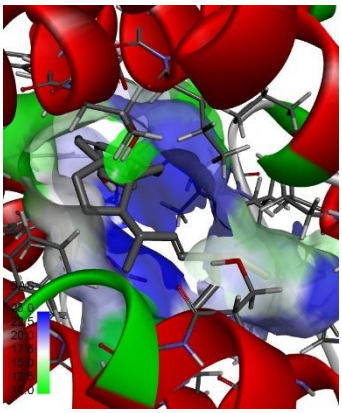

X

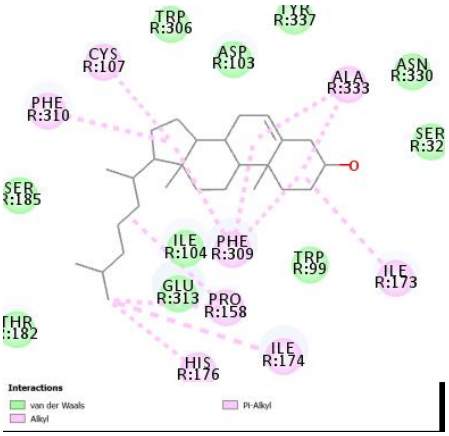

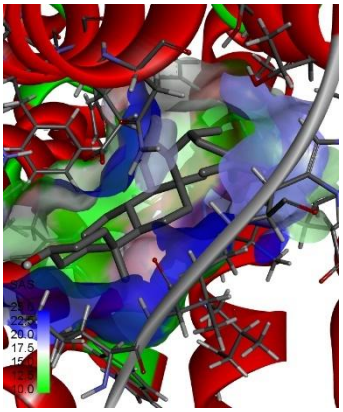

XI

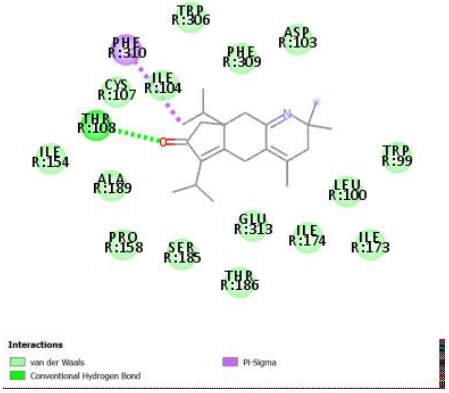

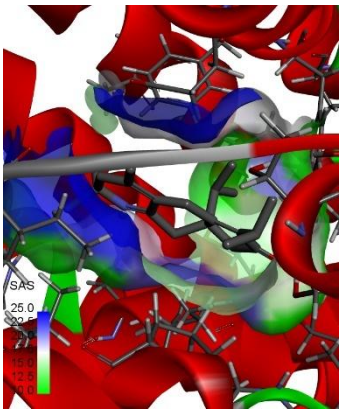

XII

Figure 3.1.2.3: 2D (left) and 3D (right) views of the molecular interactions of amino-acid residues of 5-HT1F receptor with (I) Butyrospermol (II) (3S,5S,9S,10S,13R,14R,17R)-17-[(E,2S,5S)-5-ethyl-6-methylhept-3-en-2-yl]-10,13-dimethyl-2,3,4,5,6,9,11,12,14,15,16,17-dodecahydro-1H-cyclopenta[a]phenanthren-3-ol (III) (3S,8R,9R,10R,13R,14R,17R)-17-[(2R,5R)-5,6-dimethylheptan-2-yl]-10,13-dimethyl-2,3,4,7,8,9,11,12,14,15,16,17-dodecahydro-1H-cyclopenta[a]phenanthren-3-ol (IV) (3S)-3-hydroxy-3-methyl-11-(4-oxocyclohexa-2,5-dien-1-ylidene)-2,4,6,7,8,9-hexahydropyridazino[1,2-a]indazol-1-one (V) Campesterol (VI) [3-methyl-11-(4-oxocyclohexa-2,5-dien-1-ylidene)-6,7,8,9-tetrahydropyridazino[1,2-a]indazol-1-yl]

hydrogen sulfate (VII) [11-(4-hydroxycyclohexa-2,5-dien-1-ylidene)-3-methyl-6,7,8,9-tetrahydropyridazino[1,2-a]indazol-1-yl]hydrogen sulfate (VIII) (+)-Tirucallol (IX) 3S,8R,9R,10R,13R,14R,17R)-17-[(2R,5R)-5-ethyl-6-methylheptan-2-yl]-10,13-dimethyl-2,3,4,7,8,9,11,12,14,15,16,17-dodecahydro-1H-cyclopenta[a]phenanthren-3-ol (X) (3S,8R,9R,10R,13R,14R,17R)-17-[(E,2S,5S)-5-ethyl-6-methylhept-3-en-2-yl]-10,13-dimethyl-2,3,4,7,8,9,11,12,14,15,16,17-dodecahydro-1H-cyclopenta[a]phenanthren-3-ol (XI) (3S,8R,9R,10R,13R,14R,17R)-10,13-dimethyl-17-[(2R)-6-methylheptan-2-yl]-2,3,4,7,8,9,11,12,14,15,16,17-dodecahydro-1H-cyclopenta[a]phenanthren-3-ol (XII) (8aR)-2,2,4-trimethyl-6,8a-di(propan-2-yl)-8,9-dihydrocyclopenta[g]quinolin-7-one in *Nigella sativa.*

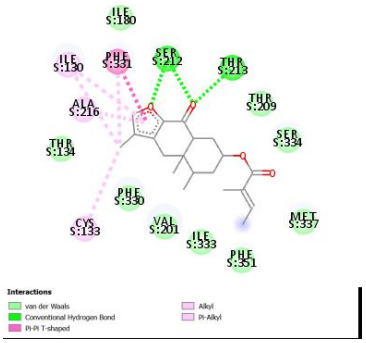

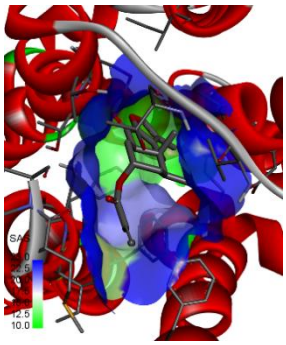

I

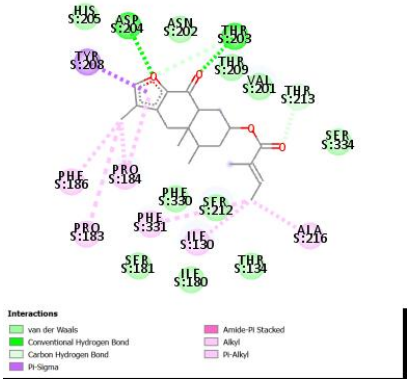

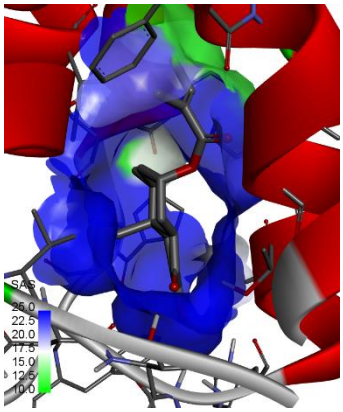

II

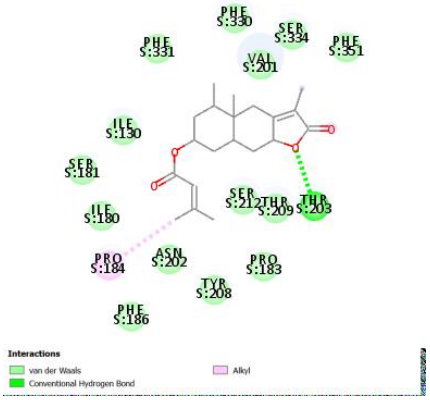
PHE S:330
SER S:334
PHE S:331
PHE S:351
VAL S:201
ILE S:130
SER S:181
SER S:212
THR S:209
THR S:203
ILE S:180
PRO S:184
ASN S:202
PRO S:183
TYR S:208
PHE S:186
Interactions
van der Waals
Alkyl
Conventional Hydrogen Bond

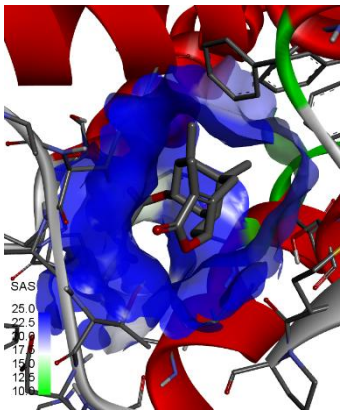
SAS
25.0

III

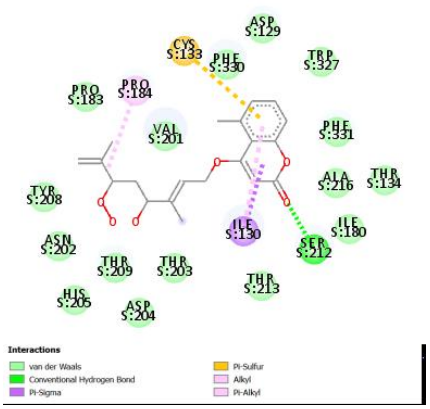
ASP S:129
CYS S:133
PHE S:330
TRP S:327
PRO S:183
PRO S:184
VAL S:201
PHE S:331
ALA S:216
THR S:134
TYR S:208
ILE S:130
ILE S:180
ASN S:202
SER S:212
THR S:209
THR S:203
THR S:213
HIS S:205
ASP S:204
Interactions
van der Waals
Conventional Hydrogen Bond
Pi-Sigma
Pi-Sulfur
Alkyl
Pi-Alkyl

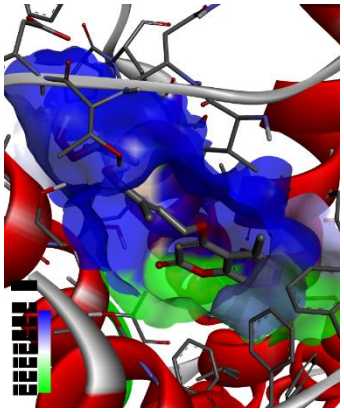

IV

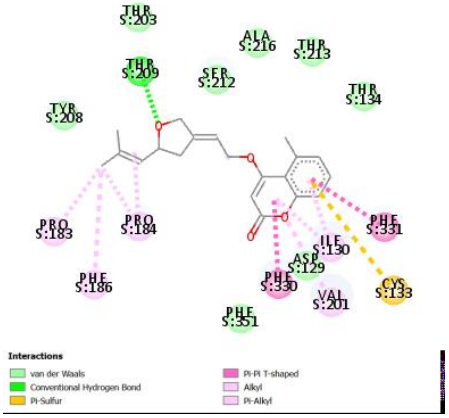
THR S:203
ALA S:216
THR S:213
THR S:209
SER S:212
THR S:134
TYR S:208
PRO S:183
PRO S:184
PHE S:331
ILE S:130
ASP S:129
PHE S:186
PHE S:330
CYS S:133
VAL S:201
PHE S:351
Interactions
van der Waals
Conventional Hydrogen Bond
Pi-Sulfur
Pi-Pi T-shaped
Alkyl
Pi-Alkyl

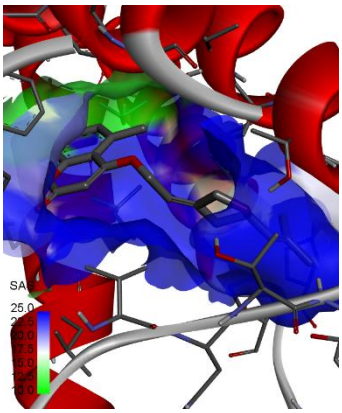
SA
25.0

V

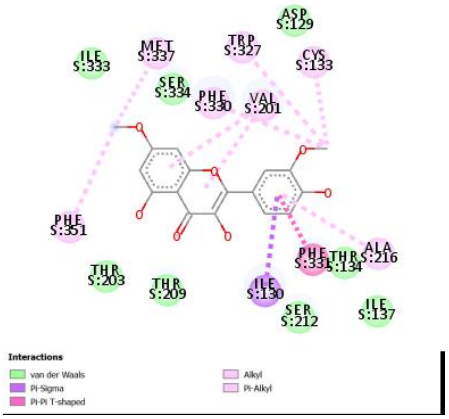

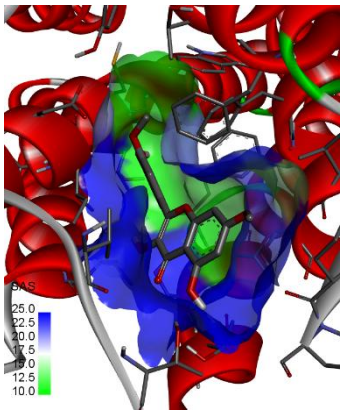

VI

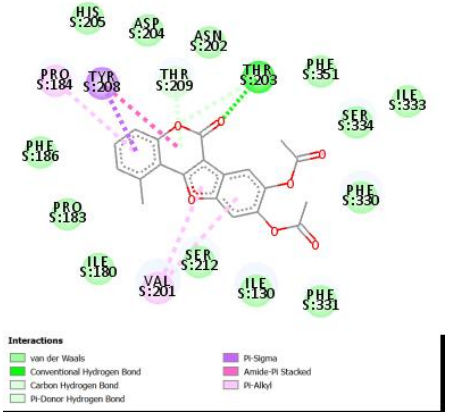

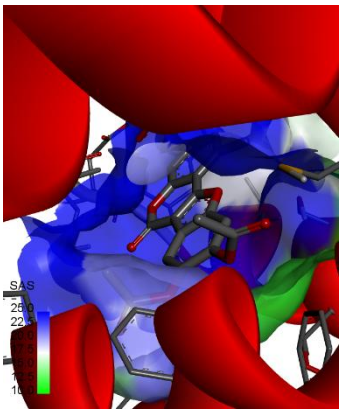

VII

Figure 3.1.3.1: 2D (left) and 3D (right) views of the molecular interactions of amino-acid residues of 5-HT1Breceptor with (I) [(4aR,5S,7S,8aR)-3,4a,5-trimethyl-9-oxo-4,5, 6, 7, 8,8a-hexahydrobenzo[f][1]benzofuran-7-yl](Z)-2-methylbut-2-enoate (II) [(4aR,5S, 7S,8aR)-3,4a,5-trimethyl-9-oxo-4,5,6,7,8,8a-hexahydrobenzo[f] [1] benzo -furan-7-yl] 2-methylbut-2-enoate (III) [(4aR,5S,7R,8aR,9aS)-3,4a,5-trimethyl-2-oxo-4,5,6,7,8,8a,9,9a-octahydrobenzo[f][1]benzofuran-7-yl]3-methylbut-2-enoate (IV) 4-[(2E,4S,6S)-6-hydroperoxy-

4-hydroxy-3,7-dimethylocta-2,7-dienoxy]-5-methylchromen-2-one (V) 5-methyl-4-[(2Z)-2-[(5R)-5-(2-methylprop-1-enyl)oxolan-3-ylidene]ethoxy]chromen-2-one (VI) Rhamnazin (VII) (9-acetyloxy-1-methyl-6-oxo-[1]benzofuro[3,2-c]chromen-8-yl) acetate in *Petasites hybridus.*

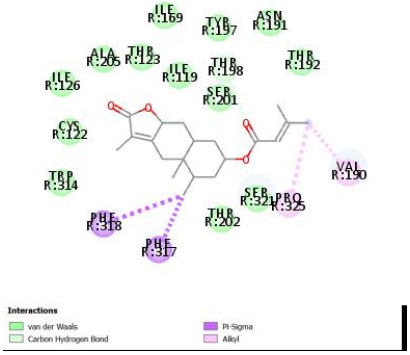

I

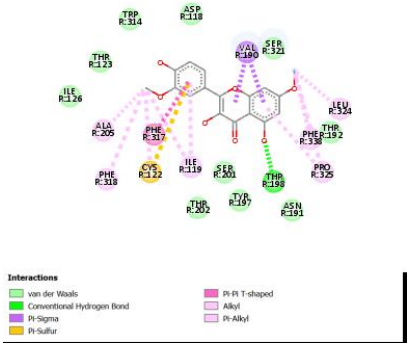

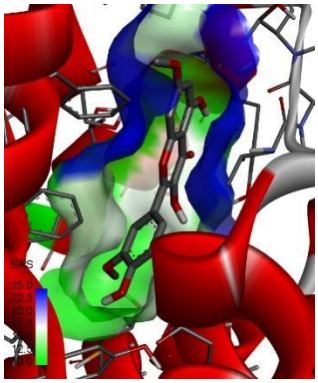

II

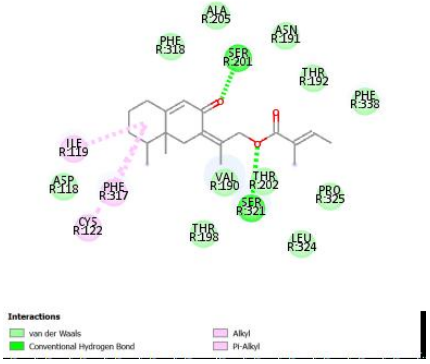
ALA R:205
ASN R:191
PHE R:318
SER R:201
THR R:192
PHE R:338
ILE R:119
ASP R:118
PHE R:317
VAL R:190
THR R:202
PRO R:325
SER R:321
CYS R:122
THR R:198
LEU R:324
Interactions
van der Waals
Conventional Hydrogen Bond
Alkyl
Pi-Alkyl

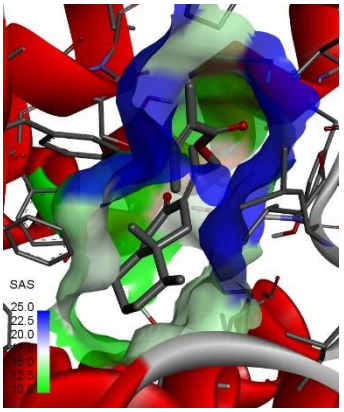
SAS
25.0
22.5
20.0

III

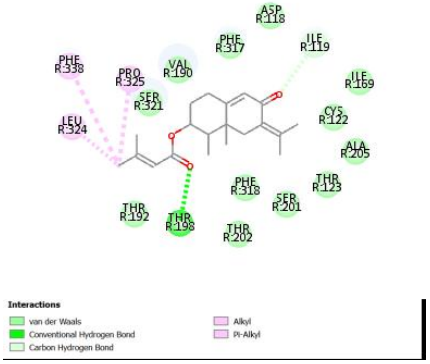
ASP R:118
PHE R:317
ILE R:119
PHE R:338
PRO R:325
VAL R:190
ILE R:169
SER R:321
CYS R:122
LEU R:324
ALA R:205
PHE R:318
THR R:123
SER R:201
THR R:192
THR R:198
THR R:202
Interactions
van der Waals
Conventional Hydrogen Bond
Carbon Hydrogen Bond
Alkyl
Pi-Alkyl

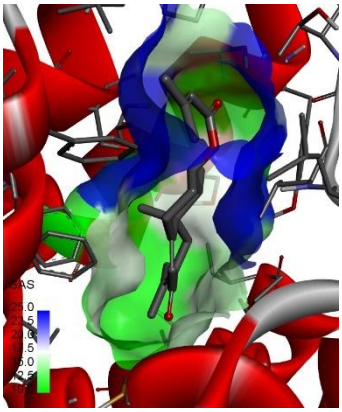
SAS
25.0
22.5
20.0

IV

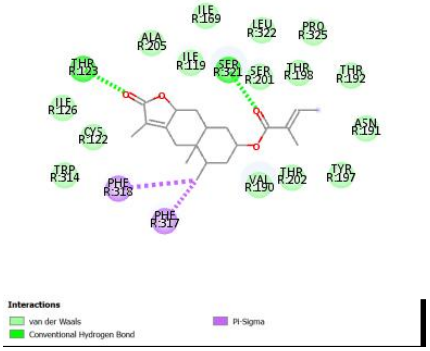
ILE R:169
LEU R:322
PRO R:325
ALA R:205
THR R:123
ILE R:119
SER R:321
SER R:201
THR R:198
THR R:192
ILE R:126
CYS R:122
ASN R:191
TRP R:314
PHE R:318
VAL R:190
THR R:202
TYR R:197
PHE R:317
Interactions
van der Waals
Conventional Hydrogen Bond
Pi-Sigma

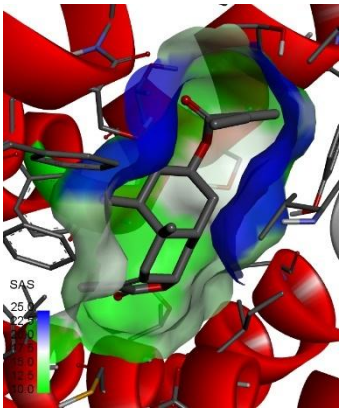
SAS
25.0
22.5
20.0

V

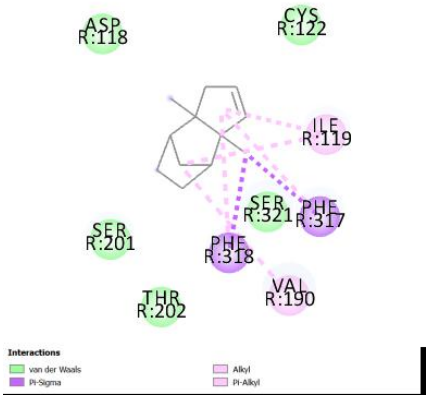
ASP
R:118
CYS
R:122
ILE
R:119
SER
R:321
PHE
R:317
SER
R:201
PHE
R:318
VAL
R:190
THR
R:202
Interactions
van der Waals
Alkyl
Pi-Sigma
Pi-Alkyl

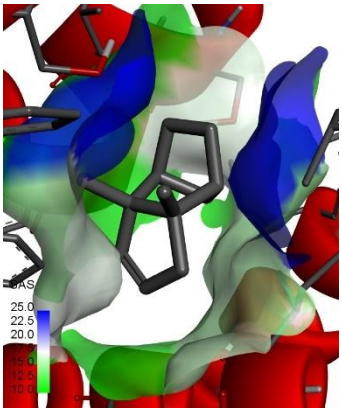
SAS
25.0
22.5
20.0

VI

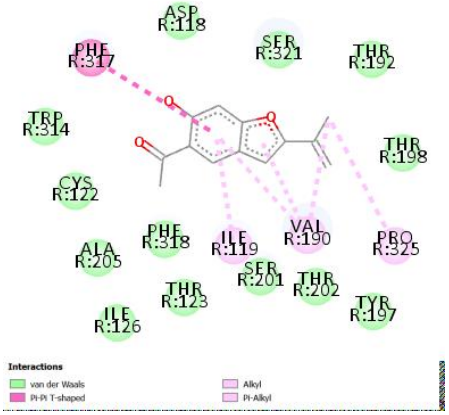
ASP
R:118
PHE
R:317
SER
R:321
THR
R:192
TRP
R:314
THR
R:198
CYS
R:122
PHE
R:318
ILE
R:119
VAL
R:190
PRO
R:325
ALA
R:205
SER
R:201
THR
R:202
THR
R:123
TYR
R:197
ILE
R:126
Interactions
van der Waals
Alkyl
Pi-Pi T-shaped
Pi-Alkyl

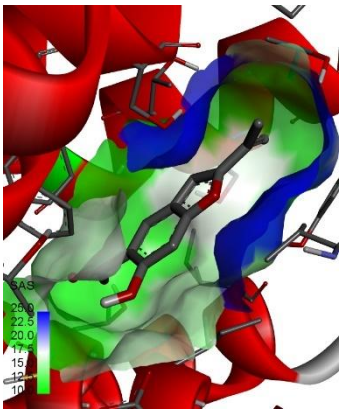
SAS
25.0
22.5
20.0

VII

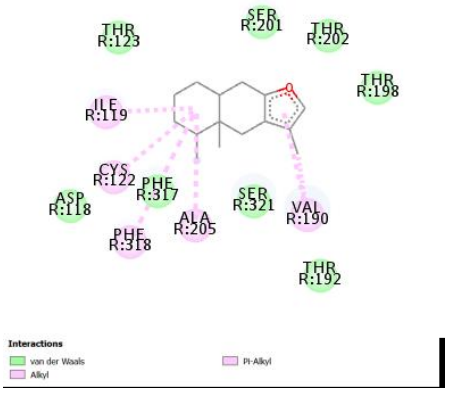
THR
R:123
SER
R:201
THR
R:202
THR
R:198
ILE
R:119
CYS
R:122
PHE
R:317
ASP
R:118
SER
R:321
VAL
R:190
ALA
R:205
PHE
R:318
THR
R:192
Interactions
van der Waals
Alkyl
Pi-Alkyl

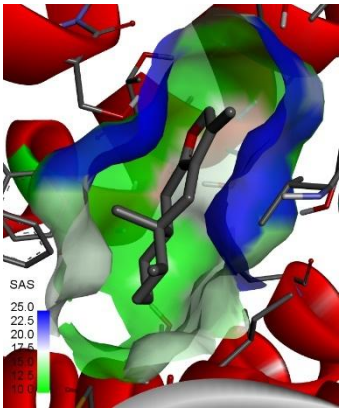
SAS
25.0
22.5
20.0

VIII

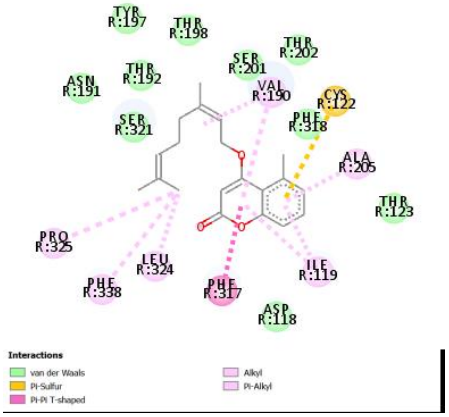
TYR R:197
THR R:198
THR R:202
SER R:201
THR R:192
ASN R:191
VAL R:190
CYS R:122
SER R:321
PHE R:318
ALA R:205
THR R:123
PRO R:325
LEU R:324
ILE R:119
PHE R:338
PHE R:317
ASP R:118
Interactions
van der Waals
Pi-Sulfur
Pi-Pi T-shaped
Alkyl
Pi-Alkyl

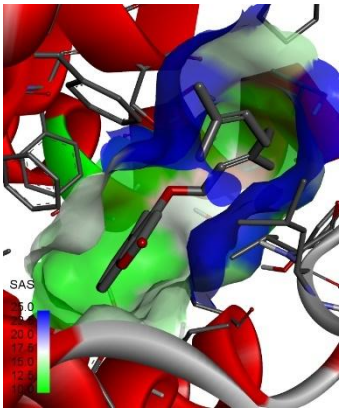
SAS

IX

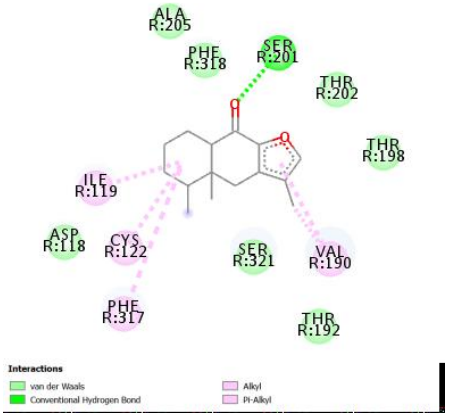
ALA R:205
PHE R:318
SER R:201
THR R:202
THR R:198
ILE R:119
ASP R:118
CYS R:122
SER R:321
VAL R:190
PHE R:317
THR R:192
Interactions
van der Waals
Conventional Hydrogen Bond
Alkyl
Pi-Alkyl

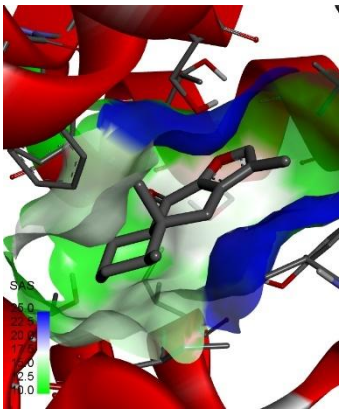
SAS

X

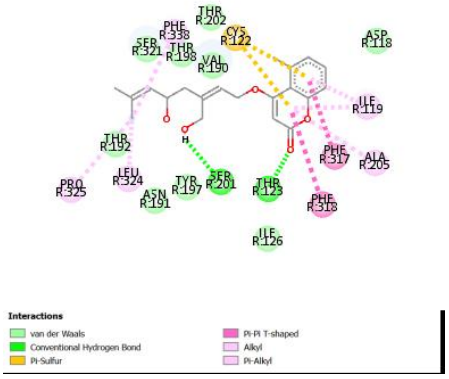
THR R:202
PHE R:338
CYS R:122
ASP R:118
SER R:321
THR R:198
VAL R:190
ILE R:119
THR R:192
PHE R:317
ALA R:205
PRO R:325
LEU R:324
TYR R:197
SER R:201
THR R:123
ASN R:191
PHE R:318
ILE R:126
Interactions
van der Waals
Conventional Hydrogen Bond
Pi-Sulfur
Pi-Pi T-shaped
Alkyl
Pi-Alkyl

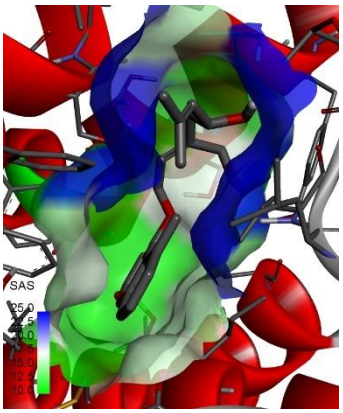
SAS

XI

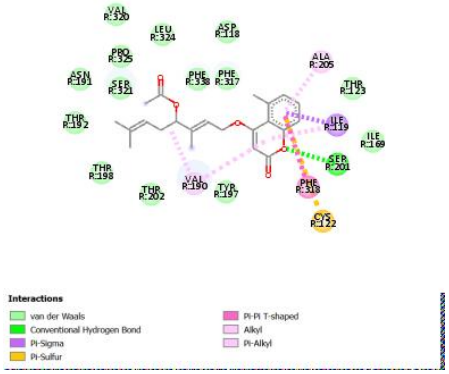
VAL R:326
LEU R:324
ASP R:118
PRO R:325
ASN R:193
SER R:321
PHE R:338
PHE R:317
ALA R:205
THR R:123
THR R:192
ILE R:119
ILE R:169
SER R:201
THR R:198
VAL R:190
TYR R:197
PHE R:318
THR R:202
CYS R:122
Interactions
van der Waals
Conventional Hydrogen Bond
Pi-Sigma
Pi-Sulfur
Pi-Pi T-shaped
Alkyl
Pi-Alkyl

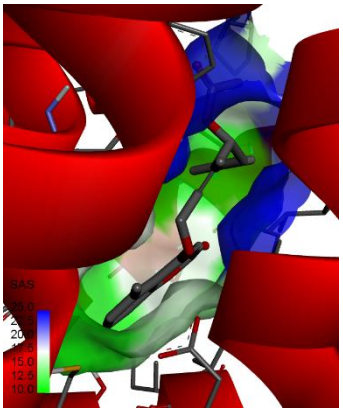
SAS
20.0
15.0
12.5
10.0

XII

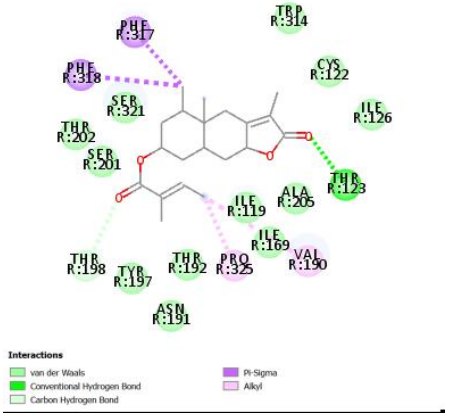
TRP R:314
PHE R:317
CYS R:122
PHE R:318
SER R:321
ILE R:126
THR R:202
SER R:201
THR R:123
ALA R:205
ILE R:119
ILE R:169
THR R:198
TYR R:197
THR R:192
PRO R:325
VAL R:190
ASN R:191
Interactions
van der Waals
Conventional Hydrogen Bond
Carbon Hydrogen Bond
Pi-Sigma
Alkyl

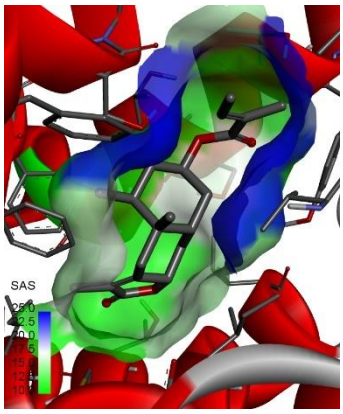
SAS

XIII

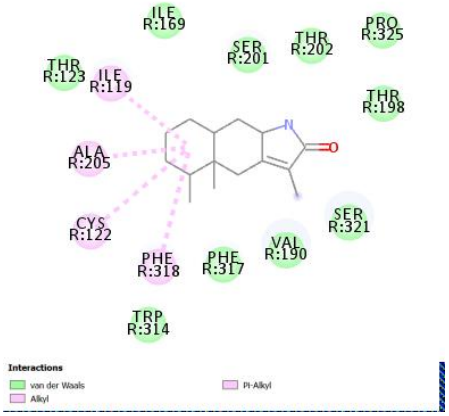
ILE R:169
PRO R:325
SER R:201
THR R:202
THR R:123
ILE R:119
THR R:198
ALA R:205
SER R:321
CYS R:122
VAL R:190
PHE R:318
PHE R:317
TRP R:314
Interactions
van der Waals
Alkyl
Pi-Alkyl

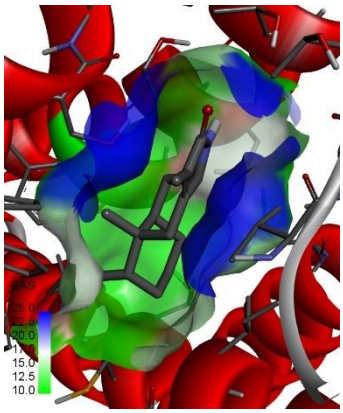
15.0
12.5
10.0

XIV

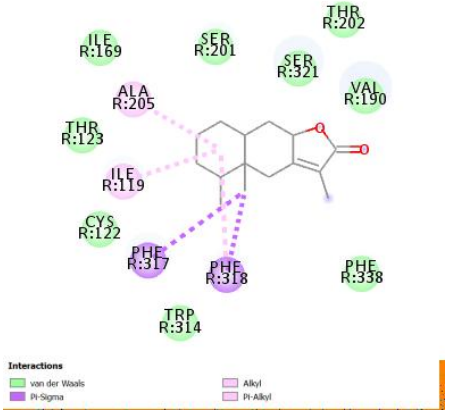
THR R:202
ILE R:169
SER R:201
SER R:321
VAL R:190
ALA R:205
THR R:123
ILE R:119
CYS R:122
PHE R:317
PHE R:318
PHE R:338
TRP R:314
Interactions
van der Waals
Alkyl
Pi-Sigma
Pi-Alkyl

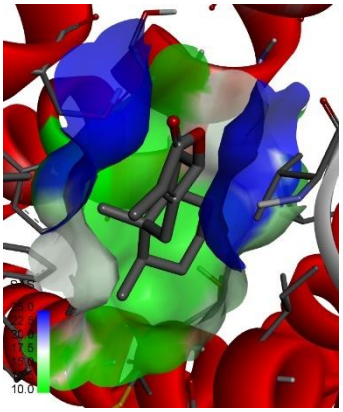
10.0

XV

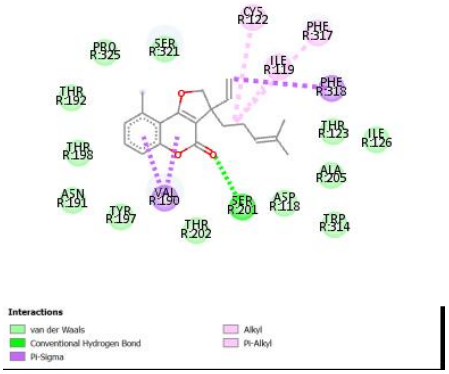
CYS R:122
PHE R:317
PRO R:325
SER R:321
ILE R:119
PHE R:318
THR R:192
THR R:123
ILE R:126
THR R:198
ALA R:205
ASN R:191
VAL R:190
TYR R:197
SER R:201
ASP R:118
THR R:202
TRP R:314
Interactions
van der Waals
Alkyl
Conventional Hydrogen Bond
Pi-Alkyl
Pi-Sigma

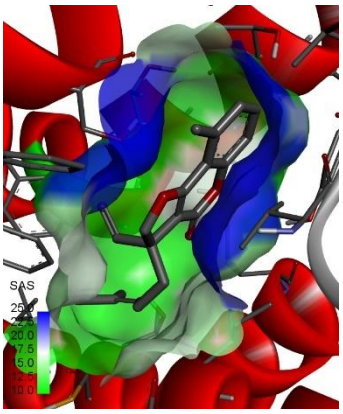
SAS

XVI

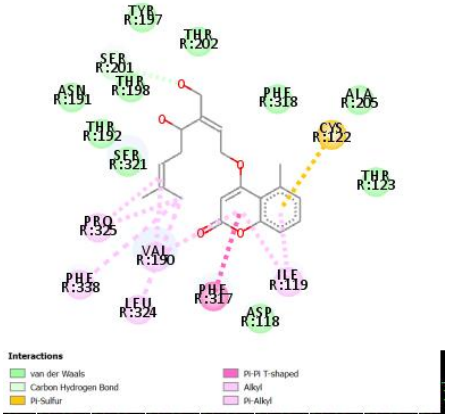
TYR R:197
THR R:202
SER R:201
ASN R:191
THR R:198
PHE R:318
ALA R:205
THR R:192
CYS R:122
SER R:321
THR R:123
PRO R:325
VAL R:190
PHE R:338
ILE R:119
PHE R:317
LEU R:324
ASP R:118
Interactions
van der Waals
Pi-Pi T-shaped
Carbon Hydrogen Bond
Alkyl
Pi-Sulfur
Pi-Alkyl

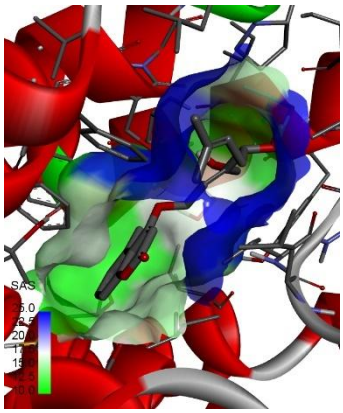
SAS

XVII

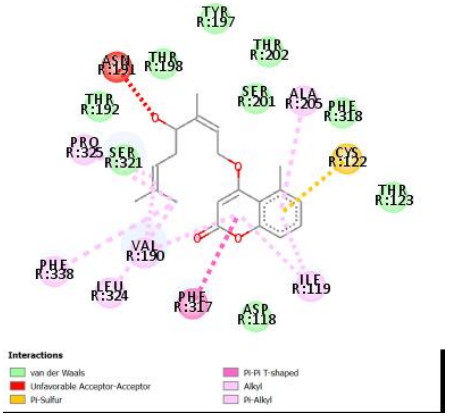
TYR R:197
THR R:202
ASN R:191
THR R:198
SER R:201
ALA R:205
PHE R:318
THR R:192
PRO R:325
SER R:321
CYS R:122
THR R:123
VAL R:190
PHE R:338
ILE R:119
LEU R:324
PHE R:317
ASP R:118
Interactions
van der Waals
Unfavorable Acceptor-Acceptor
Pi-Sulfur
Pi-Pi T-shaped
Alkyl
Pi-Alkyl

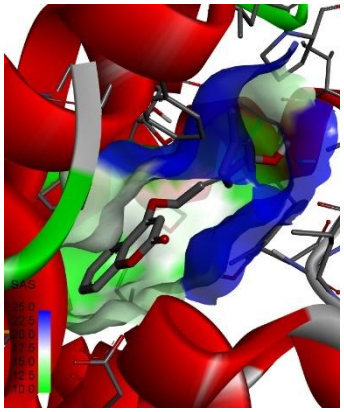

XVIII

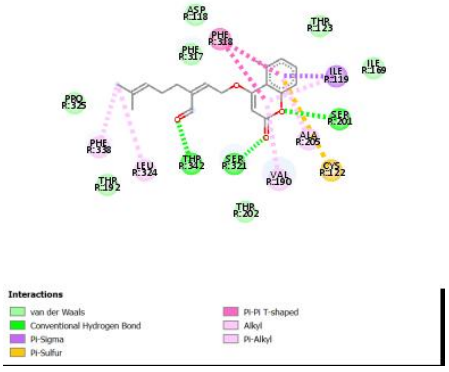
ASP R:118
THR R:123
PHE R:338
PHE R:317
ILE R:119
ILE R:189
PRO R:325
SER R:201
ALA R:205
PHE R:338
LEU R:324
THR R:342
SER R:321
VAL R:190
CYS R:122
THR R:192
THR R:202
Interactions
van der Waals
Conventional Hydrogen Bond
Pi-Sigma
Pi-Sulfur
Pi-Pi T-shaped
Alkyl
Pi-Alkyl

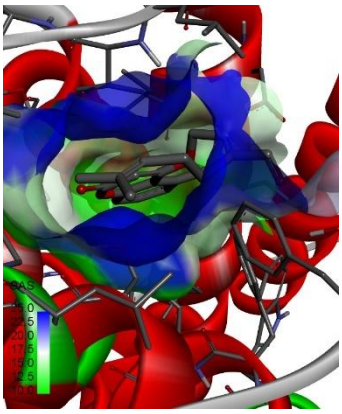

XIX

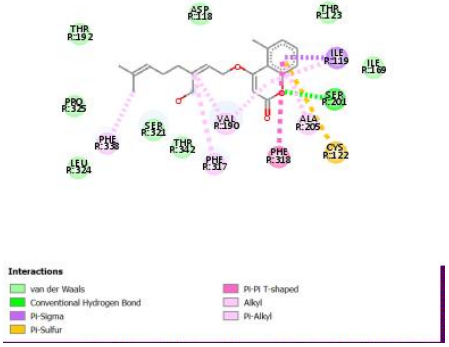
ASP R:118
THR R:123
THR R:192
ILE R:119
ILE R:189
PRO R:325
SER R:201
SER R:321
VAL R:190
ALA R:205
PHE R:338
THR R:342
PHE R:317
PHE R:318
LEU R:324
CYS R:122
Interactions
van der Waals
Conventional Hydrogen Bond
Pi-Sigma
Pi-Sulfur
Pi-Pi T-shaped
Alkyl
Pi-Alkyl

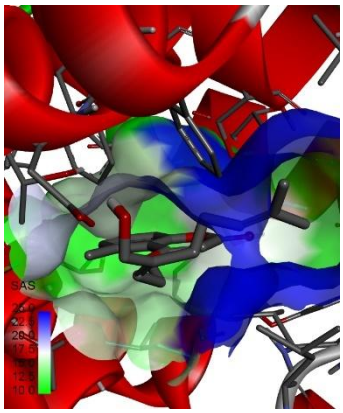

XX

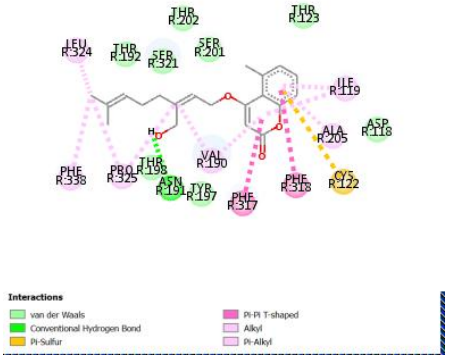

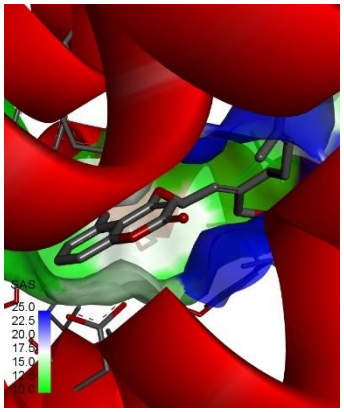

XXI

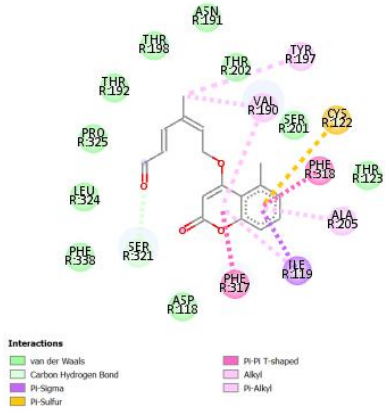

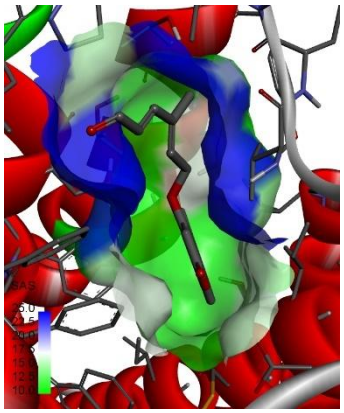

XXII

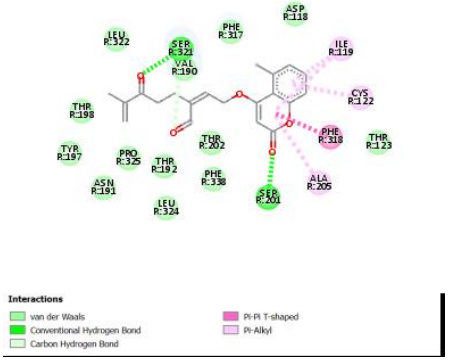

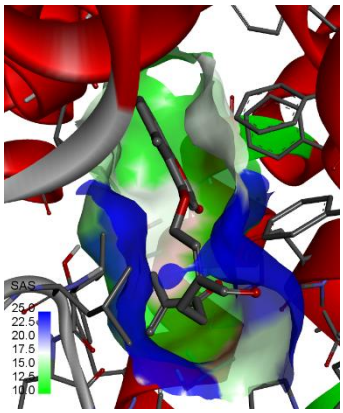

XXIII

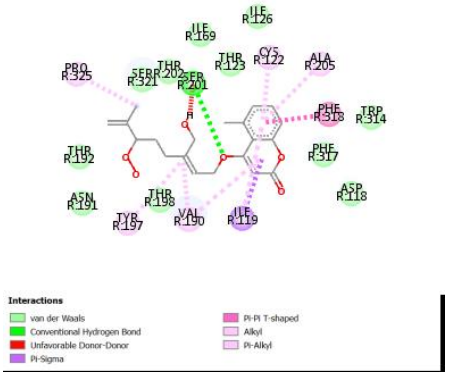

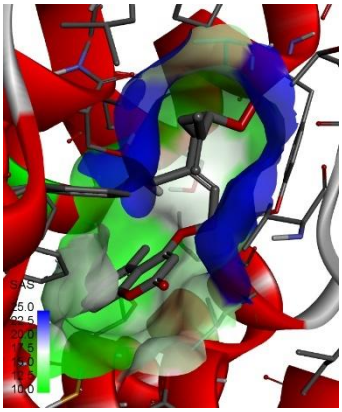

XXIV

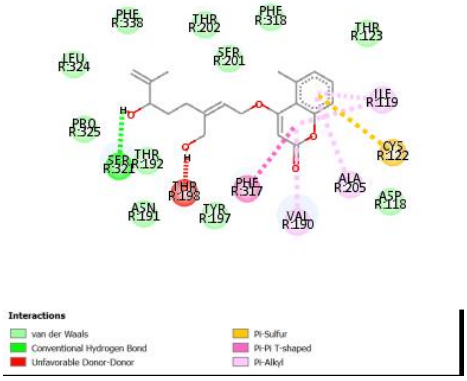

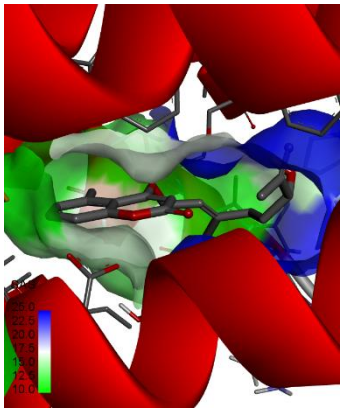

XXV

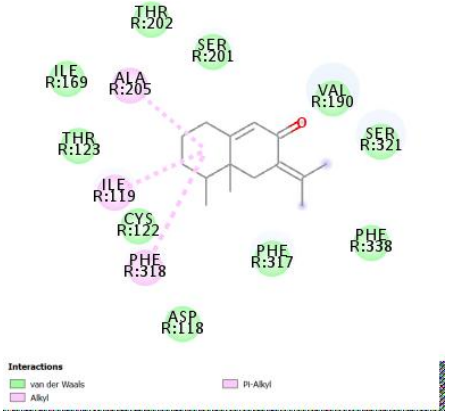

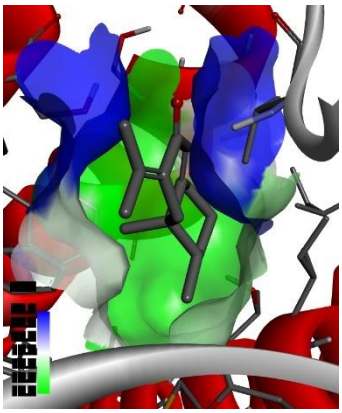

XXVI

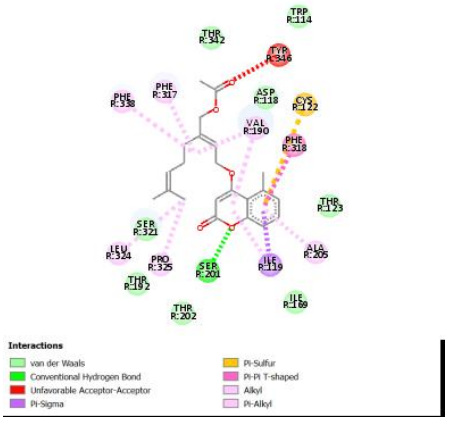

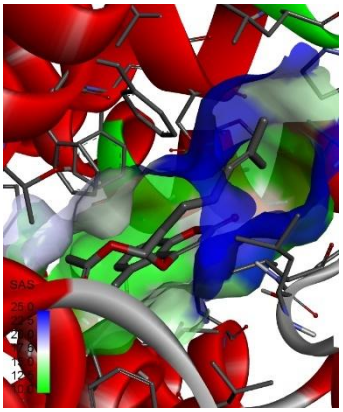

XXVII

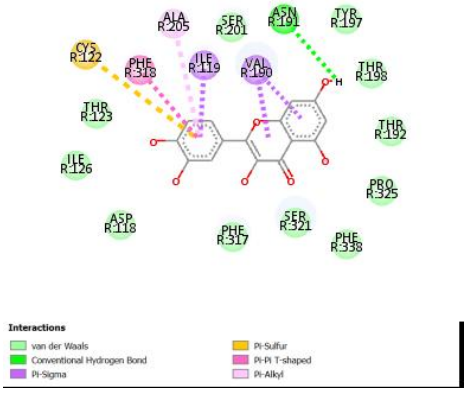

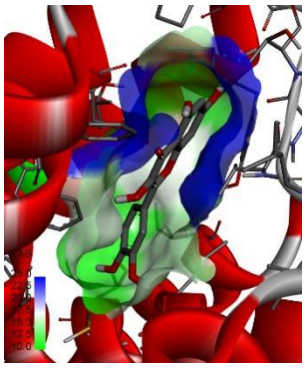

XXVIII

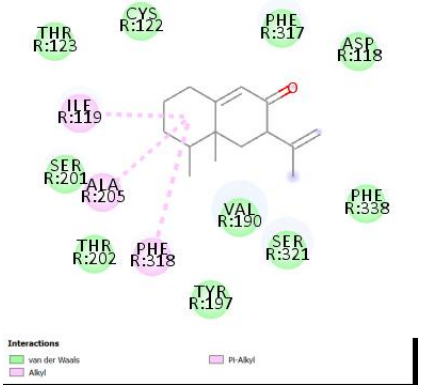

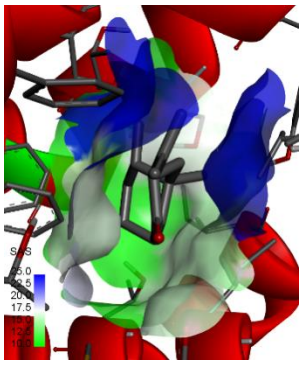

XXIX

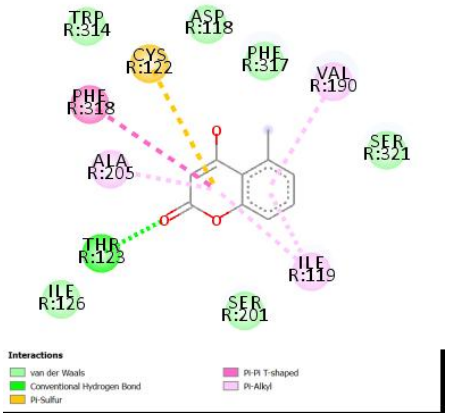

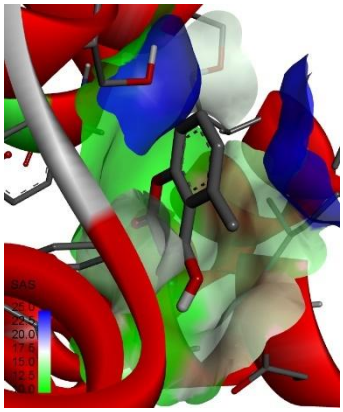

XXX

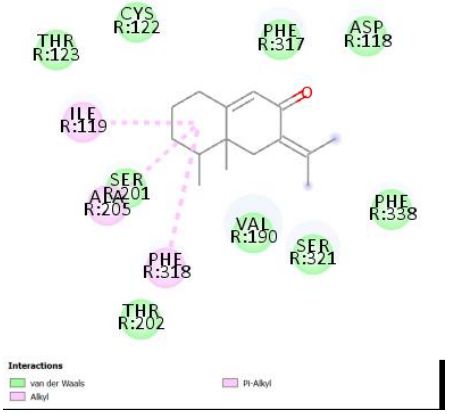

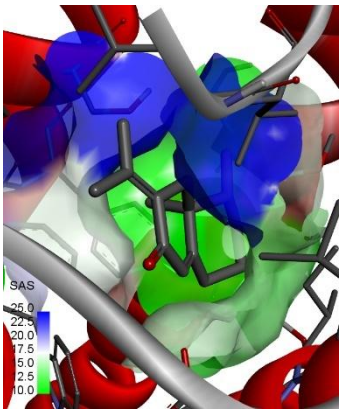

XXXI

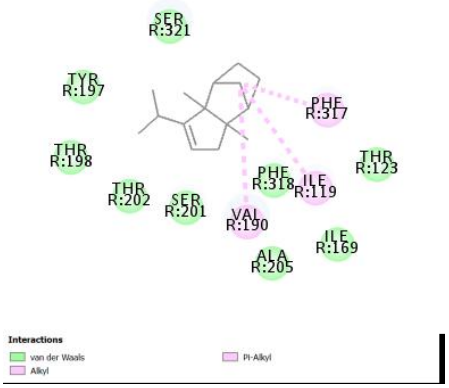

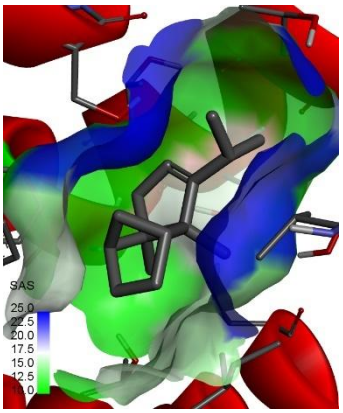

XXXII

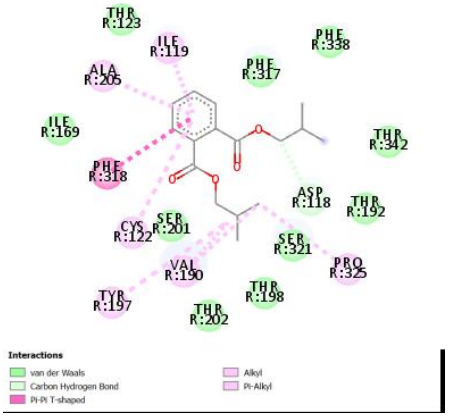

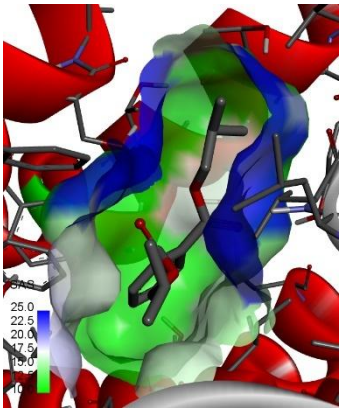

XXXIII

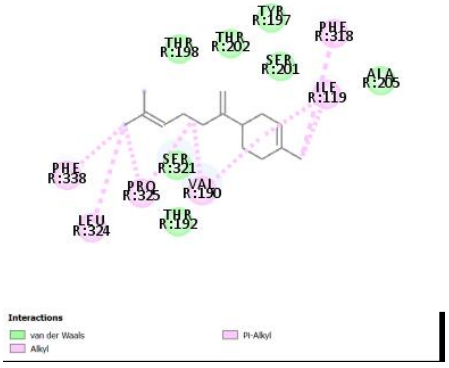

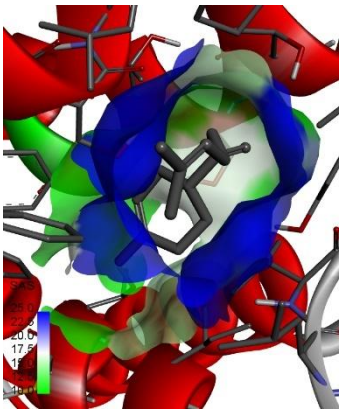

XXXIV

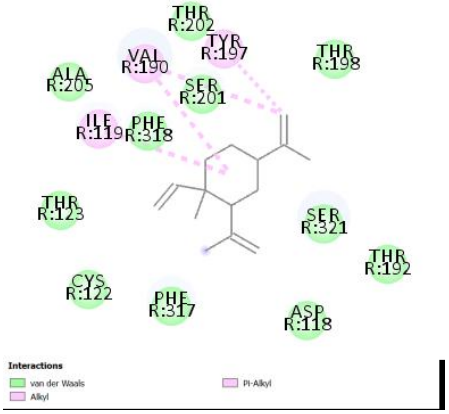

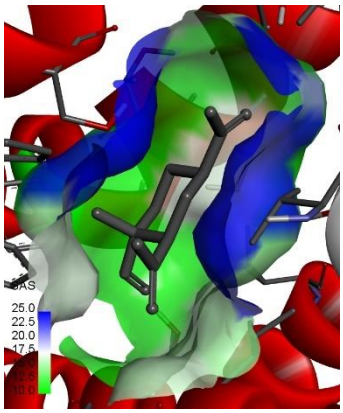

XXXV

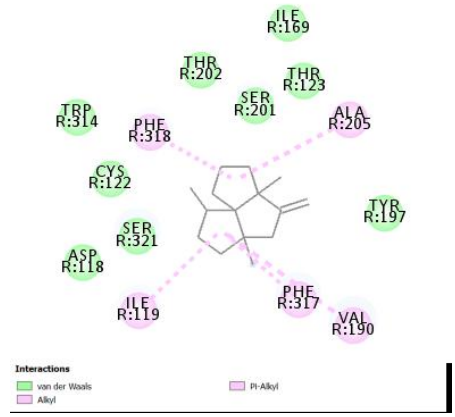

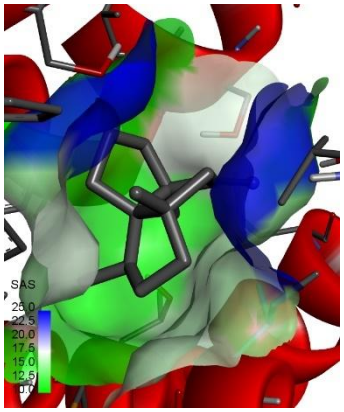

XXXVI

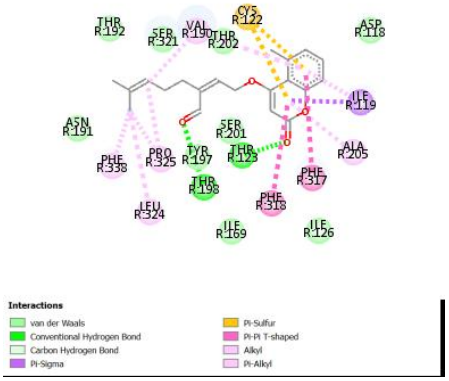

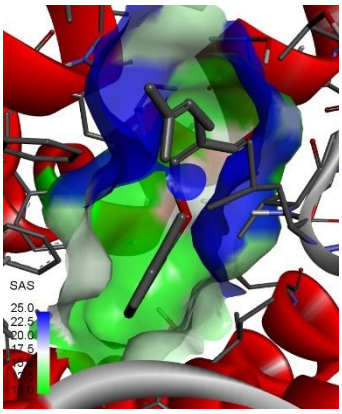

XXXVII

Figure 3.1.3.2: 2D (left) and 3D (right) views of the molecular interactions of amino-acid residues of 5-HT1D receptor with (I) [(4aR,5S,7R,8aR,9aS)-3,4a,5-trimethyl-2-oxo-4,5,6,7,8,8a,9,9a-octahydrobenzo[f][1]benzofuran-7-yl]3-methylbut-2-enoate (II) Rhamnazin (III) [(2E)-2-[(8S,8aR)-8,8a-dimethyl-3-oxo-5,6,7,8-tetrahydro-1H-naphthalen-2-ylidene]propyl] (Z)-2-methylbut-2-enoate (IV) [(1R,2R,8aR)-1,8a-dimethyl-6-oxo-7-propan-2-ylidene-2,3,4,8-tetrahydro-1H-naphthalen-2-yl] 3-methylbut-2-enoate (V) [(4aR,5S,7R,8aR,9aS)-3,4a,5-trimethyl-2-oxo-4,5,6,7,8,8a,9,9a-octahydrobenzo[f][1]benzo -furan-7-yl] (Z)-2-methylbut-2-enoate (VI) Albene (VII) Euparin (VIII) (4aR,5S,8aS)-3,4a,5-trimethyl-5,6,7,8,8a,9-

hexahydro-4H-benzo[f][1]benzofuran (IX) 4-Geranyloxy-5-methyl coumarin (X) (4aR,5S,8aR)-3,4a,5-trimethyl-4,5,6,7,8,8a-hexahydrobenzo[f][1]benzo furan-9-one (XI) 4-[(2Z,5R)-5-hydroxy-3-(hydroxymethyl)-7-methylocta-2,6-dienoxy]-5-methylchromen-2-one (XII) [(2E,4R)-3,7-dimethyl-1-(5-methyl-2-oxochromen-4-yl)oxyocta-2,6-dien-4-yl] acetate (XIII) [(4aR,5S,7R,8aR,9aS)-3,4a,5-trimethyl-2-oxo-4,5,6,7,8,8a,9,9a-octahydrobenzo[f][1]benzofuran-7-yl] (E)-2-methylbut-2-enoate (XIV) (4aR,5S,8aR,9aR)-3,4a,5-trimethyl-4,5,6,7,8,8a,9,9a-octahydro-1H-benzo[f]indol-2-one (XV) (4aR,5R,8aR, 9aR)-3,4a,5-trimethyl-4,5,6,7,8,8a,9,9a-octahydrobenzo[f][1]benzofuran-2-one (XVI) (3S)-3-ethenyl-9-methyl-3-(4-methylpent-3-enyl)-2H-furo[3,2-c]chromen-4-one (XVII) 4-[(2E,4R)-4-hydroxy-3-(hydroxymethyl)-7-methylocta-2,6-dienoxy]-5-methylchromen-2-one (XVIII) 4-[(2E,4R)-4-hydroxy-3,7-dimethylocta-2,6-dienoxy]-5-methylchromen-2-one (XIX) 4-[10-Oxo-neryloxy]-5-methylcoumarin (XX) 4-(10-Hydroxyneryloxy)-5-methylcoumarin (XXI) 4-(10-Hydroxygeranyloxy)-5-methylcoumarin (XXII)4-[5-Formyl-3-methyl-pent-2E,4E-dien-1-yl]-5-methylcoumarin (XXIII) 4-[6,10-Dioxo-neryloxy]-5-methyl coumarin (XXIV) 4-[(2Z,6S)-6-hydroperoxy-3-(hydroxymethyl)-7-methylocta-2,7-dienoxy]-5-methylchromen-2-one (XXV) 4-[(2Z,6R)-6-hydroxy-3-(hydroxymethyl)-7-methylocta-2,7-dienoxy]-5-methylchromen-2-one (XXVI) Dehydrofukinone (XXVII) [(2Z)-6-methyl-2-[2-(5-methyl-2-oxochromen-4-yl)oxyethylidene]hept-5-enyl] acetate (XXVIII) Quercetin (XXIX) Neopet -asane (XXX) 4-Hydroxy-5-methylcoumarin (XXXI) 4a,5-dimethyl-3-propan-2-ylidene-5,6,7,8-tetrahydro-4H-naphthalen-2-one (XXXII) Petasitene (XXXIII) Diisobutyl phthalate (XXXIV) (R)-beta-bisabolene (XXXV) Beta-Elemene (XXXVI) Pethybrene (XXXVII) 4-[10-Oxo-geranyloxyl]-5-methylcoumarin in *Petasites hybridus*

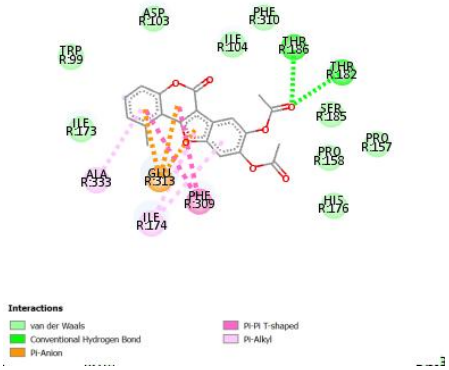
ASP R:103
PHE R:310
ILE R:104
THR R:186
TRP R:99
THR R:182
SER R:185
ILE R:173
PRO R:157
PRO R:158
ALA R:333
GLU R:313
PHE R:309
HIS R:176
ILE R:174
Interactions
van der Waals
Conventional Hydrogen Bond
Pi-Anion
Pi-Pi T-shaped
Pi-Alkyl

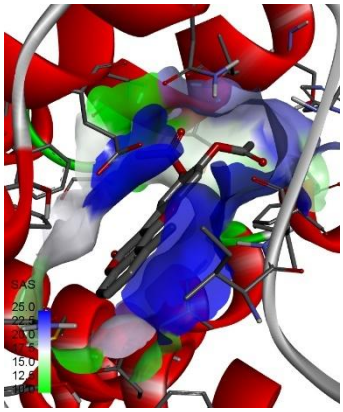

I

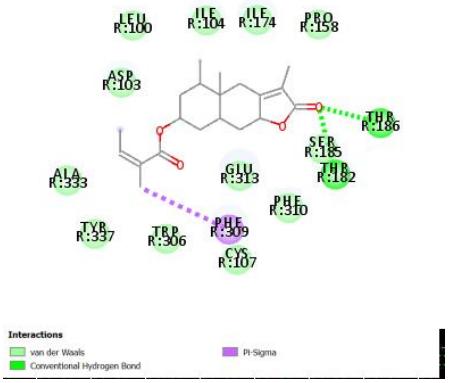
LEU R:100
ILE R:104
ILE R:174
PRO R:158
ASP R:103
THR R:186
SER R:185
ALA R:333
GLU R:313
THR R:182
PHE R:310
TYR R:337
TRP R:306
PHE R:309
CYS R:107
Interactions
van der Waals
Conventional Hydrogen Bond
Pi-Sigma

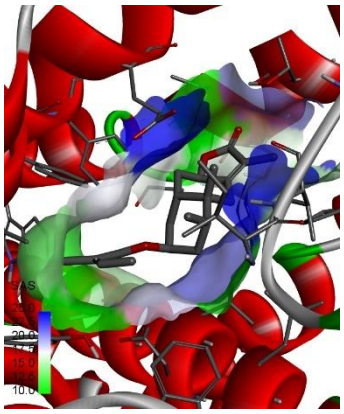

II

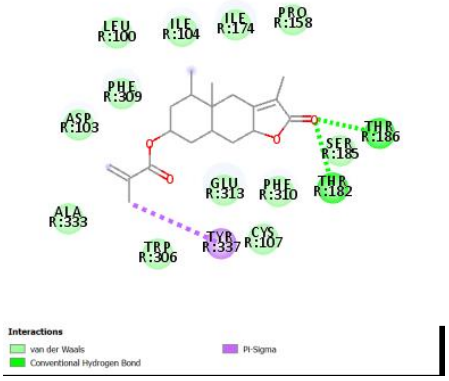
LEU R:100
ILE R:104
ILE R:174
PRO R:158
PHE R:309
ASP R:103
THR R:186
SER R:185
GLU R:313
PHE R:310
THR R:182
ALA R:333
TYR R:337
CYS R:107
TRP R:306
Interactions
van der Waals
Conventional Hydrogen Bond
Pi-Sigma

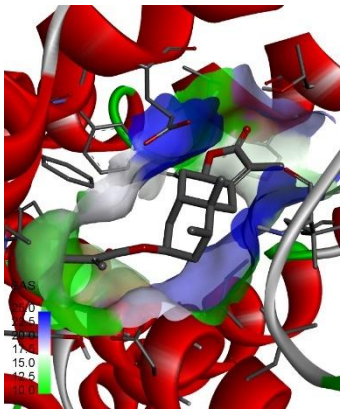

III

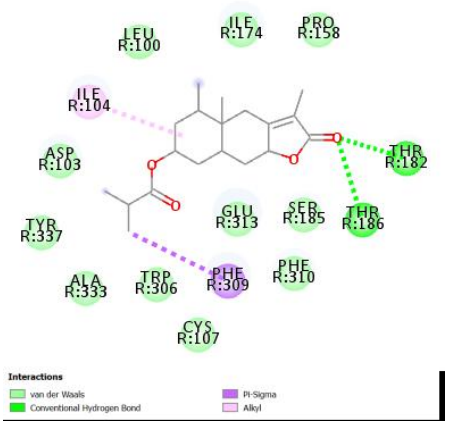
LEU R:100
ILE R:174
PRO R:158
ILE R:104
ASP R:103
THR R:182
GLU R:313
SER R:185
THR R:186
TYR R:337
PHE R:309
PHE R:310
ALA R:333
TRP R:306
CYS R:107
Interactions
van der Waals
Conventional Hydrogen Bond
Pi-Sigma
Alkyl

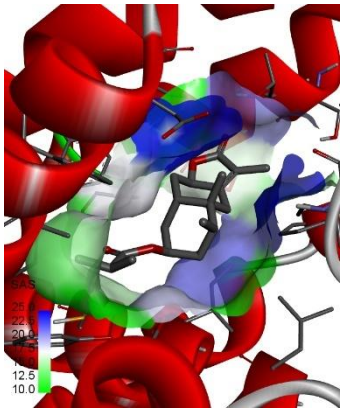
12.5
10.0

IV

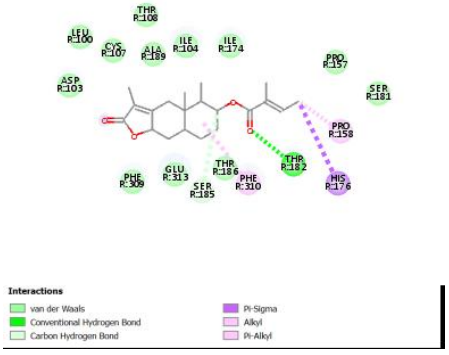
THR R:108
LEU R:100
CYS R:107
ALA R:189
ILE R:104
ILE R:174
PRO R:157
ASP R:103
SER R:181
PRO R:158
THR R:182
THR R:186
PHE R:309
GLU R:313
SER R:185
PHE R:310
MIS R:176
Interactions
van der Waals
Conventional Hydrogen Bond
Carbon Hydrogen Bond
Pi-Sigma
Alkyl
Pi-Alkyl

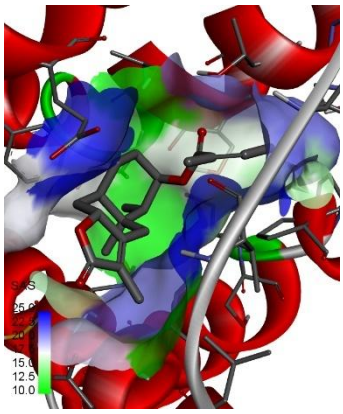
15.0
12.5
10.0

V

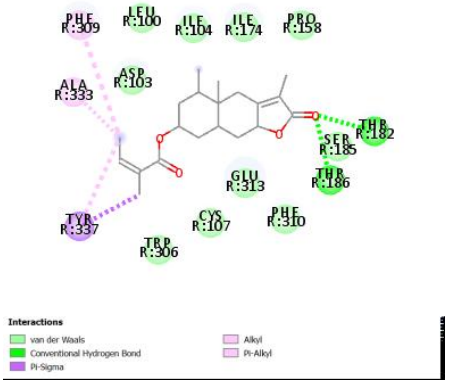
PHE R:309
LEU R:100
ILE R:104
ILE R:174
PRO R:158
ALA R:333
ASP R:103
THR R:182
SER R:185
GLU R:313
THR R:186
TYR R:337
CYS R:107
PHE R:310
TRP R:306
Interactions
van der Waals
Conventional Hydrogen Bond
Pi-Sigma
Alkyl
Pi-Alkyl

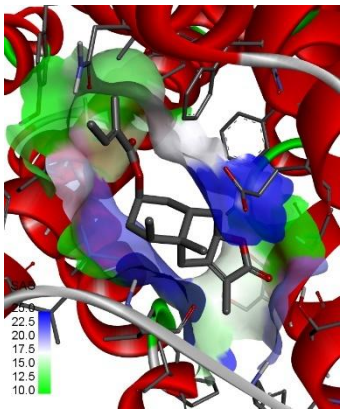
22.5
20.0
17.5
15.0
12.5
10.0

VI

Figure 3.1.3.3: 2D (left) and 3D (right) views of the molecular interactions of amino-acid residues of 5-HT1F receptor with (I) (9-acetyloxy-1-methyl-6-oxo-[1]benzofuro[3,2-c]chromen-8-yl) acetate (II) [(4aR,5S,7R,8aR,9aR)-3,4a,5-trimethyl-2-oxo-4,5,6,7,8,8a,9,9a-octahydrobenzo[f][1]benzofuran-7-yl] (Z)-2-methylbut-2-enoate (III)[(4aR,5S,7R,8aR, 9aR)-3,4a,5-trimethyl-2-oxo-4,5,6,7,8,8a,9,9aoctahydrobenzo[f][1]benzofuran-7-yl] 2-methylprop-2-enoate (IV) [(4aR,5S,7R,8aR,9aR)-3,4a,5-trimethyl-2-oxo-4,5,6,7,8,8a,9,9a-octahydro -benzo[f][1]benzofuran-7-yl] 2-methylpropanoate (V)[(4aS,5R,6R,8aR,9aR)-3,4a,5-trimethyl-2-oxo-4,5,6,7,8,8a,9,9a-octahydrobenzo[f][1]benzofuran-6-yl] (Z)-2-methylbut-2- enoate (VI)[(4aR,5S,7R,8aR,9aR)-3,4a,5-trimethyl-2-oxo-4,5,6,7,8,8a,9,9a-octahydrobenzo[f][1] -benzofuran-7-yl] (E)-2-methylbut-2-enoate in *Petasites hybridus*.

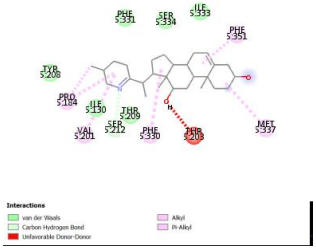

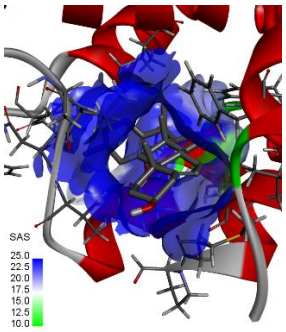

I

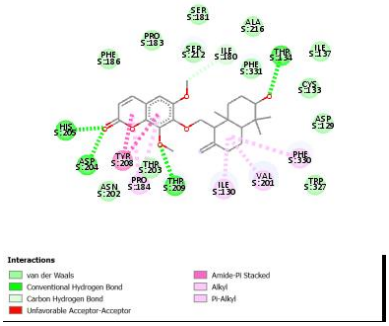

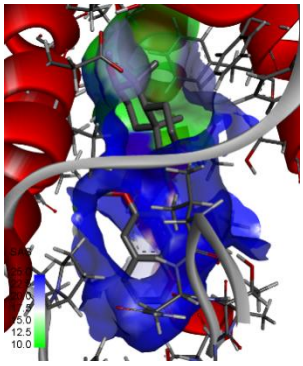

II

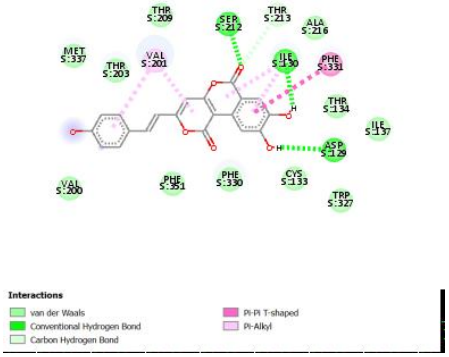
THR S:209
SER S:212
THR S:213
ALA S:216
MET S:337
THR S:203
VAL S:201
ILE S:130
PHE S:331
THR S:134
ILE S:137
ASP S:129
VAL S:200
PHE S:351
PHE S:330
CYS S:133
TRP S:327
Interactions
van der Waals
Conventional Hydrogen Bond
Carbon Hydrogen Bond
Pi-Pi T-shaped
Pi-Alkyl

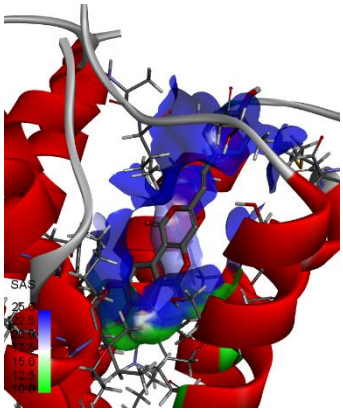
SAS

III

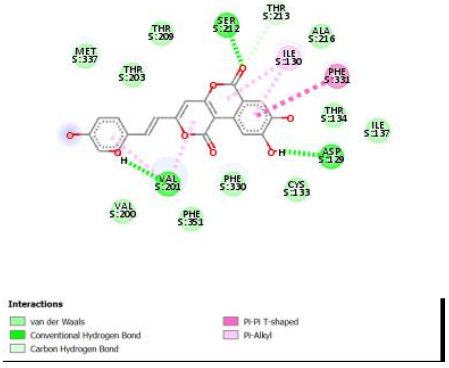
THR S:213
SER S:212
THR S:209
ALA S:216
MET S:337
ILE S:130
THR S:203
PHE S:331
THR S:134
ILE S:137
ASP S:129
VAL S:201
PHE S:330
CYS S:133
VAL S:200
PHE S:351
Interactions
van der Waals
Conventional Hydrogen Bond
Carbon Hydrogen Bond
Pi-Pi T-shaped
Pi-Alkyl

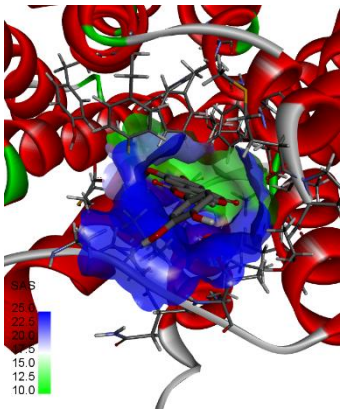
SAS
25.0
22.5
20.0
15.0
12.5
10.0

IV

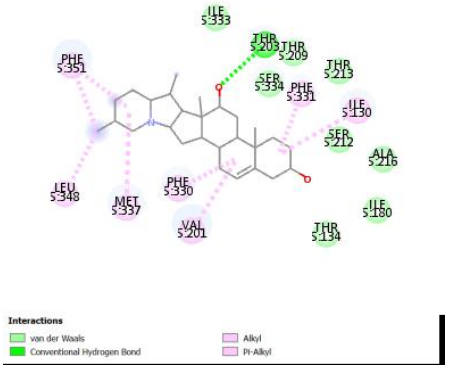
ILE S:333
THR S:203
THR S:209
PHE S:351
THR S:213
SER S:334
PHE S:331
ILE S:130
SER S:212
ALA S:216
LEU S:348
PHE S:330
MET S:337
ILE S:180
VAL S:201
THR S:134
Interactions
van der Waals
Conventional Hydrogen Bond
Alkyl
Pi-Alkyl

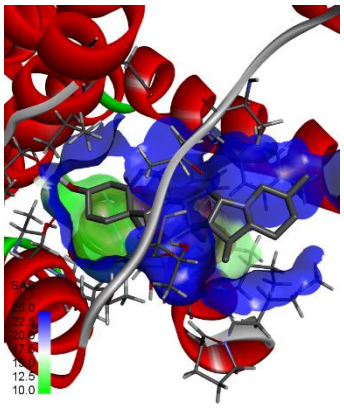
SAS
25.0
22.5
20.0
15.0
12.5
10.0

V

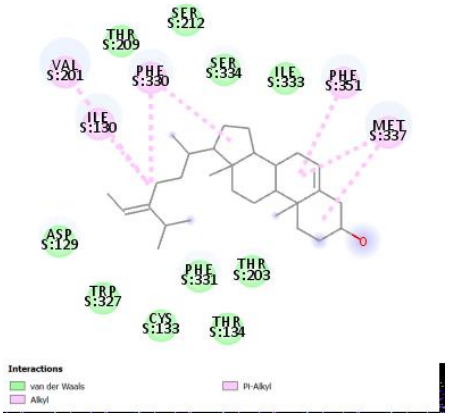
SER S:212
THR S:209
VAL S:201
PHE S:330
SER S:334
ILE S:333
PHE S:351
ILE S:130
MET S:337
ASP S:129
PHE S:331
THR S:203
TRP S:327
CYS S:133
THR S:134
Interactions
van der Waals
Alkyl
Pi-Alkyl

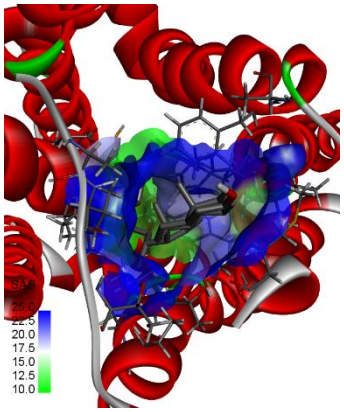
SAS
25.0
22.5
20.0
17.5
15.0
12.5
10.0

VI

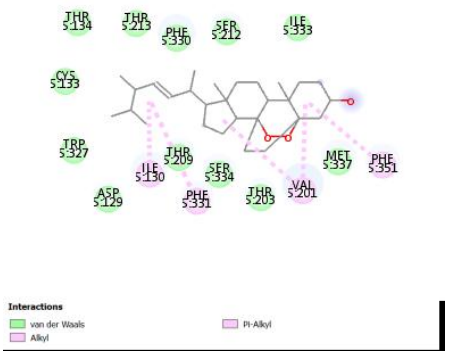
THR S:134
THR S:213
PHE S:330
SER S:212
ILE S:333
CYS S:133
TRP S:327
THR S:209
ILE S:130
SER S:334
MET S:337
PHE S:351
ASP S:129
PHE S:331
THR S:203
VAL S:201
Interactions
van der Waals
Alkyl
Pi-Alkyl

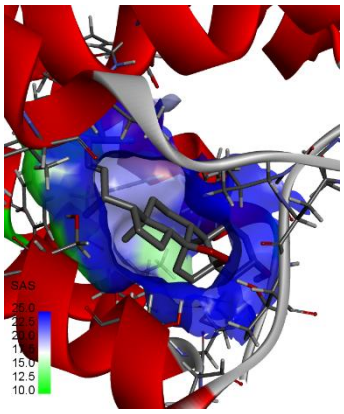
SAS
25.0
22.5
20.0
17.5
15.0
12.5
10.0

VII

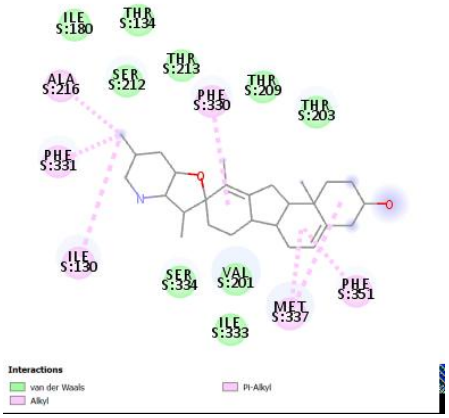
ILE S:180
THR S:134
THR S:213
ALA S:216
SER S:212
PHE S:330
THR S:209
THR S:203
PHE S:331
ILE S:130
SER S:334
VAL S:201
PHE S:351
MET S:337
ILE S:333
Interactions
van der Waals
Alkyl
Pi-Alkyl

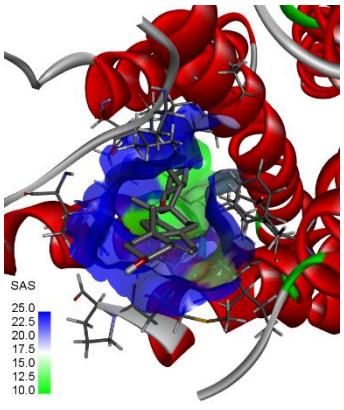
SAS
25.0
22.5
20.0
17.5
15.0
12.5
10.0

VIII

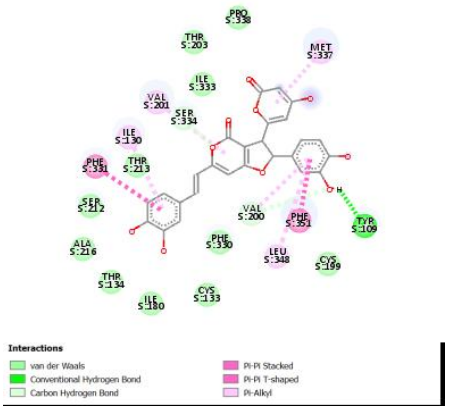

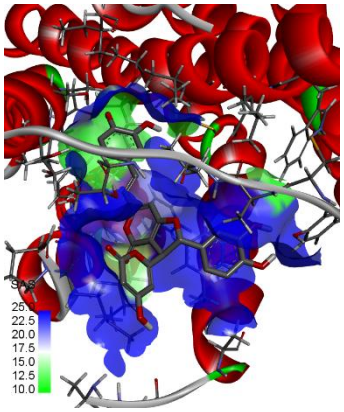

IX

Figure 3.1.4.1: 2D (left) and 3D (right) views of the molecular interactions of amino-acid residues of 5-HT1B receptor with (I) (3S,8R,9S,10R,12S,13S,14S,17R)-10,13-dimethyl-17-[(1S)-1-[(3S)-3-methyl-2,3,4,5-tetrahydropyridin-6-yl]ethyl]-2,3,4,7,8,9,11,12,14,15,16,17-dodecahydro-1H-cyclopenta[a]phenanthrene-3,12-diol (II) 7-[[(1S,4aR,6S,8aS)-6-hydroxy-5,5,8a-trimethyl-2-methylidene-3,4,4a,6,7,8-hexahydro-1H-naphthalen-1-yl]methoxy]-6,8-dimethoxychromen-2-one (III) Phelligridin C (IV) Phelligridin D (V) Rubijervine (VI) Fucosterol (VII) Ergosterol Peroxide (VIII) (3S,3'R,3'aS,6'S,6aS,6bS,7'aR,9S,11aS,11bR)-3',6',10,11b-tetramethylspiro[2,3,4,6,6a,6b,7,8,11,11a-decahydro-1H-benzo[a]fluorene-9,2'-3a,4,5,6,7,7a-hexahydro-3H-furo[3,2-b]pyridine]-3-o (IX) Hypholomine B in *Tanacetum parthenium.*

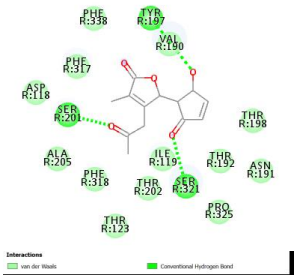

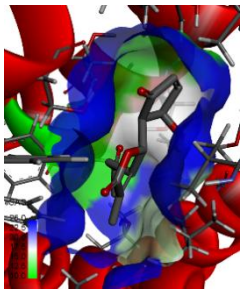

I

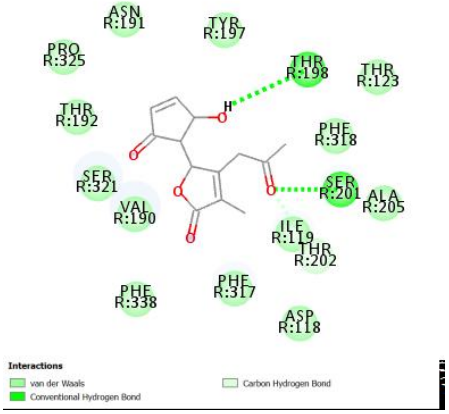
ASN R:191
TYR R:197
PRO R:325
THR R:198
THR R:123
THR R:192
PHE R:318
SER R:321
SER R:201
ALA R:205
VAL R:190
ILE R:119
THR R:202
PHE R:317
PHE R:338
ASP R:118
Interactions
van der Waals
Carbon Hydrogen Bond
Conventional Hydrogen Bond

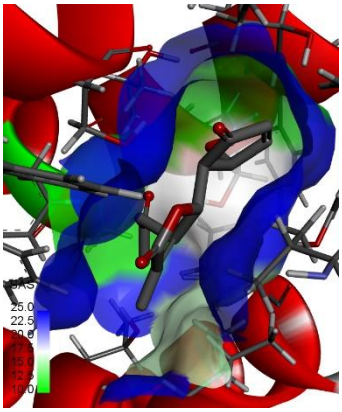

II

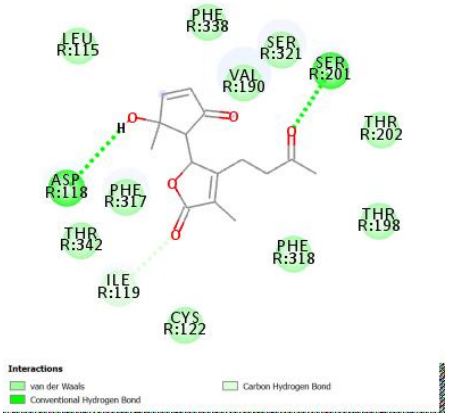
PHE R:338
LEU R:115
SER R:321
SER R:201
VAL R:190
THR R:202
ASP R:118
PHE R:317
THR R:198
THR R:342
PHE R:318
ILE R:119
CYS R:122
Interactions
van der Waals
Carbon Hydrogen Bond
Conventional Hydrogen Bond

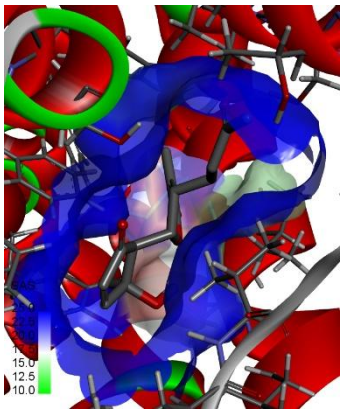

III

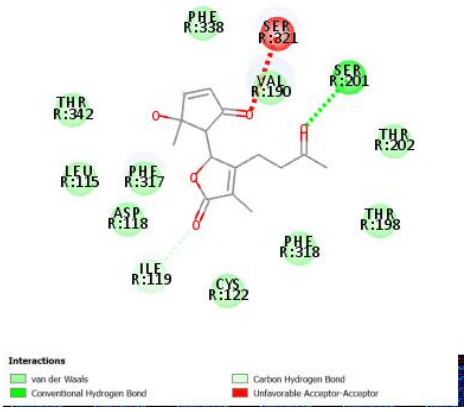
PHE R:338
SER R:321
SER R:201
VAL R:190
THR R:342
THR R:202
LEU R:115
PHE R:317
ASP R:118
THR R:198
PHE R:318
ILE R:119
CYS R:122
Interactions
van der Waals
Carbon Hydrogen Bond
Conventional Hydrogen Bond
Unfavorable Acceptor-Acceptor

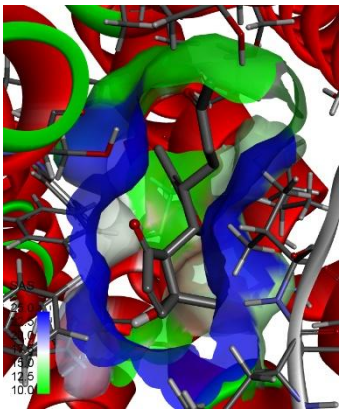

IV

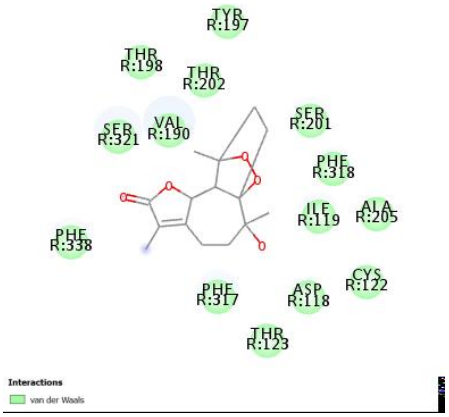
TYR R:197
THR R:198
THR R:202
SER R:201
SER R:321
VAL R:190
PHE R:318
ILE R:119
ALA R:205
PHE R:338
CYS R:122
PHE R:317
ASP R:118
THR R:123
Interactions
van der Waals

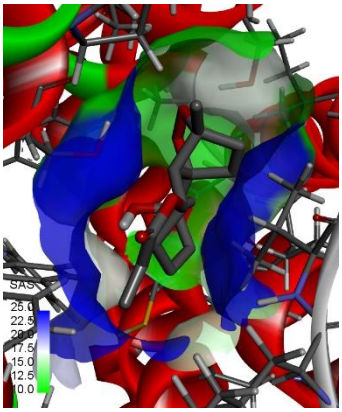
SAS
25.0
22.5
20.0
17.5
15.0
12.5
10.0

V

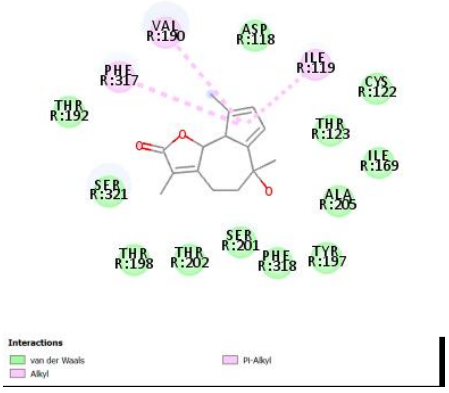
VAL R:190
ASP R:118
ILE R:119
PHE R:317
CYS R:122
THR R:192
THR R:123
ILE R:169
SER R:321
ALA R:205
SER R:201
THR R:198
THR R:202
PHE R:318
TYR R:197
Interactions
van der Waals
Pi-Alkyl
Alkyl

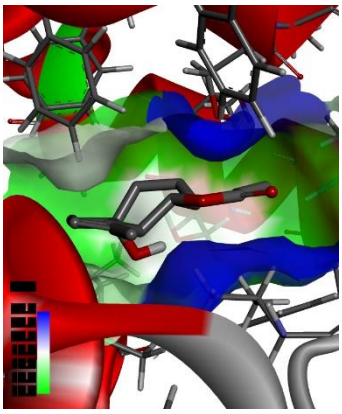

VI

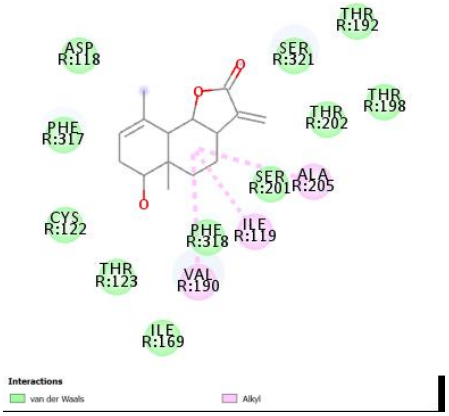
THR R:192
ASP R:118
SER R:321
THR R:198
PHE R:317
THR R:202
SER R:201
ALA R:205
CYS R:122
PHE R:318
ILE R:119
THR R:123
VAL R:190
ILE R:169
Interactions
van der Waals
Alkyl

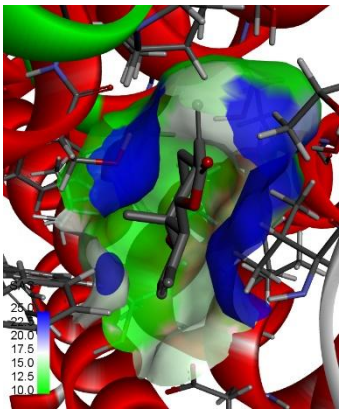
20.0
17.5
15.0
12.5
10.0

VII

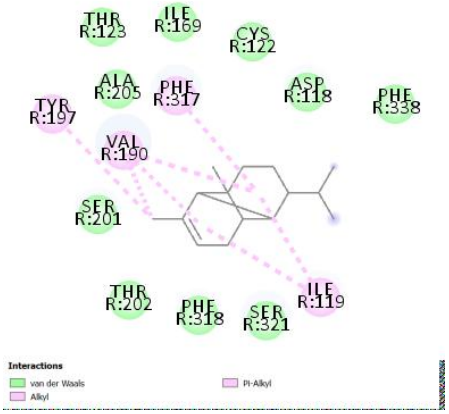
THR R:123
ILE R:169
CYS R:122
ALA R:205
PHE R:317
ASP R:118
PHE R:338
TYR R:197
VAL R:190
SER R:201
THR R:202
PHE R:318
SER R:321
ILE R:119
Interactions
van der Waals
Alkyl
Pi-Alkyl

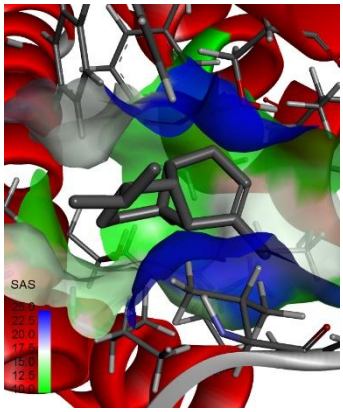
SAS

VIII

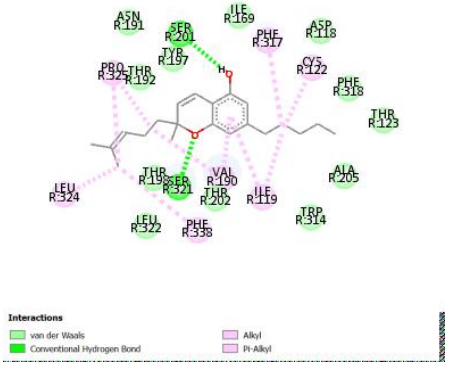
ASN R:191
SER R:201
ILE R:169
PHE R:317
ASP R:118
TYR R:197
CYS R:122
PRO R:325
THR R:192
PHE R:318
THR R:123
LEU R:324
THR R:198
SER R:321
VAL R:190
THR R:202
ILE R:119
ALA R:205
LEU R:322
PHE R:338
TRP R:314
Interactions
van der Waals
Conventional Hydrogen Bond
Alkyl
Pi-Alkyl

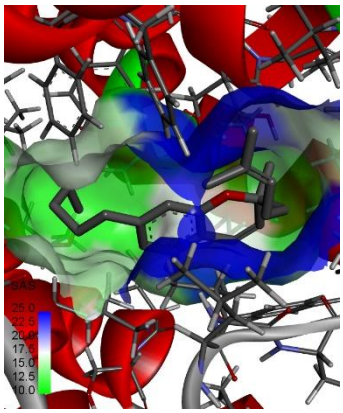
SAS

IX

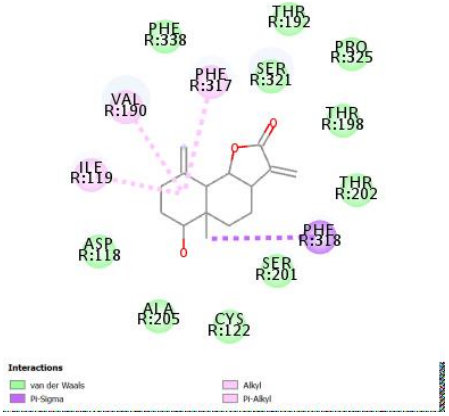
THR R:192
PHE R:338
PRO R:325
SER R:321
PHE R:317
VAL R:190
THR R:198
ILE R:119
THR R:202
ASP R:118
PHE R:318
SER R:201
ALA R:205
CYS R:122
Interactions
van der Waals
Pi-Sigma
Alkyl
Pi-Alkyl

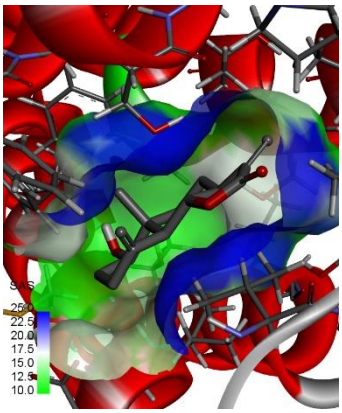

X

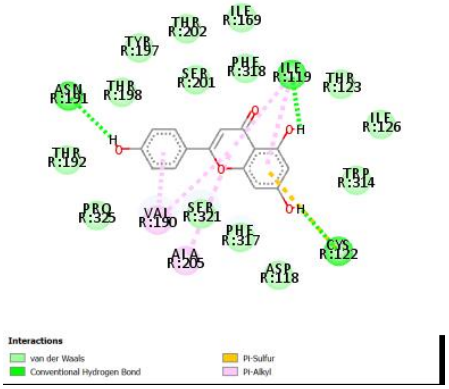
THR R:202
ILE R:169
TYR R:197
PHE R:318
ILE R:119
SER R:201
THR R:123
ASN R:191
THR R:198
ILE R:126
THR R:192
TRP R:314
PRO R:325
VAL R:190
SER R:321
PHE R:317
CYS R:122
ALA R:205
ASP R:118
Interactions
van der Waals
Conventional Hydrogen Bond
Pi-Sulfur
Pi-Alkyl

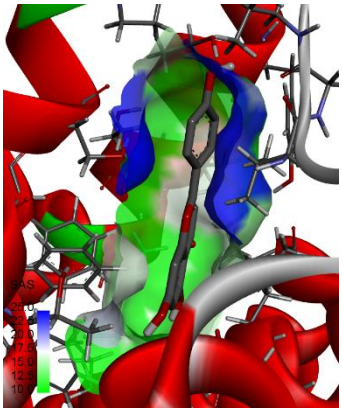

XI

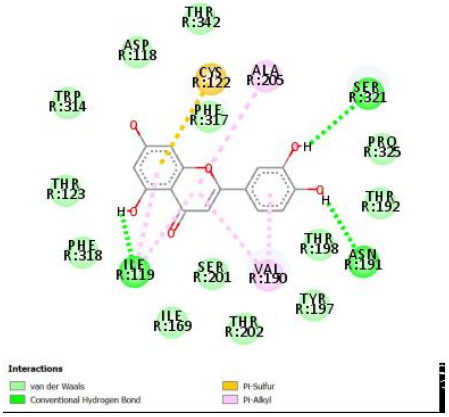
THR R:342
ASP R:118
CYS R:122
ALA R:205
SER R:321
TRP R:314
PHE R:317
PRO R:325
THR R:123
THR R:192
PHE R:318
THR R:198
ASN R:191
ILE R:119
SER R:201
VAL R:190
TYR R:197
ILE R:169
THR R:202
Interactions
van der Waals
Conventional Hydrogen Bond
Pi-Sulfur
Pi-Alkyl

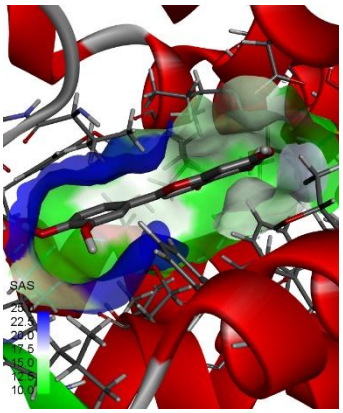

XII

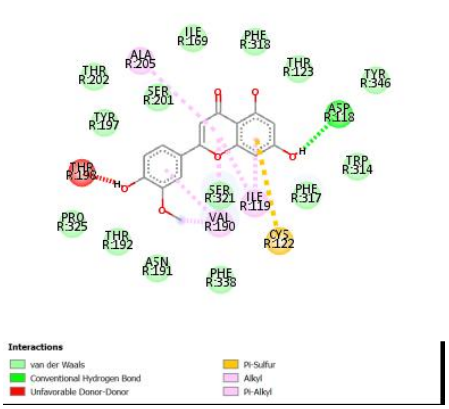
ILE R:169
PHE R:318
ALA R:205
THR R:123
THR R:202
TYR R:346
SER R:201
ASP R:118
TYR R:197
TRP R:314
SER R:321
ILE R:119
PHE R:317
PRO R:325
VAL R:190
THR R:192
CYS R:122
ASN R:191
PHE R:338
Interactions
van der Waals
Conventional Hydrogen Bond
Unfavorable Donor-Donor
Pi-Sulfur
Alkyl
Pi-Alkyl

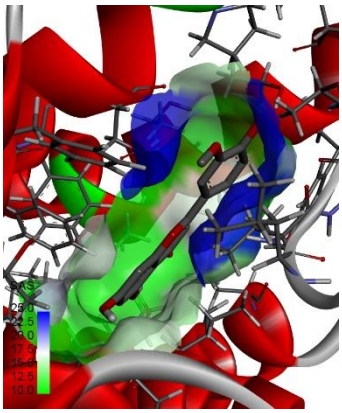

XIII

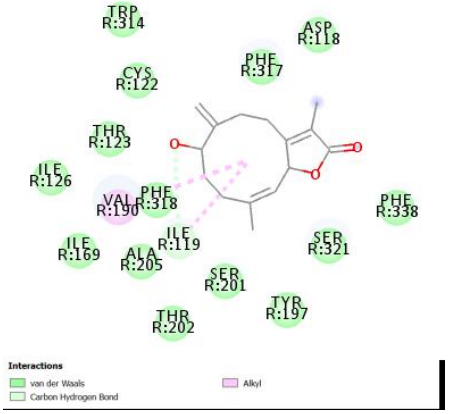
TRP R:314
ASP R:118
PHE R:317
CYS R:122
THR R:123
ILE R:126
VAL R:190
PHE R:318
PHE R:338
ILE R:169
ILE R:119
ALA R:205
SER R:321
SER R:201
TYR R:197
THR R:202
Interactions
van der Waals
Carbon Hydrogen Bond
Alkyl

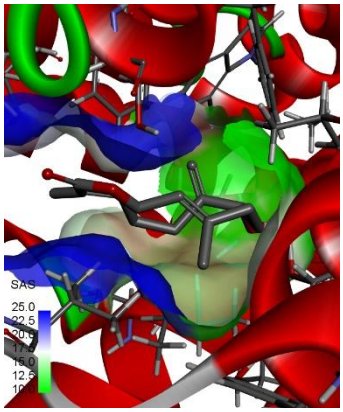
SAS
25.0

IX

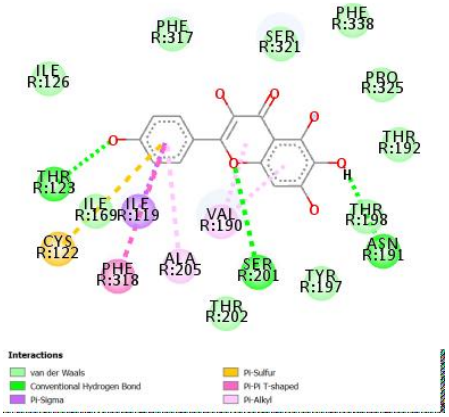
PHE R:317
SER R:321
PHE R:338
ILE R:126
PRO R:325
THR R:192
THR R:123
ILE R:169
ILE R:119
VAL R:190
THR R:198
CYS R:122
ASN R:191
PHE R:318
ALA R:205
SER R:201
TYR R:197
THR R:202
Interactions
van der Waals
Conventional Hydrogen Bond
Pi-Sigma
Pi-Sulfur
Pi-Pi T-shaped
Pi-Alkyl

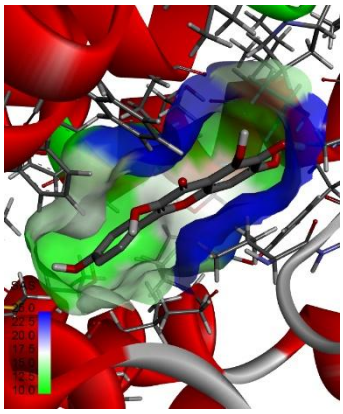

X

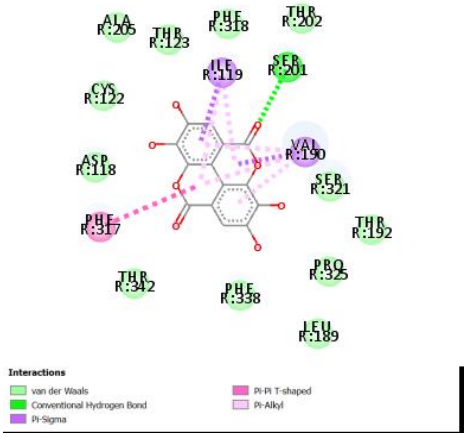
ALA R:205
THR R:123
PHE R:318
THR R:202
ILE R:119
SER R:201
CYS R:122
VAL R:190
ASP R:118
SER R:321
PHE R:317
THR R:192
PRO R:325
THR R:342
PHE R:338
LEU R:189
Interactions
van der Waals
Conventional Hydrogen Bond
Pi-Sigma
Pi-Pi T-shaped
Pi-Alkyl

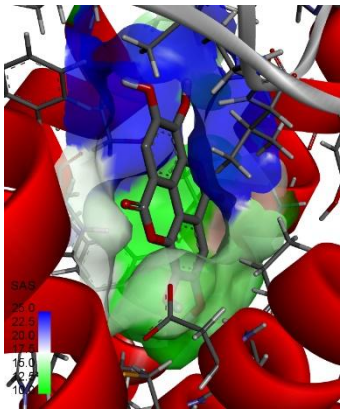
SAS
25.0

XI

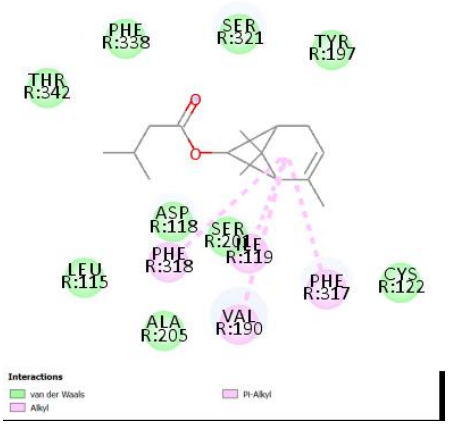
PHE R:338
SER R:321
TYR R:197
THR R:342
ASP R:118
SER R:201
ILE R:119
PHE R:318
LEU R:115
PHE R:317
CYS R:122
ALA R:205
VAL R:190
Interactions
van der Waals
Alkyl
Pi-Alkyl

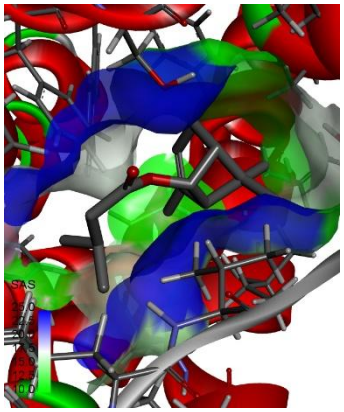

XII

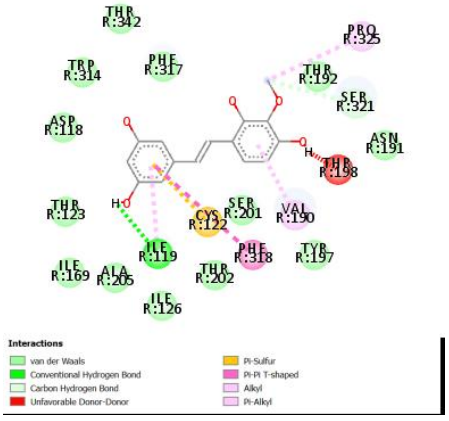
THR R:342
PRO R:325
TRP R:314
PHE R:317
THR R:192
SER R:321
ASP R:118
ASN R:191
THR R:198
THR R:123
SER R:201
VAL R:190
CYS R:122
ILE R:119
PHE R:318
TYR R:197
ILE R:169
ALA R:205
THR R:202
ILE R:126
Interactions
van der Waals
Conventional Hydrogen Bond
Carbon Hydrogen Bond
Unfavorable Donor-Donor
Pi-Sulfur
Pi-Pi T-shaped
Alkyl
Pi-Alkyl

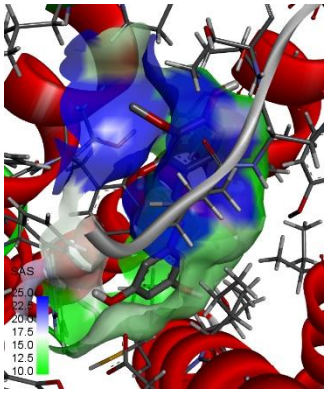

XIII

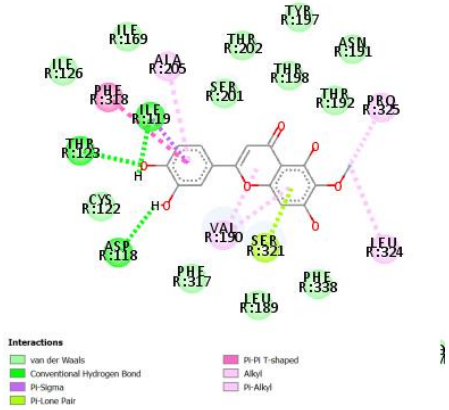
TYR R:197
ILE R:169
THR R:202
ASN R:191
ALA R:205
ILE R:126
THR R:198
SER R:201
PHE R:318
THR R:192
PRO R:325
ILE R:119
THR R:123
CYS R:122
VAL R:190
SER R:321
LEU R:324
ASP R:118
PHE R:317
PHE R:338
LEU R:189
Interactions
van der Waals
Conventional Hydrogen Bond
Pi-Sigma
Pi-Lone Pair
Pi-Pi T-shaped
Alkyl
Pi-Alkyl

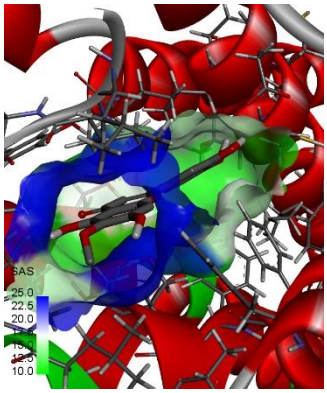

XIV

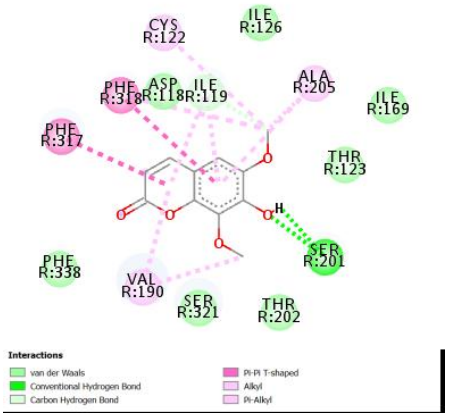
CYS R:122
ILE R:126
PHE R:318
ASP R:118
ILE R:119
ALA R:205
ILE R:169
PHE R:317
THR R:123
PHE R:338
VAL R:190
SER R:321
THR R:202
SER R:201
Interactions
van der Waals
Conventional Hydrogen Bond
Carbon Hydrogen Bond
Pi-Pi T-shaped
Alkyl
Pi-Alkyl

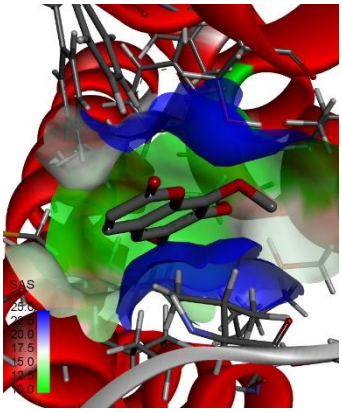

XV

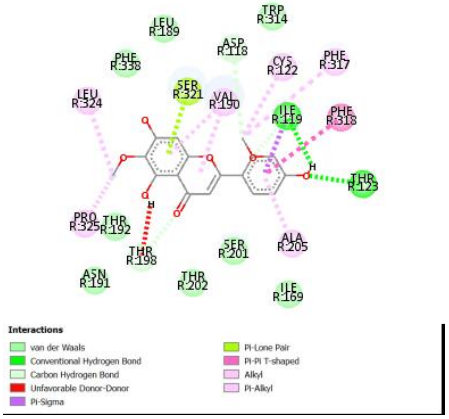
TRP R:314
LEU R:189
ASP R:118
PHE R:338
CYS R:122
PHE R:317
SER R:321
VAL R:190
LEU R:324
ILE R:119
PHE R:318
THR R:123
PRO R:325
THR R:192
THR R:198
SER R:201
ALA R:205
ASN R:191
THR R:202
ILE R:169
Interactions
van der Waals
Conventional Hydrogen Bond
Carbon Hydrogen Bond
Unfavorable Donor-Donor
Pi-Sigma
Pi-Lone Pair
Pi-Pi T-shaped
Alkyl
Pi-Alkyl

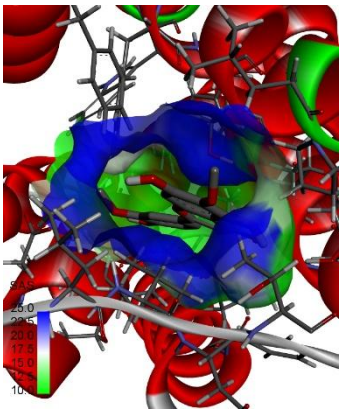

XVI

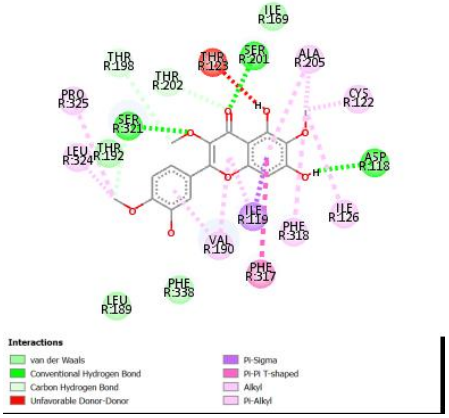
ILE R:169
THR R:198
THR R:123
SER R:201
ALA R:205
THR R:202
PRO R:325
CYS R:122
SER R:321
LEU R:324
THR R:192
ASP R:118
ILE R:119
ILE R:126
PHE R:318
VAL R:190
PHE R:317
PHE R:338
LEU R:189
Interactions
van der Waals
Conventional Hydrogen Bond
Carbon Hydrogen Bond
Unfavorable Donor-Donor
Pi-Sigma
Pi-Pi T-shaped
Alkyl
Pi-Alkyl

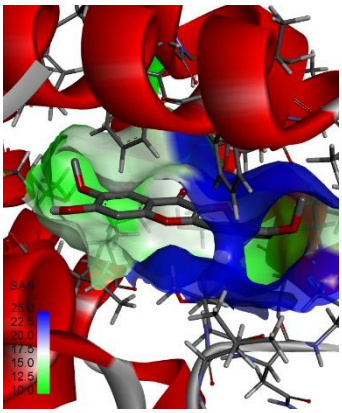

XVII

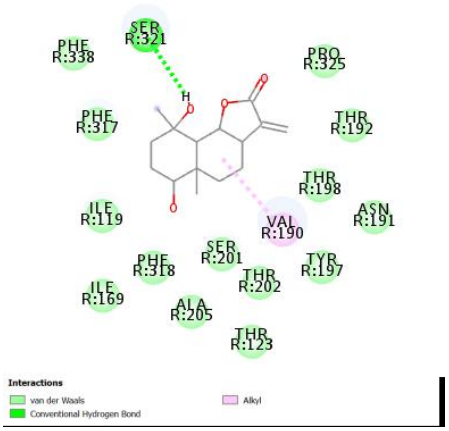
SER R:321
PHE R:338
PRO R:325
PHE R:317
THR R:192
THR R:198
ILE R:119
ASN R:191
VAL R:190
SER R:201
PHE R:318
TYR R:197
THR R:202
ILE R:169
ALA R:205
THR R:123
Interactions
van der Waals
Alkyl
Conventional Hydrogen Bond

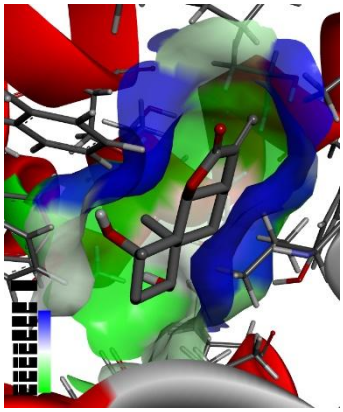

XVIII

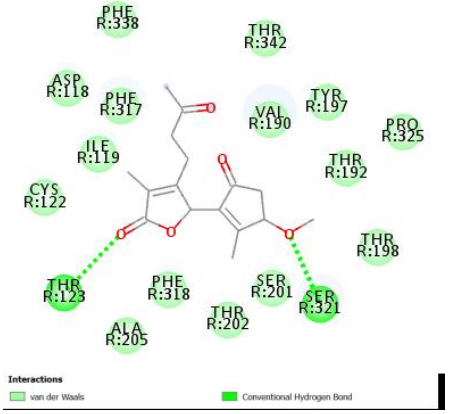
PHE R:338
THR R:342
ASP R:118
PHE R:317
TYR R:197
VAL R:190
PRO R:325
ILE R:119
THR R:192
CYS R:122
THR R:198
THR R:123
PHE R:318
SER R:201
SER R:321
THR R:202
ALA R:205
Interactions
van der Waals
Conventional Hydrogen Bond

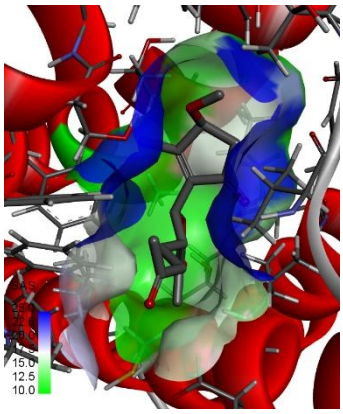

XIX

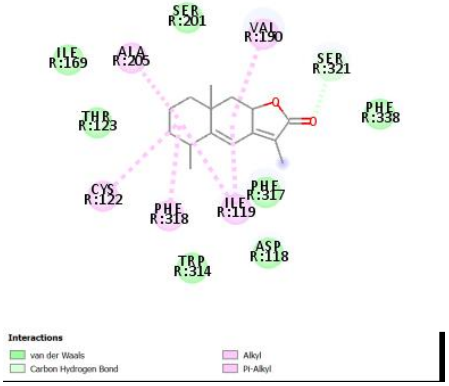
SER R:201
VAL R:190
ILE R:169
ALA R:205
SER R:321
PHE R:338
THR R:123
CYS R:122
PHE R:317
PHE R:318
ILE R:119
ASP R:118
TRP R:314
Interactions
van der Waals
Alkyl
Carbon Hydrogen Bond
Pi-Alkyl

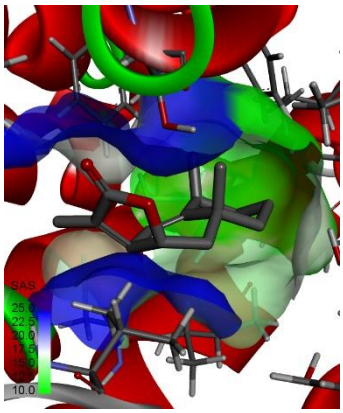

XX

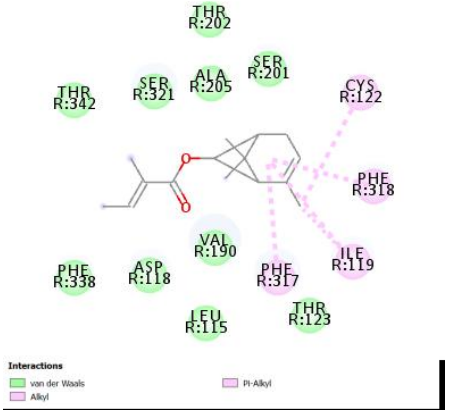

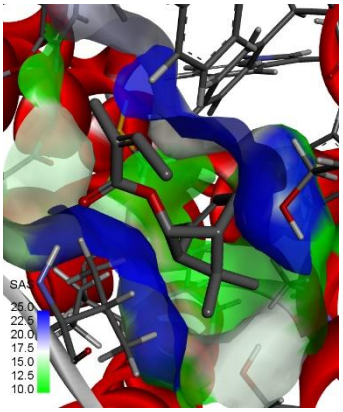

XXI

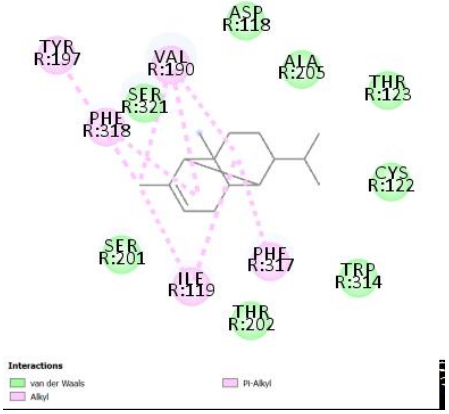

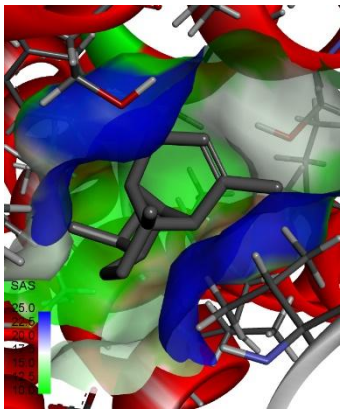

XXII

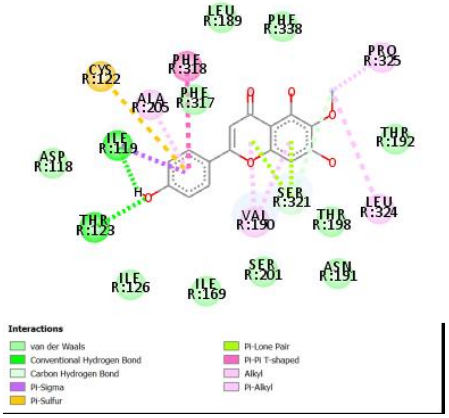

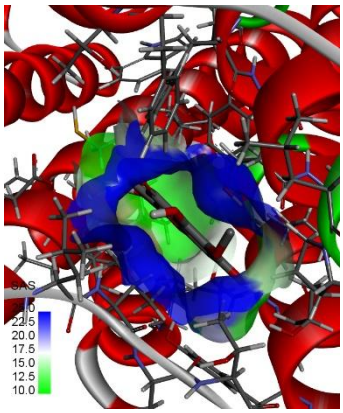

XXIII

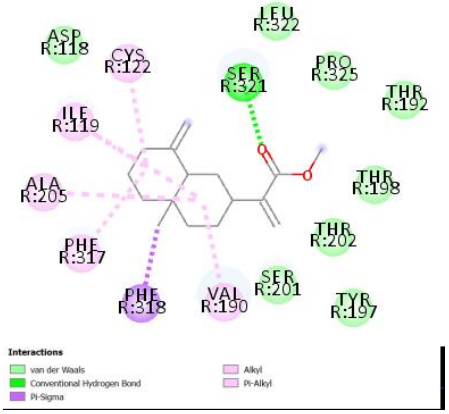

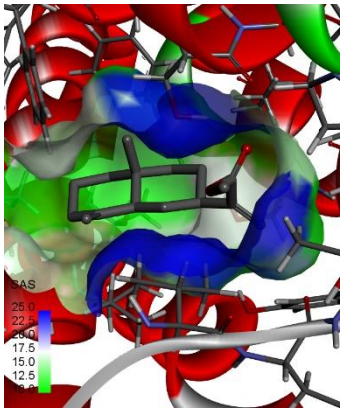

XXIV

Figure 3.1.4.2: 2D (left) and 3D (right) views of the molecular interactions of amino-acid residues of 5-HT1D receptor with (I) (4R,5S)-5-[(1S,2R)-2-hydroxy-5-oxocyclopent-3-en-1-yl]-3-methylidene-4-(2-oxopropyl)oxolan-2-one (II) (4R,5S)-5-[(1S,2S)-2-hydroxy-5-oxocyclopent-3-en-1-yl]-3-methylidene-4-(2-oxopropyl)oxolan-2-one (III) Secotana -partholide B (IV) Secotanapartholide A (V)(1S,2R,5S,9S,10S,11R)-2-hydroxy-2,11-dimethyl-6-methylidene-8,12,13-trioxatetracyclo[9.2.2.01,10.05,9] pentadec-14-en-7-one (VI)(3aS,6R,9aS,9bS)-6-hydroxy-6,9-dimethyl-3-methylidene-4,5,9a,9b-tetrahydro-3aH-azuleno[4,5-b]furan-2-one (VII) Santamarin (VIII) 1,3-dimethyl-8-propan-2-yltricyclo[4.4.0.02,7]dec-3-ene (IX) (+-)-Cannabichromene (X) Reynosin (XI) Apigenin (XII) Luteolin (XIII) Chrysoeriol (IX) Artemorin (X) 6-Hydroxykaempferol (XI) Ellagic Acid (XII) Chrysanthenyl isovalerate (XIII) 4-[(E)-2-(3,5-dihydroxyphenyl)ethenyl]-2-methoxybenzene-1,3-diol (XIV) Nepetin (XV) Isofraxidin (XVI) Jaceosidin (XVII) Jaceidin (XVIII) 1-beta-Hydroxyarbusculin A (XIX) 3-O-methyl-isosecotanapartholide (XX) (+)-Alantolactone (XXI) Chrysanthenyl angelate (XXII) (1R,2S,7S,8S)-1,3-dimethyl-8-propan-2-yltricyclo[4.4.0.02,7]dec-3-ene (XXIII) Hispidulin (XXIV) Methyl-gamma-costate in *Tanacetum parthenium.*

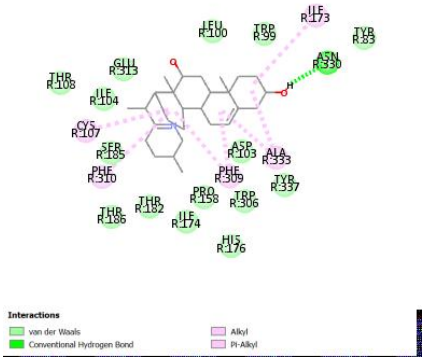
LEU R:100
TRP R:99
ILE R:173
TYR R:83
ASN R:330
GLU R:313
THR R:108
ILE R:104
CYS R:107
SER R:185
ASP R:103
ALA R:333
PHE R:310
PHE R:309
TYR R:337
PRO R:158
THR R:182
TRP R:306
THR R:186
ILE R:174
HIS R:176
Interactions
van der Waals
Conventional Hydrogen Bond
Alkyl
Pi-Alkyl

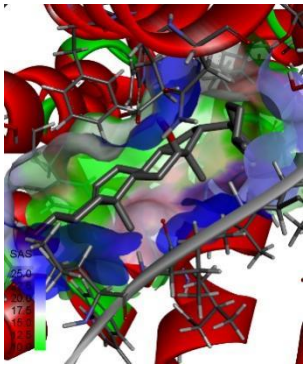
SAS
25.0
22.5
20.0
17.5

I

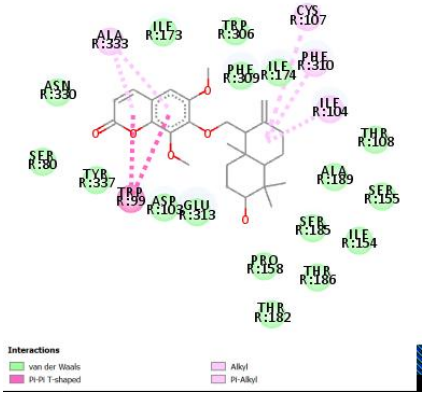
CYS R:107
ALA R:333
ILE R:173
TRP R:306
PHE R:310
PHE R:309
ILE R:174
ASN R:330
ILE R:104
THR R:108
SER R:80
TYR R:337
ALA R:189
SER R:155
TRP R:99
ASP R:103
GLU R:313
SER R:185
ILE R:154
PRO R:158
THR R:186
THR R:182
Interactions
van der Waals
Pi-Pi T-shaped
Alkyl
Pi-Alkyl

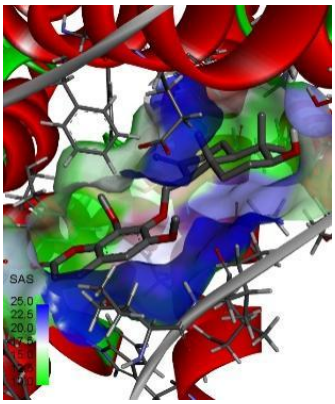
SAS
25.0
22.5
20.0

II

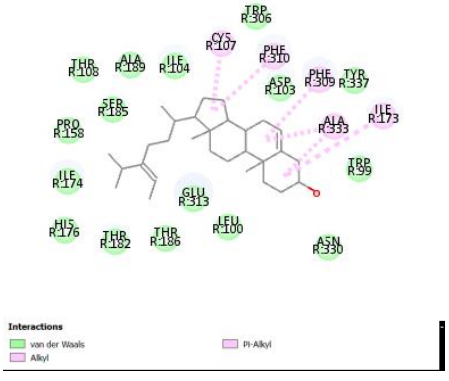
TRP R:306
CYS R:107
THR R:108
ALA R:189
ILE R:104
PHE R:310
PHE R:309
TYR R:337
ASP R:103
SER R:185
ILE R:173
PRO R:158
ALA R:333
TRP R:99
ILE R:174
GLU R:313
HIS R:176
THR R:152
THR R:186
LEU R:100
ASN R:330
Interactions
van der Waals
Alkyl
Pi-Alkyl

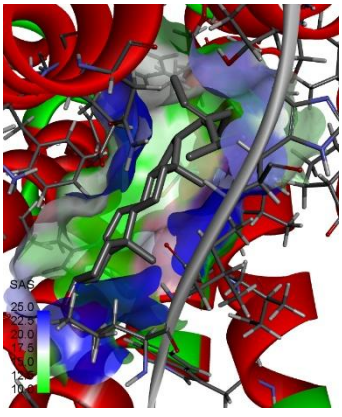
SAS
25.0
22.5
20.0

III

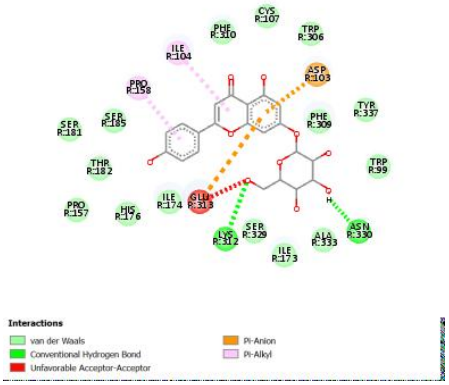
CYS R:107
PHE R:310
TRP R:306
ILE R:104
ASP R:103
PRO R:158
TYR R:337
SER R:181
SER R:185
PHE R:309
THR R:182
TRP R:99
PRO R:157
HIS R:176
ILE R:174
GLU R:313
LYS R:312
SER R:329
ALA R:333
ASN R:330
ILE R:173
Interactions
van der Waals
Conventional Hydrogen Bond
Unfavorable Acceptor-Acceptor
Pi-Anion
Pi-Alkyl

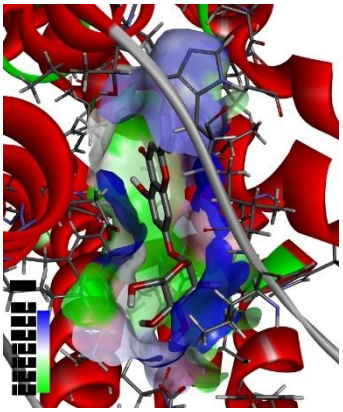

IV

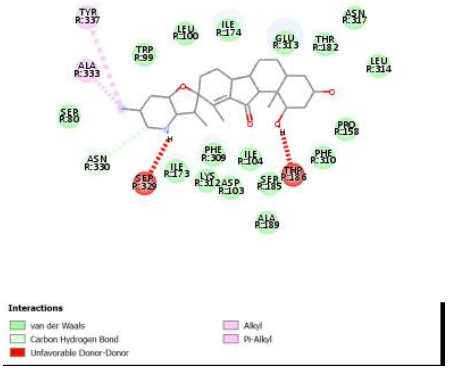
TYR R:337
LEU R:100
ILE R:174
ASN R:317
GLU R:313
THR R:182
TRP R:99
LEU R:314
ALA R:333
SER R:80
PRO R:158
PHE R:309
ILE R:104
PHE R:310
ASN R:330
ILE R:173
LYS R:312
ASP R:103
SER R:185
THR R:186
SER R:329
ALA R:189
Interactions
van der Waals
Carbon Hydrogen Bond
Unfavorable Donor-Donor
Alkyl
Pi-Alkyl

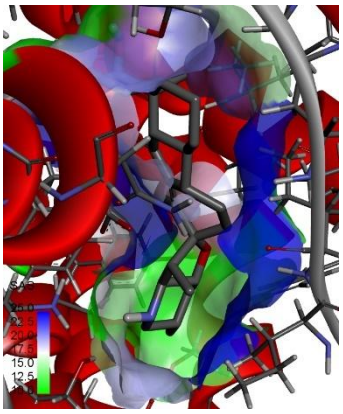

V

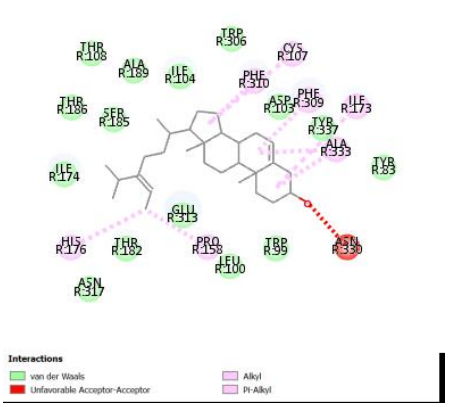
TRP R:306
THR R:108
CYS R:107
ALA R:189
ILE R:104
PHE R:310
THR R:186
SER R:185
ASP R:103
PHE R:309
ILE R:173
TYR R:337
ALA R:333
TYR R:53
ILE R:174
GLU R:313
HIS R:176
THR R:182
PRO R:158
TRP R:99
ASN R:330
LEU R:100
ASN R:317
Interactions
van der Waals
Unfavorable Acceptor-Acceptor
Alkyl
Pi-Alkyl

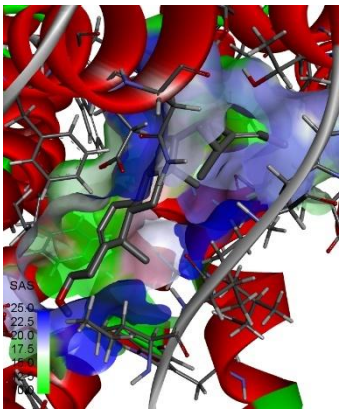
SAS
25.0
22.5
20.0
17.5

VI

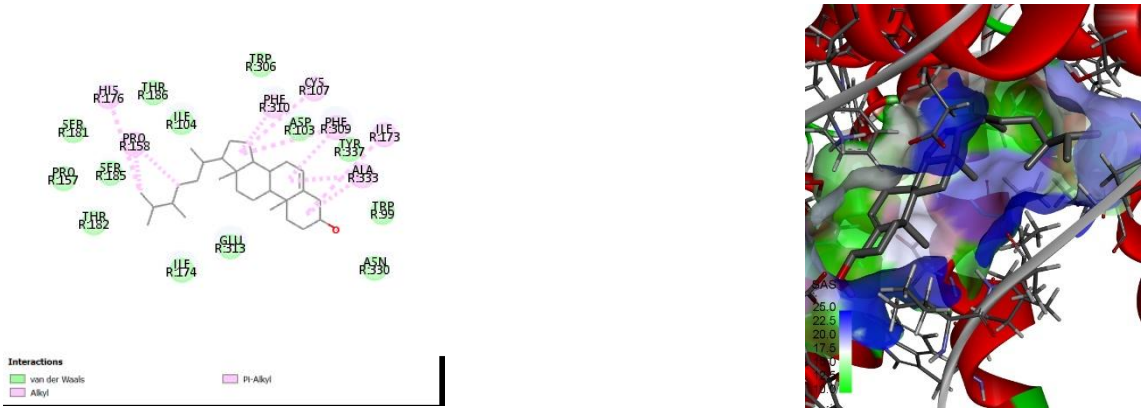

VII

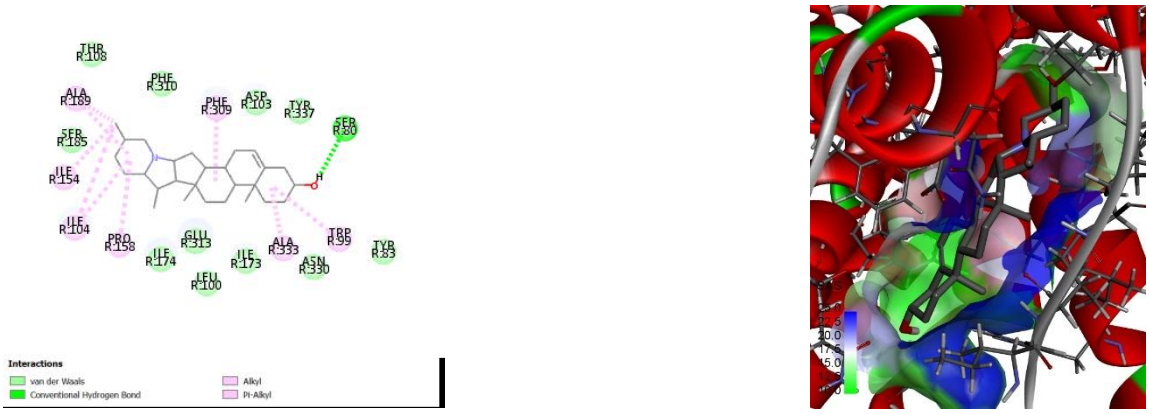

VIII

Figure 3.1.4.3: 2D (left) and 3D (right) views of the molecular interactions of amino-acid residues of 5-HT1F receptor with (I) (3S,8R,9S,10R,12S,13S,14S,17R)-10,13-dimethyl-17-[(1S)-1-[(3S)-3-methyl-2,3,4,5-tetrahydropyridin-6-yl]ethyl]-2,3,4,7,8,9,11,12,14,15,16,17-dodecahydro-1H-cyclopenta[a]phenanthrene-3,12-diol (II) 7-[[(1S,4aR,6S,8aS)-6-hydroxy-5,5,8a-trimethyl-2-methylidene-3,4,4a,6,7,8-hexahydro-1H-naphthalen-1-yl]methoxy]-6,8-dimethoxychromen-2-one (III) Fucosterol (IV) 7-(alpha-D-Glucopyranosyloxy)-5-hydroxy-2-(4-hydroxyphenyl)-4H-1-benzopyran-4-one (V) (1R,3S,3'R,3'aS,4aR,6'S,6aS,6bS,7'aR,9R,11aS,11bS)-1,3-dihydroxy-3',6',10,11b-tetramethylspiro[1,2,3,4,4a,5,6,6a,6b,7,8,11a-dodecahydrobenzo[a]fluorene-9,2'-3a,4,5,6,7,7a-hexahydro-3H-furo[3,2-b]pyridine]-11-one (VI) Isofucosterol (VII) 22,23-Dihydrobrassicasterol (VIII) Solanidine in *Tanacetum parthenium.*

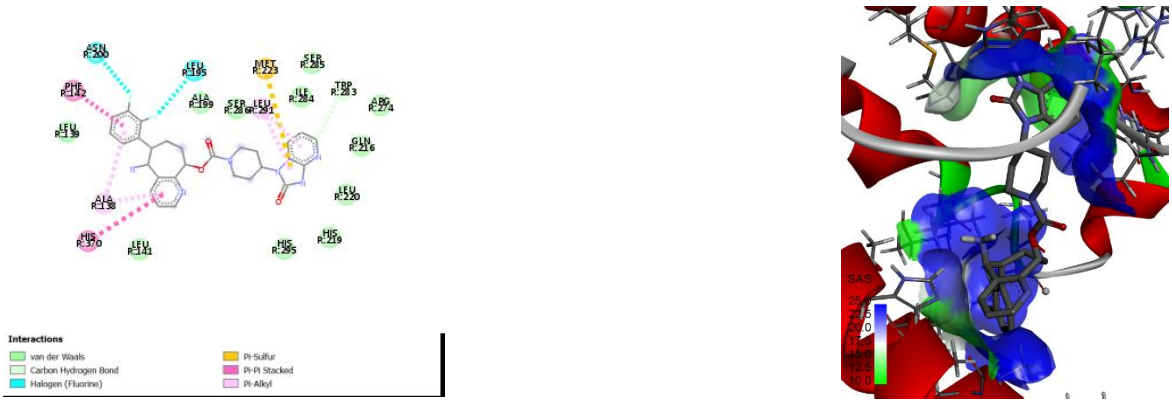

I

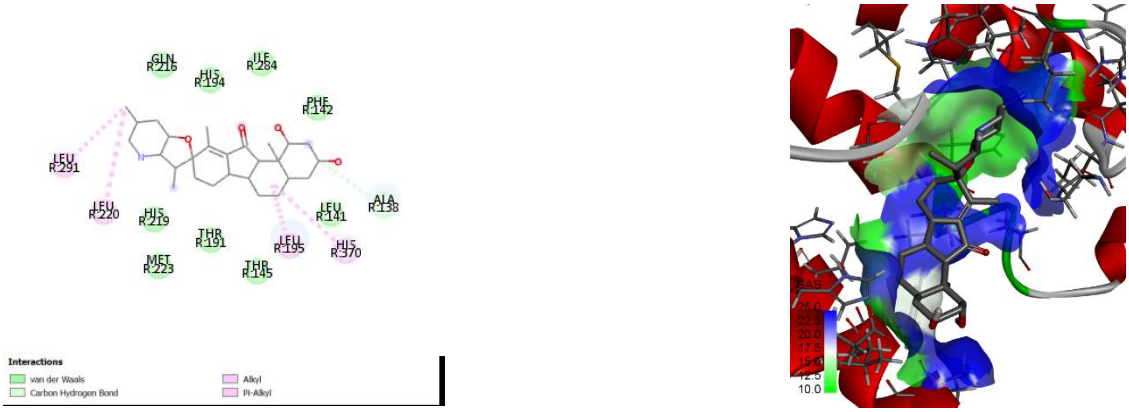

II

Figure 3.1.4.4: 2D (left) and 3D (right) views of the molecular interactions of amino-acid residues of CGRP receptor with (I) Rimegepant (II) (1R,3S,3'R,3'aS,4aR,6'S,6aS,6bS,7'aR,9R,11aS,11bS)-1,3-dihydroxy-3',6',10,11b-tetramethylspiro[1,2,3,4,4a,5,6,6a,6b,7,8,11a-dodecahydrobenzo[a]fluorene-9,2'-3a,4,5,6,7,7a-hexahydro-3H-furo[3,2-b]pyridine]-11-one in *Tanacetum parthenium.*

3.2 ADME Profiling of ligands

Table 3.2.1 ADME Profiling of ligands from Crassocephalum crepidioides

Compounds	Molecular Weight (Da)	Number of Hydrogen Acceptors	Number of Hydrogen Donors	Log $P_{O/W}$	Lipinski
[(1S,2S,3E,5R,7E,11R)-8-formyl-5-[(E)-4-hydroxy-4-methylpent-2-enyl]-1,5-dimethyl-12-oxabicyclo[9.1.0]dodeca-3,7-dien-2-yl] 3-methylbut-2-enoate	416.26	5	1	3.17	0
2-[(1S,2R,3S,9S,11S)-11-methoxy-3,9-dimethyl-3-(4-methylpent-3-enyl)-8,12-dioxatricyclo[7.2.1.01,6]dodec-5-en-2-yl]ethenyl 3-methylbut-2-enoate	430.27	5	0	4.87	0
Vibsanin T	416.26	5	1	3.97	0
[(E)-2-[(1S,5S,7R,8S,11S)-8-methyl-5-(2-oxopropyl)-11-prop-1-en-2-yl-4-oxatricyclo[6.3.1.02,6]dodec-2(6)-en-7-yl]ethenyl] 3-methylbut-2-enoate	398.25	4	0	3.89	0
(1S,4S,5R,8R,13S,14R,17S,18R)-4,5,9,9,13,20,20-heptamethyl-24-oxahexacyclo[15.5.2.01,18.04,17.05,14.08,13] tetracos-15-en-10-one	438.35	2	0	3.48	0
7-but-2-enyl-6,8-dihydroxy-3-pent-3-enyl-3,4-dihydroisochromen-1-one	302.15	4	2	3.63	0
2-(4-hydroxy-3-methoxyphenyl)-3-(hydroxymethyl)-5-[(E)-3-hydroxyprop-1-enyl]-1-benzofuran-7-ol	342.11	6	4	2.08	0
2-[(3aS,5R,8aR)-3-methyl-8-methylidene-3a,4,5,6,7,8a-hexahydro-1H-azulen-5-yl]propan-2-ol	220.18	1	1	3.51	0

[(2R,3R,4S,5R,6S)-3,5-dihydroxy-2-(hydroxymethyl)-6-(6-methoxy-2-oxochromen-7-yl)oxyoxan-4-yl] acetate	396.11	10	3	-0.32	0
2-[(3R,3aR,5S,8aS)-3-hydroperoxy-3-methyl-8-methylidene-3a,4,5,6,7,8a-hexahydroazulen-5-yl]propan-2-ol	252.17	3	2	2.25	0
[(2R,3S,4S,5R,6S)-5-acetyloxy-3,4-dihydroxy-6-(6-methoxy-2-oxochromen-7-yl)oxyoxan-2-yl]methyl acetate	438.12	11	2	-0.03	0
[(2R,3R,4S,5R,6S)-4-acetyloxy-3,5-dihydroxy-6-(6-methoxy-2-oxochromen-7-yl)oxyoxan-2-yl]methyl acetate	438.12	11	2	0.24	0
Scopolin	354.1	9	4	-0.896	0
7-butyl-6,8-dihydroxy-3-pent-3-enyl-3,4-dihydroisochromen-1-one	304.17	4	2	3.71	0
Neovibsanin I	416.26	5	1	3.55	0
[(E)-2-[(4S,6S,7S,8S,11R,15S)-4-methoxy-4,8,12,12-tetramethyl-3,13-dioxatetracyclo[6.6.2.02,6.011,15]hexadec-1-en-7-yl]ethenyl] 3-methylbut-2-enoate	430.27	5	0	4.12	0

Table 3.2.2 ADME Profiling of ligands from *Nigella sativa*

Compounds	**Molecular Weight (Da)**	**Number of Hydrogen Acceptors**	**Number of Hydrogen Donors**	**Log $P_{O/W}$**	**Lipinski**
4alpha,24-Dimethyl-5alpha-cholest-8(9)-en-3beta-ol	414.39	1	1	7.02	0
Butyrospermol	426.39	1	1	7.39	0
(3S,5S,9S,10S,13R,14R,17R)-17-[(E,2S,5S)-5-ethyl-6-methylhept-3-en-2-yl]-10,13-dimethyl-	412.37	1	1	6.38	0

2,3,4,5,6,9,11,12,14,15,16,17-dodecahydro-1H-cyclopenta[a]phenanthren-3-ol					
(3S,8R,9R,10R,13R,14R,17R)-17-[(2R,5R)-5,6-dimethylheptan-2-yl]-10,13-dimethyl-2,3,4,7,8,9,11,12,14,15,16,17-dodecahydro-1H-cyclopenta[a]phenanthren-3-ol	400.37	1	1	7.45	0
(3S)-3-hydroxy-3-methyl-11-(4-oxocyclohexa-2,5-dien-1-ylidene)-2,4,6,7,8,9-hexahydropyridazino[1,2-a]indazol-1-one	312.15	5	1	1.36	0
Campesterol	400.37	1	1	7.66	0
5-Dehydroavenasterol	410.35	1	1	6.49	0
Alpha-Spinasterol	412.37	1	1	6.66	0
24-Ethyllophenol	428.4	1	1	8.69	0
(3R,3aR,5aS,6S,7S,9aR,9bS)-3a,9b-dimethyl-7-prop-1-en-2-yl-3-[(2R,4R)-4,6,6-trimethyl-5-methylideneoctan-2-yl]spiro[1,2,3,4,5,5a,7,8,9,9a-decahydrocyclopenta[a]naphthalene-6,5'-oxolane]-2'-one	482.41	2	0	6.64	0
(+)-Obtusifoliol	426.39	1	1	6.29	0
(3S,6R)-6-[(8R,9S,10S,13R,14S,17R)-10,13-dimethyl-2,3,4,5,6,7,8,9,11,12,14,15,16,17-tetradecahydro-1H-cyclopenta[a]phenanthren-17-yl]-3-propan-2-ylheptan-1-ol	416.4	1	1	8.69	0
4-(1-methoxy-3-methyl-6,7,8,9-tetrahydropyridazino[1,2-a]indazol-11-ylidene)cyclohexa-2,5-dien-1-one	308.15	4	0	3.07	0
[3-methyl-11-(4-oxocyclohexa-2,5-dien-1-ylidene)-6,7,8,9-tetrahydropyridazino[1,2-a]indazol-1-yl] hydrogen sulfate	374.09	7	1	0.63	0
11-(4-hydroxyphenyl)-3-methyl-6,7,8,9-tetrahydropyridazino[1,2-a]indazol-10-ium-1-ol	295.14	4	2	2.27	0

6,7,8,9-Tetrahydro-11-(4-hydroxyphenyl)-3-methyl-1H-pyridazino(1,2-a)indazol-1-one	294.14	4	1	2.15	0
[11-(4-hydroxycyclohexa-2,5-dien-1-ylidene)-3-methyl-6,7,8,9-tetrahydropyridazino[1,2-a]indazol-1-yl]hydrogen sulfate	376.11	7	2	6.38	0
(6aR)-1,2-dimethoxy-6,6-dimethyl-5,6,6a,7-tetrahydro-4H-dibenzo[de,g]quinolin-6-ium-10,11-diol	342.17	5	2	0.86	0
4-(1-methoxy-3-methyl-6,7,8,9-tetrahydropyridazino[1,2-a]indazol-10-ium-11-yl)phenol	309.16	4	1	2.85	0
Nigelladine B	283.19	2	0	3.38	0
Nigelladine A	283.19	2	0	3.63	0
(8aR)-2,2,4-trimethyl-6,8a-di(propan-2-yl)-8,9-dihydrocyclopenta[g]quinolin-7-one	311.22	2	0	4.01	0
(3S)-3-hydroxy-11-(4-hydroxyphenyl)-3-methyl-2,4,6,7,8,9-hexahydropyridazino[1,2-a]indazol-10-ium-1-one	313.15	5	2	1.44	0
Salfredin B11	232.07	4	1	2.31	0
(+)-Tirucallol	426.39	1	1	6.32	0
(3S,8R,9R,10R,13R,14R,17R)-17-[(2R,5R)-5-ethyl-6-methylheptan-2-yl]-10,13-dimethyl-2,3,4,7,8,9,11,12,14,15,16,17-dodecahydro-1H-cyclopenta[a]phenanthren-3-ol	414.39	1	1	7.79	0
(3S,8R,9R,10R,13R,14R,17R)-17-[(E,2S,5S)-5-ethyl-6-methylhept-3-en-2-yl]-10,13-dimethyl-2,3,4,7,8,9,11,12,14,15,16,17-dodecahydro-1H-cyclopenta[a]phenanthren-3-ol	412.37	1	1	6.25	0
(3S,8R,9R,10R,13R,14R,17R)-10,13-dimethyl-17-[(2R)-6-methylheptan-2-yl]-2,3,4,7,8,9,11,12,14,15,16,17-dodecahydro-1H-cyclopenta[a]phenanthren-3-ol	386.35	1	1	7.54	0

Table 3.2.3. ADME Profiling of ligands from *Petasites hybridus*

Compounds	Molecular Weight (Da)	Number of Hydrogen Acceptors	Number of Hydrogen Donors	Log $P_{O/W}$	Lipinski
[(4aR,5S,7S,8aR)-3,4a,5-trimethyl-9-oxo-4,5,6,7,8,8a-hexahydrobenzo[f][1]benzofuran-7-yl](Z)-2-methylbut-2-enoate	330.18	4	0	3.42	0
[(4aR,5S,7S,8aR)-3,4a,5-trimethyl-9-oxo-4,5,6,7,8,8a-hexahydrobenzo[f][1]benzofuran-7-yl] 2-methylbut-2-enoate	330.18	4	0	3.54	0
[(4aR,5S,7R,8aR,9aS)-3,4a,5-trimethyl-2-oxo-4,5,6,7,8,8a,9,9a-octahydrobenzo[f][1]benzofuran-7-yl]3-methylbut-2-enoate	332.2	4	0	3.496	0
4-[(2E,4S,6S)-6-hydroperoxy-4-hydroxy-3,7-dimethylocta-2,7-dienoxy]-5-methylchromen-2-one	360.16	6	2	2.47	0
5-methyl-4-[(2Z)-2-[(5R)-5-(2-methylprop-1-enyl)oxolan-3-ylidene]ethoxy]chromen-2-one	330.18	4	0	4.55	0
Rhamnazin	330.07	7	3	2.06	0
(9-acetyloxy-1-methyl-6-oxo-[1]benzofuro[3,2-c]chromen-8-yl) acetate	366.07	7	0	2.53	0
[(2E)-2-[(8S,8aR)-8,8a-dimethyl-3-oxo-5,6,7,8-tetrahydro-1H-naphthalen-2-ylidene]propyl] (Z)-2-methylbut-2-enoate	316.2	3	0	3.59	0
[(1R,2R,8aR)-1,8a-dimethyl-6-oxo-7-propan-2-ylidene-2,3,4,8-tetrahydro-1H-naphthalen-2-yl] 3-methylbut-2-enoate	316.2	3	0	4.07	0
[(4aR,5S,7R,8aR,9aS)-3,4a,5-trimethyl-2-oxo-4,5,6,7,8,8a,9,9a-octahydrobenzo[f][1]benzofuran-7-yl] (Z)-2-methylbut-2-enoate	332.2	4	0	3.36	0
Pethybrene	204.19	0	0	2.93	0

Albene	162.14	0	0	3.42	0
Euparin	216.08	3	1	3.08	0
(4aR,5S,8aS)-3,4a,5-trimethyl-5,6,7,8,8a,9-hexahydro-4H-benzo[f][1]benzofuran	218.17	1	0	4.42	0
4-Geranyloxy-5-methyl coumarin	312.17	3	0	5.52	0
(4aR,5S,8aR)-3,4a,5-trimethyl-4,5,6,7,8,8a-hexahydrobenzo[f][1]benzofuran-9-one	232.15	2	0	3.55	0
4-[(2Z,5R)-5-hydroxy-3-(hydroxymethyl)-7-methylocta-2,6-dienoxy]-5-methylchromen-2-one	344.16	5	2	2.73	0
[(2E,4R)-3,7-dimethyl-1-(5-methyl-2-oxochromen-4-yl)oxyocta-2,6-dien-4-yl] acetate	370.18	5	0	4.59	0
[(4aR,5S,7R,8aR,9aS)-3,4a,5-trimethyl-2-oxo-4,5,6,7,8,8a,9,9a-octahydrobenzo[f][1]benzofuran-7-yl] (E)-2-methylbut-2-enoate	332.2	4	0	3.38	0
(4aR,5S,8aR,9aR)-3,4a,5-trimethyl-4,5,6,7,8,8a,9,9a-octahydro-1H-benzo[f]indol-2-one	233.18	2	1	2.37	0
(4aR,5R,8aR,9aR)-3,4a,5-trimethyl-4,5,6,7,8,8a,9,9a-octahydrobenzo[f][1]benzofuran-2-one	234.16	2	0	2.72	0
(3S)-3-ethenyl-9-methyl-3-(4-methylpent-3-enyl)-2H-furo[3,2-c]chromen-4-one	310.16	3	0	4.65	0
4-[(2E,4R)-4-hydroxy-3-(hydroxymethyl)-7-methylocta-2,6-dienoxy]-5-methylchromen-2-one	344.16	5	2	3.05	0
4-[(2E,4R)-4-hydroxy-3,7-dimethylocta-2,6-dienoxy]-5-methylchromen-2-one	328.17	4	1	3.79	0
4-[10-Oxo-neryloxy]-5-methylcoumarin	326.15	4	0	4.75	0
4-[10-Oxo-geranyloxyl]-5-methylcoumarin	326.15	4	0	4.81	0

4-(10-Hydroxyneryloxy)-5-methylcoumarin	328.17	4	1	4.13	0
4-(10-Hydroxygeranyloxy)-5-methylcoumarin	328.17	4	1	4.29	0
4-[5-Formyl-3-methyl-pent-2E,4E-dien-1-yl]-5-methylcoumarin	284.1	4	0	3.27	0
4-[6,10-Dioxo-neryloxy]-5-methyl coumarin	340.13	5	0	3.54	0
4-[(2Z,6S)-6-hydroperoxy-3-(hydroxymethyl)-7-methylocta-2,7-dienoxy]-5-methylchromen-2-one	360.16	6	2	2.94	0
4-[(2Z,6R)-6-hydroxy-3-(hydroxymethyl)-7-methylocta-2,7-dienoxy]-5-methylchromen-2-one	344.16	5	2	2.62	0
Dehydrofukinone	218.17	1	0	3.598	0
[(2Z)-6-methyl-2-[2-(5-methyl-2-oxochromen-4-yl)oxyethylidene]hept-5-enyl] acetate	370.18	5	0	4.96	0
Quercetin	302.04	7	5	1.45	0
Neopetasane	218.17	1	0	3.35	0
2-Hydroxy-5-methylcoumarin	176.05	3	1	1.98	0
4a,5-dimethyl-3-propan-2-ylidene-5,6,7,8-tetrahydro-4H-naphthalen-2-one	218.17	1	0	3.80	0
Petasitene	204.19	0	0	4.65	0
Diisobutyl phthalate	278.15	4	0	4.08	0
(R) -beta-bisabolene	204.19	0	0	5.09	0
Beta-Elemene	204.19	0	0	4.62	0
[(4aR,5S,7R,8aR,9aR)-3,4a,5-trimethyl-2-oxo-4,5,6,7,8,8a,9,9a-octahydrobenzo[f][1]benzofuran-7-yl] (Z)-2-methylbut-2-enoate	332.2	4	0	3.17	0
[(4aR,5S,7R,8aR,9aR)-3,4a,5-trimethyl-2-oxo-4,5,6,7,8,8a,9,9a-	318.18	4	0	3.19	0

octahydrobenzo[f][1]benzofuran-7-yl] 2-methylprop-2-enoate					
[(4aR,5S,7R,8aR,9aR)-3,4a,5-trimethyl-2-oxo-4,5,6,7,8,8a,9,9a-octahydrobenzo[f][1]benzofuran-7-yl] 2-methylpropanoate	320.2	4	0	3.498	0
[(4aS,5R,6R,8aR,9aR)-3,4a,5-trimethyl-2-oxo-4,5,6,7,8,8a,9,9a-octahydrobenzo[f][1]benzofuran-6-yl] (Z)-2-methylbut-2-enoate	332.2	4	0	3.24	0
[(4aR,5S,7R,8aR,9aR)-3,4a,5-trimethyl-2-oxo-4,5,6,7,8,8a,9,9a-octahydrobenzo[f][1]benzofuran-7-yl] (E)-2-methylbut-2-enoate	332.2	4	0	3.29	0

Table 3.2.4 ADME Profiling of ligands from *Tanacetum parthenium*

Compounds	**Molecular Weight (Da)**	**Number of Hydrogen Acceptors**	**Number of Hydrogen Donors**	**Log $P_{O/W}$**	**Lipinski**
(3S,8R,9S,10R,12S,13S,14S,17R)-10,13-dimethyl-17-[(1S)-1-[(3S)-3-methyl-2,3,4,5-tetrahydropyridin-6-yl]ethyl]-2,3,4,7,8,9,11,12,14,15,16,17-dodecahydro-1H-cyclopenta[a]phenanthrene-3,12-diol	413.33	3	2	4.62	0
7-[[(1S,4aR,6S,8aS)-6-hydroxy-5,5,8a-trimethyl-2-methylidene-3,4,4a,6,7,8-hexahydro-1H-naphthalen-1-yl]methoxy]-6,8-dimethoxychromen-2-one	442.24	6	1	3.70	0
Phelligridin C	364.06	7	3	2.798	0
Phelligridin D	380.05	8	4	2.26	0
Rubijervine	413.33	3	2	3.85	0
Fucosterol	412.37	1	1	7.696	0

Ergosterol Peroxide	428.33	3	1	4.60	0
Hypholomine B	490.09	10	5	2.75	0
(3S,3'R,3'aS,6'S,6aS,6bS,7'aR,9S,11aS,11bR)-3',6',10,11b-tetramethylspiro[2,3,4,6,6a,6b,7,8,11,11a-decahydro-1H-benzo[a]fluorene-9,2'-3a,4,5,6,7,7a-hexahydro-3H-furo[3,2-b]pyridine]-3-o	411.31	3	2	3.24	0
(4R,5S)-5-[(1S,2R)-2-hydroxy-5-oxocyclopent-3-en-1-yl]-3-methylidene-4-(2-oxopropyl)oxolan-2-one	250.08	5	1	0.01	0
(4R,5S)-5-[(1S,2S)-2-hydroxy-5-oxocyclopent-3-en-1-yl]-3-methylidene-4-(2-oxopropyl)oxolan-2-one	250.08	5	1	-0.21	0
Secotanapartholide B	278.12	5	1	0.48	0
Secotanapartholide A	278.12	5	1	0.17	0
Methyl-gamma-costate	248.18	2	0	3.62	0
(1S,2R,5S,9S,10S,11R)-2-hydroxy-2,11-dimethyl-6-methylidene-8,12,13-trioxatetracyclo[9.2.2.01,10.05,9]pentadec-14-en-7-one	278.12	5	1	1.04	0
(3aS,6R,9aS,9bS)-6-hydroxy-6,9-dimethyl-3-methylidene-4,5,9a,9b-tetrahydro-3aH-azuleno[4,5-b]furan-2-one	246.13	3	1	2.09	0
Santamarin	248.14	3	1	2.07	0
1,3-dimethyl-8-propan-2-yltricyclo[4.4.0.02,7]dec-3-ene	204.19	0	0	5.22	0
(+-)-Cannabichromene	314.22	2	1	6.85	0
Reynosin	248.14	3	1	1.75	0
Apigenin	270.05	5	3	2.98	0
Luteolin	286.05	6	4	2.25	0

Chrysoeriol	300.06	6	3	2.67	0
Artemorin	248.14	3	1	1.22	0
Hispidulin	300.06	6	3	2.58	0
6-Hydroxykaempferol	302.04	7	5	1.62	0
Ellagic Acid	302.01	8	4	0.95	0
Chrysanthenyl isovalerate	236.18	2	0	4.395	0
4-[(E)-2-(3,5-dihydroxyphenyl)ethenyl]-2-methoxybenzene-1,3-diol	274.08	5	4	2.51	0
Nepetin	316.06	7	4	2.09	0
Isofraxidin	222.05	5	1	0.95	0
Jaceosidin	330.07	7	3	2.38	0
Jaceidin	360.08	8	3	2.12	0
1-beta-Hydroxyarbusculin A	266.15	4	2	0.99	0
3-O-methyl-isosecotanapartholide	292.13	5	0	1.09	0
(+)-Alantolactone	232.15	2	0	3.03	0
Chrysanthenyl angelate	234.16	2	0	3.97	0
(1R,2S,7S,8S)-1,3-dimethyl-8-propan-2-yltricyclo[4.4.0.02,7]dec-3-ene	204.19	0	0	5.17	0
7-(alpha-D-Glucopyranosyloxy)-5-hydroxy-2-(4-hydroxyphenyl)-4H-1-benzopyran-4-one	432.11	10	6	1.04	0
(1R,3S,3'R,3'aS,4aR,6'S,6aS,6bS,7'aR,9R,11aS,11bS)-1,3-dihydroxy-3',6',10,11b-tetramethylspiro[1,2,3,4,4a,5,6,6a,6b,7,8,11a-	443.3	5	3	3.05	0

dodecahydrobenzo[a]fluorene-9,2'-3a,4,5,6,7,7a-hexahydro-3H-furo[3,2-b]pyridine]-11-one					
Isofucosterol	412.37	1	1	7.47	0
22,23-Dihydrobrassicasterol	400.37	1	1	7.45	0
Solanidine	397.33	2	1	4.54	0

3.3 Toxicity Prediction

Table 3.3.1 Toxicity prediction of selected ligands from *Crassocephalum crepidioides*

Compounds	Skin Sensitivity	Carcinogenicity	Respiratory Toxicity	Neurotoxicity	Ototoxicity	Hematotoxicity	Nephrotoxicity	Genotoxicity
[(1S,2S,3E,5R,7E,11R)-8-formyl-5-[(E)-4-hydroxy-4-methylpent-2-enyl]-1,5-dimethyl-12-oxabicyclo[9.1.0]dodeca-3,7-dien-2-yl] 3-methylbut-2-enoate	0.9889	0.8015	0.8303	0.7400	0.3328	0.2719	0.7417	0.9993
3-[(1S,2R,3S,9S,11S)-11-methoxy-3,9-dimethyl-3-(4-methylpent-3-enyl)-8,12-dioxatricyclo[7.2.1.01,6]dodec-5-en-2-yl]ethenyl 3-methylbut-2-enoate	0.9786	0.3671	0.7628	0.7302	0.4250	0.1594	0.3807	0.1437
Vibsanin T	0.9923	0.7158	0.7159	0.6476	0.4666	0.3499	0.9392	0.9958
[(E)-2-[(1S,5S,7R,8S,11S)-8-methyl-5-(2-oxopropyl)-11-prop-1-en-2-yl-4-oxatricyclo[6.3.1.02,6]dodec-	0.9964	0.8972	0.8070	0.8833	0.6772	0.8924	0.9542	0.9475

2(6)-en-7-yl]ethenyl] 3-methylbut-2-enoate								
(1S,4S,5R,8R,13S,14R,17S,18R)-4,5,9,9,13,20,20-heptamethyl-24 oxahexacyclo[15.5.2.01,18.04,17.05,14.08,13]tetracos-15-en-10-one	0.9656	0.8577	0.9437	0.2680	0.4137	0.5909	0.7501	0.7451
7-but-2-enyl-6,8-dihydroxy-3-pent-3-enyl-3,4-dihydroisochromen-1-one	0.9979	0.1995	0.7938	0.0727	0.2420	0.0706	0.6468	0.7121
2-(4-hydroxy-3-methoxyphenyl)-3-(hydroxymethyl)-5-[(E)-3-hydroxyprop-1-enyl]-1-benzofuran-7-ol	0.9081	0.7869	0.4767	0.0388	0.2742	0.1265	0.0840	0.7350
2-[(3aS,5R,8aR)-3-methyl-8-methylidene-3a,4,5,6,7,8a-hexahydro-1H-azulen-5-yl]propan-2-ol	0.8362	0.8315	0.4417	0.2693	0.3910	0.5974	0.4438	0.1807
[(2R,3R,4S,5R,6S)-3,5-dihydroxy-2-(hydroxymethyl)-6-(6-methoxy-2-oxochromen-7-yl)oxyoxan-4-yl] acetate	0.9272	0.4750	0.0199	0.0300	0.7428	0.4158	0.5907	0.8485
2-[(3R,3aR,5S,8aS)-3-hydroperoxy-3-methyl-8-methylidene-3a,4,5,6,7,8a-hexahydroazulen-5-yl]propan-2-ol	0.9637	0.7612	0.5580	0.4997	0.4697	0.4486	0.3455	0.5243
[(2R,3S,4S,5R,6S)-5-acetyloxy-3,4-dihydroxy-6-(6-methoxy-2-oxochromen-7-yl)oxyoxan-2-yl]methyl acetate	0.9854	0.6783	0.0073	0.0343	0.5955	0.5756	0.7495	0.9900
[(2R,3R,4S,5R,6S)-4-acetyloxy-3,5-dihydroxy-6-(6-methoxy-2-oxochromen-7-yl)oxyoxan-2-yl]methyl acetate	0.9082	0.5754	0.0100	0.0294	0.5852	0.4963	0.6277	0.9453
Scopolin	0.9462	0.4899	0.0271	0.0239	0.8048	0.3649	0.6049	0.8540
7-butyl-6,8-dihydroxy-3-pent-3-enyl-3,4-dihydroisochromen-1-one	0.9979	0.1030	0.8513	0.0647	0.2851	0.0917	0.7009	0.0303

Neovibsanin I	0.9984	0.6229	0.7248	0.8994	0.7488	0.6955	0.9225	0.7012
[(E)-2-[(4S,6S,7S,8S,11R,15S)-4-methoxy-4,8,12,12-tetramethyl-3,13-dioxatetracyclo[6.6.2.02,6.011,15]hexadec-1-en-7-yl]ethenyl] 3-methylbut-2-enoate	0.9929	0.6214	0.6599	0.7691	0.3735	0.2901	0.7664	0.8478

Table 3.3.2 Toxicity prediction of selected ligands from *Nigella sativa*

Compounds	**Skin Sensitivity**	**Carcinogenicity**	**Respiratory Toxicity**	**Neurotoxicity**	**Ototoxicity**	**Hematotoxicity**	**Nephrotoxicity**	**Genotoxicity**
4alpha,24-Dimethyl-5alpha-cholest-8(9)-en-3beta-ol	0.9374	0.8491	0.7347	0.0394	0.5946	0.6503	0.7361	0.0082
Butyrospermol	0.8560	0.7772	0.8163	0.0753	0.4831	0.2622	0.4312	0.0532
(3S,5S,9S,10S,13R,14R,17R)-17-[(E,2S,5S)-5-ethyl-6-methylhept-3-en-2-yl]-10,13-dimethyl-2,3,4,5,6,9,11,12,14,15,16,17-dodecahydro-1H-cyclopenta[a]phenanthren-3-ol	0.9843	0.8241	0.9412	0.2657	0.5633	0.4678	0.6685	0.0569
(3S,8R,9R,10R,13R,14R,17R)-17-[(2R,5R)-5,6-dimethylheptan-2-yl]-10,13-dimethyl-2,3,4,7,8,9,11,12,14,15,16,17-dodecahydro-1H-cyclopenta[a]phenanthren-3-ol	0.9295	0.8504	0.7236	0.1062	0.4349	0.2539	0.4672	0.0141
(3S)-3-hydroxy-3-methyl-11-(4-oxocyclohexa-2,5-dien-1-ylidene)-2,4,6,7,8,9-hexahydropyridazino[1,2-	0.9752	0.9554	0.0876	0.4110	0.4627	0.8392	0.8754	0.9703

a]indazol-1-one								
Campesterol	0.9470	0.8749	0.7985	0.0658	0.4236	0.2966	0.4672	0.0112
5-Dehydroavenasterol	0.9769	0.7373	0.9715	0.1381	0.5423	0.3798	0.5874	0.1529
Alpha-Spinasterol	0.9404	0.8508	0.9615	0.0921	0.6121	0.6649	0.6712	0.0216
24-Ethyllophenol	0.4717	0.3040	0.6990	0.5298	0.9185	0.1320	0.0576	1.2080
(3R,3aR,5aS,6S,7S,9aR,9bS)-3a,9b-dimethyl-7-prop-1-en-2-yl-3-[(2R,4R)-4,6,6-trimethyl-5-methylideneoctan-2-yl]spiro[1,2,3,4,5,5a,7,8,9,9a-decahydrocyclopenta[a]naphthalene-6,5'-oxolane]-2'-one	0.8976	0.7960	0.6977	0.2742	0.6660	0.5160	0.6544	0.2014
(+)-Obtusifoliol	0.9701	0.8494	0.7767	0.0250	0.5255	0.6950	0.8029	0.1125
(3S,6R)-6-[(8R,9S,10S,13R,14S,17R)-10,13-dimethyl-2,3,4,5,6,7,8,9,11,12,14,15,16,17-tetradecahydro-1H-cyclopenta[a]phenanthren-17-yl]-3-propan-2-ylheptan-1-ol	0.9989	0.9182	0.9735	0.2915	0.6273	0.4692	0.7274	0.0002
4-(1-methoxy-3-methyl-6,7,8,9-tetrahydropyridazino[1,2-a]indazol-11-ylidene)cyclohexa-2,5-dien-1-one	0.8455	0.8126	0.8305	0.8045	0.3144	0.7387	0.3458	0.8804
[3-methyl-11-(4-oxocyclohexa-2,5-dien-1-ylidene)-6,7,8,9-tetrahydropyridazino[1,2-a]indazol-1-yl] hydrogen sulfate	0.9710	0.4980	0.7997	0.1072	0.3112	0.6205	0.2415	0.9954

11-(4-hydroxyphenyl)-3-methyl-6,7,8,9-tetrahydropyridazino[1,2-a]indazol-10-ium-1-ol	0.9992	0.5860	0.9321	0.5993	0.0226	0.0065	0.2048	0.9999
6,7,8,9-Tetrahydro-11-(4-hydroxyphenyl)-3-methyl-1H-pyridazino(1,2-a)indazol-1-one	0.5885	0.6053	0.7452	0.8565	0.2435	0.4245	0.4375	0.9644
[11-(4-hydroxycyclohexa-2,5-dien-1-ylidene)-3-methyl-6,7,8,9-tetrahydropyridazino[1,2-a]indazol-1-yl]hydrogen sulfate	0.8497	0.3354	0.7147	0.0924	0.3412	0.2979	0.2781	0.9638
(6aR)-1,2-dimethoxy-6,6-dimethyl-5,6,6a,7-tetrahydro-4H-dibenzo[de,g]quinolin-6-ium-10,11-diol	0.7728	0.4643	0.9971	0.5717	0.1456	0.0223	0.0911	0.4847
4-(1-methoxy-3-methyl-6,7,8,9-tetrahydropyridazino[1,2-a]indazol-10-ium-11-yl)phenol	0.9988	0.7311	0.8931	0.8296	0.0209	0.0109	0.2103	0.9999
Nigelladine B	0.9700	0.9080	0.6750	0.7504	0.5579	0.7840	0.9401	0.9275
Nigelladine A	0.9646	0.9003	0.7085	0.6907	0.5156	0.7152	0.9048	0.7218
(8aR)-2,2,4-trimethyl-6,8a-di(propan-2-yl)-8,9-dihydrocyclopenta[g]quinolin-7-one	0.9727	0.8864	0.7568	0.8718	0.6381	0.7012	0.8274	0.9673
Salfredin B11	0.9915	0.9316	0.4938	0.5141	0.3860	0.7308	0.8988	0.9183
(+)-Tirucallol	0.9789	0.8352	0.8779	0.1593	0.4815	0.4981	0.7305	0.0997
(3S)-3-hydroxy-11-(4-hydroxyphenyl)-3-methyl-2,4,6,7,8,9-hexahydropyridazino[1,2-a]indazol-10-ium-1-one	0.9997	0.8744	0.1958	0.4347	0.0438	0.0124	0.6105	0.9999

(3S,8R,9R,10R,13R,14R,17R)-17-[(2R,5R)-5-ethyl-6-methylheptan-2-yl]-10,13-dimethyl-2,3,4,7,8,9,11,12,14,15,16,17-dodecahydro-1H-cyclopenta[a]phenanthren-3-ol	0.9860	0.6479	0.8328	0.1420	0.4960	0.2248	0.4692	0.0010
(3S,8R,9R,10R,13R,14R,17R)-17-[(E,2S,5S)-5-ethyl-6-methylhept-3-en-2-yl]-10,13-dimethyl-2,3,4,7,8,9,11,12,14,15,16,17-dodecahydro-1H-cyclopenta[a]phenanthren-3-ol	0.9825	0.8350	0.9019	0.2778	0.5874	0.4573	0.6053	0.1157
(3S,8R,9R,10R,13R,14R,17R)-10,13-dimethyl-17-[(2R)-6-methylheptan-2-yl]-2,3,4,7,8,9,11,12,14,15,16,17-dodecahydro-1H-cyclopenta[a]phenanthren-3-ol	0.9378	0.8570	0.6696	0.0472	0.4782	0.2241	0.3992	0.0052

Table 3.3.3 Toxicity prediction of selected ligands from *Petasites hybridus*

Compounds	**Skin Sensitivity**	**Carcinogenicity**	**Respiratory Toxicity**	**Neurotoxicity**	**Ototoxicity**	**Hematotoxicity**	**Nephrotoxicity**	**Genotoxicity**
[(4aR,5S,7S,8aR)-3,4a,5-trimethyl-9-oxo-4,5,6,7,8,8a-hexahydrobenzo[f][1]benzofuran-7-yl](Z)-2-methylbut-2-enoate	0.5905	0.9427	0.6370	0.1883	0.2526	0.4150	0.7753	0.9465
[(4aR,5S,7S,8aR)-3,4a,5-trimethyl-9-oxo-4,5,6,7,8,8a-hexahydrobenzo[f][1]benzofuran-7-yl] 2-methylbut-2-enoate	0.6981	0.9497	0.6935	0.2152	0.3242	0.5143	0.8243	0.9437
[(4aR,5S,7R,8aR,9aS)-3,4a,5-trimethyl-2-oxo-4,5,6,7,8,8a,9,9a-octahydrobenzo[f][1]benzofuran-7-yl]3-methylbut-2-enoate	0.9999	0.9882	0.5883	0.9599	0.3723	0.8657	0.9951	0.9915

4-[(2E,4S,6S)-6-hydroperoxy-4-hydroxy-3,7-dimethylocta-2,7-dienoxy]-5-methylchromen-2-one	0.9926	0.9488	0.7170	0.6344	0.6636	0.7765	0.8816	0.9940
6-methyl-4-[(2Z)-2-[(5R)-5-(2-methylprop-1-enyl)oxolan-3-ylidene]ethoxy]chromen-2-one	0.9954	0.9155	0.5000	0.5030	0.1355	0.0813	0.3372	0.9378
Rhamnazin	0.5200	0.7068	0.7957	0.0577	0.1181	0.1869	0.0958	0.6323
(9-acetyloxy-1-methyl-6-oxo-[1]benzofuro[3,2-c]chromen-8-yl) acetate	0.7259	0.6513	0.3457	0.0847	0.0736	0.4126	0.0259	0.7927
Pethybrene	0.6928	0.7826	0.8457	0.4331	0.3434	0.4210	0.5555	0.2022
[(2E)-2-[(8S,8aR)-8,8a-dimethyl-3-oxo-5,6,7,8-tetrahydro-1H-naphthalen-2-ylidene]propyl] (Z)-2-methylbut-2-enoate	0.9654	0.9449	0.5185	0.2785	0.2602	0.5650	0.7947	0.9053
[(1R,2R,8aR)-1,8a-dimethyl-6-oxo-7-propan-2-ylidene-2,3,4,8-tetrahydro-1H-naphthalen-2-yl] 3-methylbut-2-enoate	0.9082	0.7608	0.7347	0.7718	0.3246	0.5966	0.4965	0.5551
[(4aR,5S,7R,8aR,9aS)-3,4a,5-trimethyl-2-oxo-4,5,6,7,8,8a,9,9a-octahydrobenzo[f][1]benzofuran-7-yl] (Z)-2-methylbut-2-enoate	0.9997	0.9910	0.4624	0.8764	0.2975	0.7621	0.9930	0.9851
Albene	0.9009	0.9269	0.9204	0.3328	0.1538	0.1046	0.3416	0.3215
Euparin	0.5569	0.7484	0.8032	0.2329	0.2347	0.4181	0.1807	0.6707
(4aR,5S,8aS)-3,4a,5-trimethyl-5,6,7,8,8a,9-hexahydro-4H-benzo[f][1]benzofuran	0.5678	0.8786	0.8189	0.1431	0.2254	0.3585	0.3282	0.1088

4-Geranyloxy-5-methyl coumarin	0.8709	0.6798	0.8821	0.4231	0.3494	0.3530	0.2498	0.2735
(4aR,5S,8aR)-3,4a,5-trimethyl-4,5,6,7,8,8a-hexahydrobenzo[f][1]benzofuran-9-one	0.5227	0.9365	0.7544	0.1406	0.2359	0.4961	0.2473	0.7072
4-[(2Z,5R)-5-hydroxy-3-(hydroxymethyl)-7-methylocta-2,6-dienoxy]-5-methylchromen-2-one	0.9380	0.8520	0.7899	0.2769	0.4792	0.2526	0.1854	0.7096
[(2E,4R)-3,7-dimethyl-1-(5-methyl-2-oxochromen-4-yl)oxyocta-2,6-dien-4-yl] acetate	0.9341	0.7658	0.7312	0.4915	0.5085	0.5839	0.6098	0.9676
[(4aR,5S,7R,8aR,9aS)-3,4a,5-trimethyl-2-oxo-4,5,6,7,8,8a,9,9a-octahydrobenzo[f][1]benzofuran-7-yl] (E)-2-methylbut-2-enoate	0.9997	0.9912	0.5610	0.9124	0.3300	0.8026	0.9945	0.9949
(4aR,5S,8aR,9aR)-3,4a,5-trimethyl-4,5,6,7,8,8a,9,9a-octahydro-1H-benzo[f]indol-2-one	0.6831	0.5990	0.7092	0.2681	0.4171	0.6168	0.5290	0.4146
(4aR,5R,8aR,9aR)-3,4a,5-trimethyl-4,5,6,7,8,8a,9,9a-octahydrobenzo[f][1]benzofuran-2-one	0.9597	0.7979	0.4186	0.2306	0.2991	0.6444	0.8345	0.1612
(3S)-3-ethenyl-9-methyl-3-(4-methylpent-3-enyl)-2H-furo[3,2-c]chromen-4-one	0.8183	0.7454	0.5051	0.5898	0.2624	0.4556	0.3991	0.1646
4-[(2E,4R)-4-hydroxy-3-(hydroxymethyl)-7-methylocta-2,6-dienoxy]-5-methylchromen-2-one	0.6331	0.7440	0.7208	0.2035	0.6153	0.2672	0.2781	0.7821
4-[(2E,4R)-4-hydroxy-3,7-dimethylocta-2,6-dienoxy]-5-methylchromen-2-one	0.4597	0.7119	0.6201	0.1674	0.5711	0.2921	0.2871	0.5822
4-[10-Oxo-neryloxy]-5-methylcoumarin	0.6264	0.6219	0.7641	0.4333	0.2414	0.3115	0.2339	0.3254
4-[10-Oxo-geranyloxyl]-5-methylcoumarin	0.7359	0.6713	0.8661	0.4458	0.1564	0.2050	0.1902	0.3920

4-(10-Hydroxyneryloxy)-5-methylcoumarin	0.8796	0.5306	0.8718	0.4223	0.2944	0.2792	0.2317	0.3113
4-(10-Hydroxygeranyloxy)-5-methylcoumarin	0.9352	0.4277	0.8790	0.1254	0.1700	0.1402	0.0713	0.0483
4-[5-Formyl-3-methyl-pent-2E,4E-dien-1-yl]-5-methylcoumarin	0.2993	0.8407	0.7023	0.3825	0.2611	0.3231	0.2559	0.8801
4-[6,10-Dioxo-neryloxy]-5-methyl coumarin	0.3803	0.7106	0.7661	0.4097	0.2924	0.3922	0.1468	0.8032
4-[(2Z,6S)-6-hydroperoxy-3-(hydroxymethyl)-7-methylocta-2,7-dienoxy]-5-methylchromen-2-one	0.9995	0.6888	0.4091	0.0738	0.3156	0.2938	0.1019	0.7133
4-[(2Z,6R)-6-hydroxy-3-(hydroxymethyl)-7-methylocta-2,7-dienoxy]-5-methylchromen-2-one	0.9879	0.6284	0.8331	0.0574	0.3306	0.2207	0.1313	0.2694
Dehydrofukinone	0.8338	0.8618	0.6745	0.3595	0.2287	0.5119	0.5051	0.2854
[(2Z)-6-methyl-2-[2-(5-methyl-2-oxochromen-4-yl)oxyethylidene]hept-5-enyl] acetate	0.9645	0.5696	0.8220	0.1994	0.0525	0.1709	0.1165	0.1332
Quercetin	0.8969	0.6002	0.6737	0.0086	0.1637	0.0325	0.0106	0.9749
Neopetasane	0.9313	0.8319	0.7117	0.3854	0.2018	0.6024	0.4986	0.7251
4-Hydroxy-5-methylcoumarin	0.5019	0.7001	0.8672	0.1926	0.1222	0.2182	0.2128	0.7722
4a,5-dimethyl-3-propan-2-ylidene-5,6,7,8-tetrahydro-4H-naphthalen-2-one	0.7522	0.7122	0.6014	0.6323	0.3421	0.6255	0.3819	0.1212

Petasitene	0.5577	0.8144	0.8119	0.4733	0.3930	0.3303	0.4119	0.2798
Diisobutyl phthalate	0.4726	0.5477	0.0313	0.0880	0.1565	0.0046	0.0219	0.0005
(S)-beta-bisabolene	0.9742	0.6482	0.8667	0.4946	0.1465	0.4002	0.3362	0.0061
Beta-Elemene	0.9185	0.8879	0.8727	0.4009	0.2471	0.5303	0.2233	0.2153
[(4aR,5S,7R,8aR,9aR)-3,4a,5-trimethyl-2-oxo-4,5,6,7,8,8a,9,9a-octahydrobenzo[f][1]benzofuran-7-yl] (Z)-2-methylbut-2-enoate	0.9855	0.9271	0.3596	0.5817	0.2719	0.3451	0.9492	0.8525
[(4aR,5S,7R,8aR,9aR)-3,4a,5-trimethyl-2-oxo-4,5,6,7,8,8a,9,9a-octahydrobenzo[f][1]benzofuran-7-yl] 2-methylprop-2-enoate	0.9913	0.9338	0.3656	0.7586	0.3814	0.3727	0.9286	0.7734
[(4aR,5S,7R,8aR,9aR)-3,4a,5-trimethyl-2-oxo-4,5,6,7,8,8a,9,9a-octahydrobenzo[f][1]benzofuran-7-yl] 2-methylpropanoate	0.9848	0.8292	0.5244	0.7937	0.4834	0.5896	0.9750	0.9215
[(4aS,5R,6R,8aR,9aR)-3,4a,5-trimethyl-2-oxo-4,5,6,7,8,8a,9,9a-octahydrobenzo[f][1]benzofuran-6-yl] (Z)-2-methylbut-2-enoate	0.9957	0.8632	0.2818	0.4013	0.2148	0.4632	0.8250	0.8268
[(4aR,5S,7R,8aR,9aR)-3,4a,5-trimethyl-2-oxo-4,5,6,7,8,8a,9,9a-octahydrobenzo[f][1]benzofuran-7-yl] (E)-2-methylbut-2-enoate	0.9858	0.9285	0.4626	0.6757	0.3058	0.3998	0.9594	0.9427

Table 3.3.4 Toxicity prediction of selected ligands from *Tanacetum parthenium*

Compounds	Skin Sensitivity	Carcinogenicity	Respiratory Toxicity	Neurotoxicity	Ototoxicity	Hematotoxicity	Nephrotoxicity	Genotoxicity
(3S,8R,9S,10R,12S,13S,14S,17R)-10,13-dimethyl-17-[(1S)-1-[(3S)-3-methyl-2,3,4,5-tetrahydropyridin-6-yl]ethyl]-2,3,4,7,8,9,11,12,14,15,16,17-dodecahydro-1H-cyclopenta[a]phenanthrene-3,12-diol	0.9934	0.9772	0.9128	0.0726	0.5007	0.1622	0.6909	0.012
7-[[(1S,4aR,6S,8aS)-6-hydroxy-5,5,8a-trimethyl-2-methylidene-3,4,4a,6,7,8-hexahydro-1H-naphthalen-1-yl]methoxy]-6,8-dimethoxychromen-2-one	0.1978	0.7251	0.5380	0.2048	0.4160	0.2153	0.2160	0.6495
Phelligridin C	0.9797	0.7754	0.2422	0.0179	0.2972	0.0413	0.0581	0.9397
Phelligridin D	0.9974	0.6456	0.1824	0.0022	0.5747	0.0260	0.0227	0.9500
Rubijervine	0.9622	0.9287	0.8790	0.1087	0.3633	0.1672	0.5990	0.0128
Fucosterol	0.9165	0.7824	0.8273	0.0681	0.4419	0.3294	0.5698	0.0187
Ergosterol Peroxide	0.9884	0.9195	0.8034	0.0314	0.6012	0.0502	0.3672	0.0768
Hypholomine B	0.9981	0.5578	0.2432	0.0025	0.5845	0.0075	0.0072	0.9996

(3S,3'R,3'aS,6'S,6aS,6bS,7'aR,9S,11aS,11bR)-3',6',10,11b-tetramethylspiro[2,3,4,6,6a,6b,7,8,11,11a-decahydro-1H-benzo[a]fluorene-9,2'-3a,4,5,6,7,7a-hexahydro-3H-furo[3,2-b]pyridine]-3-o	0.9794	0.7269	0.6853	0.3032	0.7581	0.1625	0.5483	0.1577
(4R,5S)-5-[(1S,2R)-2-hydroxy-5-oxocyclopent-3-en-1-yl]-3-methylidene-4-(2-oxopropyl)oxolan-2-one	0.9975	0.6994	0.6109	0.5740	0.4426	0.9303	0.8934	0.9958
(4R,5S)-5-[(1S,2S)-2-hydroxy-5-oxocyclopent-3-en-1-yl]-3-methylidene-4-(2-oxopropyl)oxolan-2-one	0.9987	0.7241	0.4842	0.7245	0.4087	0.9297	0.9306	0.9989
Secotanapartholide B	0.9989	0.8926	0.5109	0.9135	0.4541	0.7350	0.9774	0.8053
Secotanapartholide A	0.9960	0.7683	0.4138	0.7838	0.4304	0.7866	0.9687	0.8455
Methyl-gamma-costate	0.9616	0.7436	0.8738	0.3700	0.3499	0.4718	0.6320	0.0822
(1S,2R,5S,9S,10S,11R)-2-hydroxy-2,11-dimethyl-6-methylidene-8,12,13-trioxatetracyclo[9.2.2.01,10.05,9]pentadec-14-en-7-one	0.9939	0.5144	0.8115	0.4200	0.5000	0.2380	0.2974	0.6730
(3aS,6R,9aS,9bS)-6-hydroxy-6,9-dimethyl-3-methylidene-4,5,9a,9b-tetrahydro-3aH-azuleno[4,5-b]furan-2-one	0.9951	0.9066	0.7058	0.8080	0.4304	0.6949	0.8759	0.9697
Santamarin	0.9834	0.9171	0.4719	0.3689	0.3876	0.6697	0.7403	0.7506
1,3-dimethyl-8-propan-2-yltricyclo[4.4.0.02,7]dec-3-ene	0.0503	0.6647	0.6514	0.4655	0.6667	0.2111	0.0722	0.0040

(+-)-Cannabichromene	0.8925	0.1264	0.9120	0.2548	0.5230	0.2221	0.4892	0.0001
Reynosin	0.9821	0.9162	0.4838	0.5824	0.4865	0.5100	0.7485	0.6330
Apigenin	0.6452	0.7934	0.7773	0.0606	0.0678	0.0432	0.0214	0.9872
Luteolin	0.9286	0.6893	0.7290	0.0116	0.1532	0.0285	0.0099	0.9858
Chrysoeriol	0.7209	0.7580	0.8365	0.0446	0.0752	0.0669	0.0344	0.9482
Artemorin	0.9871	0.7273	0.2527	0.5599	0.4436	0.6900	0.8205	0.3832
Hispidulin	0.7327	0.6889	0.7459	0.0926	0.1035	0.0890	0.0479	0.9446
6-Hydroxykaempferol	0.9845	0.5793	0.5144	0.0076	0.3853	0.0291	0.0086	0.9714
Ellagic Acid	0.8955	0.6663	0.2773	0.0027	0.3716	0.1537	0.0390	0.9534
Chrysanthenyl isovalerate	0.4289	0.5297 .	0.3830	0.6667	0.6535	0.3309	0.2065	0.0529
4-[(E)-2-(3,5-dihydroxyphenyl)ethenyl]-2-methoxybenzene-1,3-diol	0.8766	0.5281	0.6745	0.2084	0.1692	0.0673	0.1165	0.8640
Nepetin	0.9481	0.5668	0.7044	0.0179	0.2245	0.0606	0.0236	0.9401

Isofraxidin	0.3915	0.7376	0.6914	0.3689	0.1456	0.3281	0.2125	0.5985
Jaceosidin	0.7820	0.6482	0.8201	0.0682	0.1160	0.1365	0.0799	0.8043
Jaceidin	0.7925	0.6931	0.7044	0.1075	0.1570	0.1842	0.1111	0.5329
1-beta-Hydroxyarbusculin A	0.9988	0.9576	0.6285	0.3480	0.4755	0.7122	0.9228	0.8443
3-O-methyl-isosecotanapartholide	0.9997	0.9351	0.1982	0.9177	0.6343	0.9154	0.9845	0.9068
(+)-Alantolactone	0.9934	0.8753	0.7846	0.7884	0.5039	0.8563	0.8394	0.8858
Chrysanthenyl angelate	0.4005	0.5115	0.4168	0.4896	0.4717	0.2220	0.1452	0.1278
(1R,2S,7S,8S)-1,3-dimethyl-8-propan-2-yltricyclo[4.4.0.02,7]dec-3-ene	0.8745	0.6054	0.4975	0.2718	0.4332	0.5007	0.2156	0.1030
7-(alpha-D-Glucopyranosyloxy)-5-hydroxy-2-(4-hydroxyphenyl)-4H-1-benzopyran-4-one	0.9578	0.3146	0.0558	0.0068	0.8161	0.0598	0.1961	0.8575
(1R,3S,3'R,3'aS,4aR,6'S,6aS,6bS,7'aR,9R,11aS,11bS)-1,3-dihydroxy-3',6',10,11b-tetramethylspiro[1,2,3,4,4a,5,6,6a,6b,7,8,11a-dodecahydrobenzo[a]fluorene-9,2'-3a,4,5,6,7,7a-hexahydro-3H-furo[3,2-b]pyridine]-11-one	0.9930	0.9230	0.8801	0.6783	0.6472	0.2048	0.8567	0.7343
Isofucosterol	0.9896	0.8457	0.9121	0.0266	0.3187	0.1638	0.4255	0.0223

22,23-Dihydrobrassicasterol	0.9726	0.8998	0.6541	0.0478	0.4851	0.3572	0.6068	0.0026
Solanidine	0.9274	0.9128	0.7936	0.0918	0.4220	0.2316	0.4743	0.0110

CHAPTER FOUR

DISCUSSION

4 DISCUSSION

Sumatriptan is clinically used for the acute treatment of migraine attacks, with or without aura, providing relief from migraine pain and associated symptoms such as nausea, photophobia, and phonophobia. It is not indicated for migraine prevention (Tfelt-Hansen and Saxena, 2001). Lasmiditan is used for the acute treatment of migraines in adults, especially in patients who cannot take triptans due to cardiovascular risk and is not indicated for preventive therapy (Goadsby et al., 2019). Rimegepant has dual clinical use in migraines, serving both as an acute treatment to terminate migraine attacks and as a preventive therapy to reduce the frequency of migraine days in adults (Blair, 2023). Donitriptan was developed for the acute treatment of migraine attacks, but it has never been commercially marketed, and its clinical use remains investigational (Dukat, 2001).

4.1 Binding Affinity

Crassocephalum crepidioides has been widely used in African traditional medicine for the treatment of wounds, inflammation, fever, headache, and gastrointestinal disorders, reflecting its analgesic and anti-inflammatory properties (Osei *et al*., 2021; Saganuwan, 2014). Nigella sativa, commonly known as black seed, is valued in traditional medicine for the treatment of cough, asthma, fever, and general body pain, consistent with its ethnomedicinal applications across Asia and Africa. The plant has been reported to grow successfully in northern Nigeria, particularly in states such as Kano, Kaduna, and Borno, where the climatic conditions favor its cultivation

(Mohammed *et al*., 2019; Suleiman *et al*., 2020). It is locally known and used in traditional medicine for managing respiratory ailments and fever (Kareem *et al*., 2019). Petasites hybridus, known as butterbur, is clinically recognized for its efficacy in migraine prophylaxis, with standardized root and leaf extracts shown to reduce migraine frequency and severity in controlled studies (Lipton *et al*., 2006; Allais *et al,* 2006). Tanacetum parthenium, or feverfew, is scientifically established as an effective agent for the prevention and reduction of migraine attacks, with its bioactive compounds such as parthenolide contributing to its therapeutic effect (Pareek *et al*., 2011; British Herbal Medicine Association, 2024).

Molecular docking studies of plant-derived compounds help identify potential drug candidates for migraine management by predicting how these compounds interact with migraine-related receptors such as 5-HT_1B, 5-HT_1D, 5-HT_1F, and CGRP receptors. By evaluating docking scores, researchers can determine compounds with strong binding affinity and possible therapeutic activity, guiding further development of effective anti-migraine agents (Kumar *et al*., 2022; Khan *et al*., 2021). Exploring alternatives to these drugs are necessary because despite their effectiveness in treating migraine, they have specific limitations. These drawbacks as highlighted in chapter one led to the need to investigate alternative anti-migraine agents, including plant-derived compounds, that could provide similar efficacy with improved safety, tolerability, and accessibility.

Molecular docking produces a docking score, which quantifies the predicted binding affinity between a ligand and its protein target. A stronger (more negative) docking score suggests a more stable and likely biologically active interaction (Wang and Zhu, 2016; Dar and Mir, 2017). In drug discovery, including migraine research, docking scores allow efficient screening of plant-derived or synthetic compounds against key receptors, guiding the identification of lead

candidates for development. Identifying the active site and binding amino acids in target proteins enabled site-specific docking and allowed prediction of ligand activity based on the number and quality of interactions with key residues (Meng *et al*., 2011; Ferreira *et al*., 2015).

Different ligands bound to amino acids in the target protein via various interactions such as conventional hydrogen bond, Van der Waals, Carbon Hydrogen Bond, Pi-Pi Stacked, Pi-Pi T-shaped, Pi-Alkyl, Alkyl, Pi-Sigma, Pi-Sulfur, Pi-Donor Hydrogen Bond, Pi-Lone Pair, Pi-Anion, Attractive Charge, Halogen(F), Amide-Pi Stacked, Unfavourable Donor-Donor, Unfavourable Acceptor-Acceptor, and Unfavourable Bump. Among these interactions, the conventional hydrogen bond is the most significant and will be used to predict potential ligand activity in vivo.

4.1.1 Crassocephalum crepidioides

Sixteen (16) compounds (including the four standard ligands) interacted with one or more of the target proteins, exhibiting varying binding affinities, as shown in **Table 3.1.1;** binding affinities ranged from -9.2 to -9.4kcal/mol for 5-HT1B, -6.9 to -7.6kcal/mol for 5-HT1D, and -9.8 to -10.1 kcal/mol for 5-HT1F receptors with the first value in each range corresponding to the binding affinities of the respective standards Donitriptan, Sumatriptan, and Lasmiditan. No Compound had a binding affinity equal to or stronger than that of Rimegepant (-9.1kcal/mol).

For Serotonin 1B receptor, Vibsanin T and Compound 11188728 exhibited the highest binding affinity (-9.4kcal/mol) and each formed one conventional hydrogen bond. Compound 15385431, despite exhibiting the highest binding affinity, did not form any conventional hydrogen bond while Compound 162889473 exhibited the lowest binding affinity and formed a conventional hydrogen bond. The ligands bound only to ^{209}THR amino acid residue to form the conventional hydrogen bond.

The docking was done at an exhaustiveness of 8 and the auto grid measurement was:

	X	Y	Z
Center	87.3412	64.2975	66.1044
Dimensions (Angstrom)	28.8494	42.5011	22.7417

For Serotonin 1D receptor, Compound 162915438 exhibited the highest binding affinity(-7.6kcal/mol) and formed two conventional hydrogen bonds and 7-but-2-enyl-6,8-dihydroxy-3-pent-3-enyl-3,4-dihydroisochromen-1-one with a binding affinity of -7.3kcal/mol did not form any conventional hydrogen bond. Ligands bound to the active site amino acids in the order: ^{201}SER = ^{321}SER > ^{118}ASP= ^{123}THR= ^{198}THR > ^{119}ILE= ^{342}THR.

The docking was done at an exhaustiveness of 8 and the auto grid measurement was:

	X	Y	Z
Center	97.9385	121.8423	111.2780
Dimensions (Angstrom)	17.0576	17.5505	14.1128

Compound 12068760 exhibited the highest binding affinity(-10.1kcal/mol) against Serotonin 1F receptor and formed two conventional hydrogen bonds while Neovibsanin I formed the highest conventional hydrogen bond (3). Both compounds exhibited a higher binding affinity than Lasmiditan(-9.1kcal/mol). These enhanced affinities imply that both compounds possess a higher intrinsic potential for potency relative to Lasmiditan, suggesting their capability to serve as potent modulators or agonists at the 5-HT$_1$F receptor binding site.

The docking was done at an exhaustiveness of 8 and the auto grid measurement was:

	X	Y	Z
Center	126.3774	135.3406	120.5837
Dimensions (Angstrom)	22.9100	19.9385	16.5087

4.1.2 Nigella sativa

Twenty eight (**28**) compounds (including the four Standards) interacted with one or more of the target proteins, exhibiting varying binding affinities, as shown in **Table 3.1.2;** binding affinities ranged from -9.2 to -10.5kcal/mol for 5-HT1B, -6.9 to -8.6kcal/mol for 5-HT1D, and -9.8 to -11 kcal/mol for 5-HT1F receptors with the first value in each range corresponding to the binding affinities of the respective standards Donitriptan, Sumatriptan, and Lasmiditan. No Compound had a binding affinity equal to or greater than that of Rimegepant (-9.1kcal/mol).

For Serotonin 1B receptor, Butyrospermol exhibited the highest binding affinity(-10.5kcal/mol) and only Compound 163185263 formed conventional hydrogen bond (1), Compound 163185263 and Compound 56924079 exhibited a binding affinity(-9.2kcal/mol) same as Donitriptan.

The docking was done at an exhaustiveness of 8 and the auto grid measurement was:

	X	Y	Z
Center	87.7376	64.7423	66.6879
Dimensions (Angstrom)	29.7469	40.4459	22.6369

For Serotonin 1D receptor, Compound 102575929 exhibited the highest binding affinity(-8.6kcal/mol) but did not form any conventional hydrogen bond. All the compounds except Compound 162958795 exhibited a binding affinity higher than Sumatriptan. Compound 163104975 and Compound 118717505 formed the highest conventional hydrogen bond (2). Ligands bound to the active site amino acids in the order: ^{321}SER = ^{201}SER > ^{123} THR= ^{198}THR. Other compounds interacted with some of the active site amino acids using weak forces like the van der Waal's force and pi bond.

The docking was done at an exhaustiveness of 8 and the auto grid measurement was:

	X	Y	Z
Center	98.1901	121.4703	111.7462
Dimensions (Angstrom)	17.5609	17.5073	13.3934

For Serotonin 1F receptor, Butyrospermol and Compound 124762119 exhibited the highest binding affinity (-11kcal/mol) but neither formed a conventional hydrogen bond. Compound 102575929 formed the most conventional hydrogen bond (3). Some of the compounds also formed one conventional hydrogen bond as shown in **Figure 3.1.2.3.**

Ligands bound to the active site amino acids in the order: ^{108}THR > ^{330}ASN > ^{182}THR = ^{185}THR = ^{317}ASN.

The exhaustiveness of docking was 8 and the auto grid measurement was:

	X	Y	Z
Center	125.6715	135.1914	120.9494
Dimensions (Angstrom)	23.6186	18.9835	15.0986

4.1.3 Petasites hybridus

Forty seven (**47**) compounds (including the four Standards) interacted with one or more of the target proteins, exhibiting varying binding affinities, as shown in **Table 3.1.3;** binding affinities ranged from -9.2 to -9.4kcal/mol for 5-HT1B, -6.9 to -9kcal/mol for 5-HT1D, and -9.8 to -10.3kcal/mol for 5-HT1F receptors with the first value in each range corresponding to the binding affinities of the respective standards Donitriptan, Sumatriptan, and Lasmiditan. No Compound had a binding affinity equal to or greater than that of Rimegepant (-9.0kcal/mol).

For Serotonin 1B receptor, Compound 163193385 exhibited the highest binding affinity of -9.4kcal/mol and formed only one conventional hydrogen bond. Compound 101596893 and Compound 162963127 formed the most conventional hydrogen bonds (2) while some of the compounds formed one conventional hydrogen bond. All the compounds interacted with some of the active site amino acids using weak forces as shown in **Figure 3.1.3.1.** Ligands bound to the active site amino acids in the order: ^{203}THR > ^{212}SER > 204ASP = ^{209}THR = ^{213}THR.

The docking was done at an exhaustiveness of 8 and the auto grid measurement was:

	X	Y	Z
Center	87.9814	64.7708	66.3145
Dimensions (Angstrom)	30.9186	40.5029	22.6173

For Serotonin 1D receptor, 4-[(2E,4R)-4-hydroxy-3,7-dimethylocta-2,6-dienoxy]-5-methylchromen-2-one exhibited the highest binding affinity of -9kcal/mol but did not form any conventional hydrogen bond while 4-[10-Oxo-neryloxy]-5-methylcoumarin formed the most conventional hydrogen bond (3). Some of the compounds formed one or two conventional hydrogen bonds and all the compounds interacted with some of the active site amino acids using weak forces. Ligands bound to the active site amino acids in the order: ^{201}SER > ^{321}SER > ^{123}THR > ^{191}ASN = ^{198}THR > ^{342}THR.

The docking was done at an exhaustiveness of 8 and the auto grid measurement was:

	X	Y	Z
Center	98.4850	121.5335	111.6248
Dimensions (Angstrom)	16.7621	17.2510	13.6364

For Serotonin 1F receptor, [(4aR,5S,7R,8aR,9aR)-3,4a,5-trimethyl-2-oxo-4,5,6,7,8,8a,9,9a-octahydrobenzo[f][1]benzofuran-7-yl](Z)-2-methylbut-2-enoate exhibited the strongest bonding affinity of -10.3kcal/mol and also formed the most conventional hydrogen bonds (2) as four other compounds. All the compounds formed one or more conventional hydrogen bonds and

interacted with some of the active site amino acids using weak forces. Ligands bound to the active site amino acids in the order: ^{182}THR > ^{186}THR.

The docking was done at an exhaustiveness of 8 and the auto grid measurement was:

	X	Y	Z
Center	125.8544	135.3055	120.8639
Dimensions (Angstrom)	22.8661	19.0087	14.9277

4.1.4 Tanacetum parthenium

Forty three (**43**) compounds(including the four standards) interacted with one or more of the target proteins, exhibiting varying binding affinities, as shown in **Table 3.1.4;** binding affinities ranged from -9.7 to -11kcal/mol for 5-HT1B, -6.9 to -8.7kcal/mol for 5-HT1D, -9.8 to -10.8kcal/mol for 5-HT1F receptors and -9.1 to -9.2kcal/mol for CGRP receptors with the first value in each range corresponding to the binding affinities of the respective standards Donitriptan, Sumatriptan, Lasmiditan, and Rimegepant.

For Serotonin 1B receptor, Compound 102328535 exhibited the strongest binding affinity (-11kcal/mol) and formed the most conventional hydrogen bond (4) while other compounds exhibited a binding affinity stronger than Donitriptan except Fucosterol (-9.7kcal/mol). Phelligridin C and Phelligridin D each formed three conventional hydrogen bonds, Rubijervine formed only one conventional hydrogen bond while the other compounds did not form any conventional hydrogen bond. All the compounds interacted with some of the active site amino

acids using weak forces. Ligands bound to the active site amino acids in the order: ^{212}SER = ^{129}ASP > ^{205}HIS = ^{204}ASP = ^{209}THR = ^{134}THR = ^{130}ILE = ^{201}VAL = ^{203}THR.

The docking was done at an exhaustiveness of 8 and the auto grid measurement was:

	X	Y	Z
Center	87.8118	64.4231	66.0010
Dimensions (Angstrom)	31.3564	41.0103	21.7053

For Serotonin 1D receptor, Compound 14219462 exhibited the strongest binding affinity (-8.7kcal/mol) but did not form any conventional hydrogen bond. Compound 101254614 Apigenin, Luteolin, 6-Hydroxykaempferol, Nepetin and Jaceidin (which exhibited same binding affinity of -6.9kcal/mol as Sumatriptan and three other compounds) formed the most conventional hydrogen bond (3). Some of the compounds formed one or two conventional hydrogens as shown in **Figure 3.1.4.2.** Ligands bound to the active site amino acids in the order: ^{201}SER > ^{321}SER > ^{119}ILE > ^{118}ASP = ^{123}THR > ^{191}ASN > ^{197}TYR = ^{198}THR = ^{122}CYS.

The docking was done at an exhaustiveness of 8 and the auto grid measurement was:

	X	Y	Z
Center	98.1657	121.3910	111.3669
Dimensions (Angstrom)	17.0817	17.5359	14.1522

For Serotonin 1F receptor, Compound 101861833 exhibited the strongest binding affinity of -10.8kcal/mol and formed only one conventional hydrogen bond as Solanidine, while 7-(alpha-D-

Glucopyranosyloxy)-5-hydroxy-2-(4-hydroxyphenyl)-4H-1-benzopyran-4-one formed the most conventional hydrogen bond (2). The other compounds did not form any conventional bond and all the compounds interacted with some of the active site amino acids using weak forces. Ligands bound to the active site amino acids in the order: ^{330}ASN > ^{312}LYS = ^{180}SER.

The docking was done at an exhaustiveness of 8 and the auto grid measurement was:

	X	Y	Z
Center	125.5871	135.2578	120.2738
Dimensions (Angstrom)	23.2946	20.0191	15.7277

For the CGRP receptor, Compound 16723933 bound to receptor, exhibited a binding affinity of -9.2kcal/mol and did not form any conventional hydrogen bond but interacted with some of the active site amino acids using weak forces.

Docking was done at an exhaustiveness of 8 and the auto grid measurement was:

	X	Y	Z
Center	88.6429	122.0087	94.9672
Dimensions (Angstrom)	29.4955	28.8040	25.1891

It is important to note that some compounds were found in more than one plant, while others appeared in only one, and some from either group interacted with two or more receptors, indicating broader binding potential. This can be seen in **Table 3.1.2; Table 3.1.3**; and **Table 3.1.4.**

4.2 ADMET Profiling

Absorption, Distribution, Metabolism, and Excretion (ADME) studies are essential for evaluating the drug-likeness of compounds prior to synthesis, thereby reducing the likelihood of pharmacokinetic-related failures during drug development (Di *et al*., 2012). Several predictive models exist for assessing drug-likeness; however, in this study, Lipinski's Rule of Five was employed. According to Lipinski (1997), an orally active drug should not violate more than one of the following criteria: hydrogen bond donors ≤ 5, hydrogen bond acceptors ≤ 10, molecular weight ≤ 500 Daltons, and an octanol–water partition coefficient (log P) ≤ 5. All compounds presented in **Tables 3.1.1 to 3.1.4** adhered to these parameters, indicating favorable drug-likeness and ADME properties, and suggesting efficient absorption, distribution, and metabolism with minimal risk of poor permeability or solubility.

Crassocephalum crepidioides compounds with the most favourable binding affinity and interactions with the respective receptors as discussed earlier passed Lipinski's rule of five, which indicate a strong favourable passive permeability and potential oral bioavailability. Their molecular weights in the range of 252.17 – 430.27 Da, 0 – 2 number of hydrogen bond donors, and lipophilicity values between 2.25 – 4.87 clearly indicate good drug likeness. 7-but-2-enyl-6,8-dihydroxy-3-pent-3-enyl-3,4-dihydroisochromen-1-one has the lowest predicted toxicity with average critical systemic risk of 11.43%, with risks for Hematotoxicity (7.06%) and Neurotoxicity (7.27%) being exceptionally low. Its Log P of 3.63 is ideal for balanced solubility and absorption. Compound 162889473, 7-but-2-enyl-6,8-dihydroxy-3-pent-3-enyl-3,4-dihydroisochromen-1-one, Compound 12068760 are the most promising compounds as these phytochemicals achieved optimal ADME characteristics and the highest predicted systemic

safety profile**.** Neovibsanin I is a strong secondary lead, but modification is required due to high risk of systemic toxicity.

The ligands from *Nigella sativa* with the most favourable binding affinity and interactions with the respective receptors as discussed earlier passed Lipinski's rule of five, which indicate a strong favourable passive permeability and potential oral bioavailability. Their molecular weights range from 338.38 – 440.5 Da, number of hydrogen bond donors is between 1 – 2, and lipophilicity values between 2.25–10.5 clearly indicate a normal drug likeness potential. Despite strong interaction, best systemic safety profiles of Butyrospermol and Compound 162958795 with their receptors, their high lipophilicity of 7.39 and 7.02 could indicate potential issues with formulation and solubility in aqueous environments. Compound 118717505 with lipophilicity value of 2.25 indicates balance solubility but its high risk of systemic toxicity could be a challenge. Many of the Compounds, including Butyrospermol and Compound 162958795 from Nigella sativa show promise as multi-target drug leads but need modification to enhance water solubility.

Petasites hybridus compounds with the most favourable binding affinity and interactions with the respective receptors as discussed earlier passed Lipinski's rule of five, which indicate a strong favourable passive permeability and potential oral bioavailability. Their molecular weights range from 326.15– 332.2 Da, number of hydrogen bond donors is between 0 – 1, and lipophilicity values between 3.17 – 4.75 clearly indicate an excellent balanced drug likeness potential. Compound 101996395 lipophilicity value of 3.17 indicates close optimal solubility and absorption with a good safety profile. Compound 163057208, 4-[10-Oxo-neryloxy]-5-methylcoumarin and Compound 162963127 have the lowest predicted toxicity.

Tanacetum parthenium compounds with the most favourable binding affinity and interactions with the respective receptors as discussed earlier passed Lipinski's rule of five, which indicate a strong favourable passive permeability and potential oral bioavailability. These compounds show a lipophilicity variability between 0.01–7.696 with only Fucosterol having a value greater than 5 and more than half with Log PO/W value between 2 and 4, number of hydrogen bond donors between 1–5, and relatively small molecular weight ranges between 252.09–439.36 Da, favouring absorption and distribution, thus indicating optimal potential drug likeness. Compound 102328535, Phelligridin C and Phelligridin D possess highly desirable physicochemical property for a drug intended for oral administration, with a balanced systemic toxicity profile. Compound 101861833 is highly unfavourable for predicted oral bioavailability and highly toxic, despite having a very strong binding affinity.

CHAPTER FIVE

CONCLUSION

Molecular docking and ADMET analysis of phytochemical constituents from *Crassocephalum crepidioides*, *Nigella sativa*, *Petasites hybridus*, and *Tanacetum parthenium* confirmed the claimed effective traditional use of the plants and provided evidence that supports their use for the management of migraine. The study showed that compounds from these plants can be effective with good oral bioavailability and safer alternatives to current migraine treatments.

This study showed that phytoconstituents from the selected medicinal plants were successfully obtained and certain compounds from the various plants bind to selected important receptors associated with migraine with better affinity than the reference drugs. These findings also revealed the muti-target activity of some phytoconstituents in *Nigella sativa, Petasites hybridus*, and *Tanacetum parthenium,* and validate the established effectiveness of *Petasites hybridus*, and *Tanacetum parthenium* against migraine, thus these plants contain a high number of lead compounds for development of antimigraine drugs.

Tanacetum parthenium and *Nigella sativa* contained compounds that formed the most stable, high- affinity complexes. The significant binding affinity, stable interactions and very optimal bioavailability and low toxicity risk associated with *Crassocephalum crepidioides* compounds confirm that this plant possess potential anti-migraine properties and are suitable for formulation as oral drugs following successful further developments.

REFERENCES

Aderinto, N., Olatunji, G., Kokori, E., Ogieuhi, I. J., Babalola, A. E., Ukoaka, B., Moradeyo, A., Egbunu, E., Afolabi, S., Yusuf, I. A., and Aboje, J. E. (2024). Prevalence, characteristics, and treatment outcomes of migraine headache in Nigeria: a systematic review and meta-analysis. *The Journal of Headache and Pain*, *25*(1), Article 172.

Allais, G., Mailland, E., D'Andrea, G., and Bussone, G. (2006). *Petasites hybridus* (butterbur) in migraine prophylaxis. *European Neurology Review*, *1*(2), 34–36.

American Academy of Family Physicians. (2018). Migraine: acute and preventive treatment. *American Family Physician*, *97*(7), 441–450.

American Academy of Neurology. (2012). Evidence-based guideline update: Pharmacologic treatment for episodic migraine prevention in adults: Report of the Quality Standards Subcommittee of the American Academy of Neurology and the American Headache Society. *Neurology*, *78*(17), 1337–1345.

Amiri, H., Ziaeifar, M., and Sepehri, G. (2022). The global prevalence and incidence of migraine headache: a systematic review and meta-analysis. *Current Pain and Headache Reports*, *26*(2), 79–87.

Amiri, Z., Ghelichi, L., Aghaie, A., Esmaillzadeh, A., Aligholi, E., and Toghiani, M. (2022). Migraine severity, disability, and duration...

Aoh, A. (2024). 'Mechanisms and clinical applications of CGRP antagonists.', *Headache: The Journal of Head and Face Pain*, *64*(1), 58–69.

Ashina, M., Buse, D. C., Pozo-Rosich, P., and Kurth, T. (2021). 'Diagnosis and Management of Migraine: A Review', *JAMA*, *326*(18), 1845–1855.

Ashina, M., Buse, D. C., Reuter, U., Pozo-Rosich, P., Irimia, P., and Dodick, D. W. (2021). Safety and tolerability of CGRP monoclonal antibodies in the treatment of migraine...

Baldwin, B. G. (2009). A fully resolved backbone phylogeny reveals numerous dispersals and explosive diversifications throughout the history of Asteraceae. *Proceedings of the National Academy of Sciences*, *106*(25), 10185–10190.

Baldwin, B. G. (2009). The Compositae or Asteraceae family, with notes on its evolution and phylogeny.

Banerjee, S., Schramm, C., Meringer, M., Gohlke, H., and O'Boyle, N. M. (2022). Open Babel: An open chemical toolbox. *Journal of Chemical Information and Modeling*, *62*(12), 2736–2744.

Blair, H. A. (2023). Rimegepant: A review in the acute and preventive treatment of migraine. *Drugs*, *83*(1), 77–88.

Boinpally, R., Jakate, A., Lipton, R. B., and Periclou, A. (2024). Clinical Pharmacology of Rimegepant: A Review of its Pharmacokinetics, Pharmacodynamics, and Drug-Drug Interactions. *Clinical Pharmacokinetics*, *63*(4), 389–403.

British Herbal Medicine Association. (2024). *British Herbal Compendium: A handbook of scientific information on medicinal plants.*

Burley, S. K. (2022). The Protein Data Bank: A community resource for structural biology and drug discovery. *Structure*, *30*(9), 1163–1169.

Cady, R. K., and Cady, J. A. (2012). Acute treatment of migraine: an overview of the literature. *The Journal of Headache and Pain*, *13*(S1), S19–S25.

Colman, R. F., Brown, T. P., Biondi, D. M., Spierings, E. L., and Tepper, S. J. (2005). Triptans vs. ergotamine: a systematic review and meta-analysis. *Cephalalgia*, *25*(10), 871–880.

Dar, T. A., and Mir, M. A. (2017). Molecular docking: approaches, types, and applications. In: *Molecular Docking and Drug Design.* Academic Press, pp. 1–25.

Derry, C. J., Wiffen, P. J., Moore, R. A., and Tfelt-Hansen, P. (2014). Triptans for the acute treatment of migraines in adults: a Cochrane review update. *Cochrane Database of Systematic Reviews*, (5), CD002915.

Dodick, D. W., Goadsby, P. J., Lipton, R. B., Olesen, J., and Silberstein, S. D. (2019). Frovatriptan for the acute treatment of migraine. *Expert Opinion on Pharmacotherapy*, *20*(9), 1083–1094.

Dong, H., Yang, M., Qin, Z., Li, Y., Chen, Y., and Li, J. (2024). Global, regional, and national burden of migraine in 204 countries and territories, 1990–2021: a systematic analysis. *The Lancet Neurology*, *23*(1), 77–93.

Dukat, M. (2001). Donitriptan (BMS-204154). *Current Opinion in Investigational Drugs*, *2*(10), 1438–1443.

Edvinsson, L. (2022). The CGRP pathway in migraine: from basic science to clinical translation. *The Journal of Headache and Pain*, *23*(1), Article 89.

Ferreira, L. G., Dos Santos, R. N., Oliva, G., and Andricopulo, A. D. (2015). 'Molecular Docking and Dynamics Simulation: A Powerful Combination for Structure-Based Drug Design', *Current Drug Targets*, *16*(2), 86–92.

GBD 2019. (2019). Global Burden of Disease Study 2019.

GBD 2021. (2021). Global Burden of Disease Study 2021.

Goadsby, P. J., Lipton, R. B., and Ferrari, M. D. (2002). Triptans: an update on the current evidence and future possibilities. *Current Opinion in Neurology*, *15*(3), 253–257.

Goadsby, P. J., Sprenger, T., and Dodick, D. W. (2019). Lasmiditan for the acute treatment of migraine. *The Lancet Neurology*, *18*(9), 830–841.

Goadsby, P. J., Silberstein, S. D., Lipton, R. B., and Dodick, D. W. (2023). The CGRP pathway in migraine: new insights and treatment implications.

Headache Classification Committee of the International Headache Society (IHS). (2018). The International Classification of Headache Disorders, 3rd edition (ICHD-3). *Cephalalgia*, *38*(1), 1–211.

Hoffmann, J., and May, A. (2017). Diagnosis and management of migraine. *The Lancet*, *390*(10113), 2715–2723.

Iyengar, S., Johnson, K. W., and Ossipov, M. H. (2019). CGRP and the trigeminal nervous system: mechanisms and clinical implications. *Neuropharmacology*, 157, 107629.

Kareem, M. A., Ladan, M. J., Garba, Y., and Suleiman, M. (2019). Ethnomedicinal survey of plants used for managing respiratory ailments and fever in Kano State, Nigeria. *Journal of Ethnopharmacology*, 239, 111956.

Khan, M. K. A., Khan, M. I., and Al-Wabel, N. A. (2021). Molecular docking and dynamics simulation of thymoquinone against serotonin receptors. *Journal of Molecular Structure*, 1243, 130825.

Kleeberg-Hartmann, J. (2021). *Petasites hybridus* extract inhibits CGRP release from trigeminal afferents via modulation of TRPA1 and TRPV1 channels. *Cephalalgia*, *41*(4), 456–469.

Kumar, V. (2022). Molecular docking studies of phytochemicals from *Crassocephalum crepidioides* against 5-HT1B receptor. *Journal of Molecular Graphics and Modelling*, 116, 108269.

Lipton, R. B., Diener, H. C., Marmura, M. J., Muse, D., and Szegedi, M. (2006). *Petasites hybridus* root (butterbur) is an effective preventive treatment for migraine. *Neurology*, *67*(10), 1779–1786.

Meng, E. C., Pettersen, E. F., Couch, G. S., Huang, C. C., and Ferrin, T. E. (2011). Tools for molecular modeling and visualization in UCSF Chimera.

Mohammed, A., Yahaya, G., and Yahaya, Y. (2019). Survey of traditional uses of *Nigella sativa* in northern Nigeria. *Journal of Ethnopharmacology*, 239, 111956.

Olesen, J. (2018). ICHD-3: A paradigm shift in headache classification. *The Journal of Headache and Pain*, *19*(1), 1–3.

Osei, A. K. (2021). Review of the ethnomedicinal uses, phytochemistry, and pharmacology of *Crassocephalum crepidioides*. *Journal of Ethnopharmacology*, 280, 114488.

Osonuga, B. N., Olukoya, F. O., and Abimbola, O. T. (2025). The economic and social burden of migraine in Nigeria: a community-based study. *The Lancet Regional Health - Africa*, *12*(1), 100345.

Pareek, A. (2011). Feverfew (*Tanacetum parthenium* L.): A systematic review. *Pharmacognosy Reviews*, *5*(9), 103–110.

Saganuwan, A. S. (2014). Ethnobotanical survey of medicinal plants used for the treatment of headaches in Makurdi, Benue State, Nigeria. *International Journal of Research in Pharmacy and Chemistry*, *4*(3), 661–670.

Shafqat, R. A. (2020). Triptans vs. CGRP antagonists: a comparative efficacy and safety review. *Expert Review of Neurotherapeutics*, *20*(8), 811–825.

Silberstein, S. D. (2019). Headache and migraine. *Neurology*, *93*(15), 652–660.

Suleiman, M., Abubakar, G., and Yusuf, A. (2020). Ethnobotanical survey of medicinal plants used for the treatment of respiratory ailments in Kaduna State, Nigeria. *Journal of Ethnopharmacology*, 261, 113063.

Tfelt-Hansen, P., and Saxena, P. R. (2001). Triptans: a new generation of drugs for the acute treatment of migraine. *Current Opinion in Neurology*, *14*(3), 343–349.

Villalón, C. M., and Olesen, J. (2009). The role of CGRP in the pathophysiology of migraine and efficacity of CGRP receptor antagonists. *Pharmacology & Therapeutics*, 124(1), 1–16.

Wang, G., and Zhu, W. (2016). 'Molecular Docking for Drug Discovery and Development: A Widely Used Approach but Far from Perfect', *Future Medicinal Chemistry*.

World Health Organization (WHO). (2021). Migraine: a global health priority.